# EFFECTS OF HALOPHILIC PEPTIDE FUSION ON SOLUBILITY AND STABILITY OF D-PHENYLGLYCINE AMINOTRANSFERASE

**HOSSEIN JAVID**

**A THESIS SUBMITED IN PARTIAL FULFILLMENT
OF THE REQUIREMENTS FOR
THE DEGREE OF DOCTOR OF PHILOSOPHY
(MICROBIOLOGY)
FACULTY OF GRADUATE STUDIES
MAHIDOL UNIVERSITY
2014**

Thesis
entitled

# EFFECTS OF HALOPHILIC PEPTIDE FUSION ON SOLUBILITY AND STABILITY OF D-PHENYLGLYCINE AMINOTRANSFERASE


……..

Mr. Hossein Javid
Candidate

……..

Asst. Prof. Suthep Wiyakrutta, Ph.D.
Major advisor

……..

Prof. Vithaya Meevootisom, Ph.D.
Co-advisor

……..

Lect. Nuttawee Niamsiri
Co-advisor

……..

Lect. Chartchai Changsen, Ph.D.
Co-advisor

……..

Prof. Banchong Mahaisavariya,
M.D., Dip Thai Board of Orthopedics
Dean
Faculty of Graduate Studies
Mahidol University

……..

Lect. Padungsri Dubbs, Ph.D.
Program Director
Doctor of Philosophy Program in
Microbiology, Faculty of Science
Mahidol University

Thesis
entitled

# EFFECTS OF HALOPHILIC PEPTIDE FUSION ON SOLUBILITY AND STABILITY OF D-PHENYLGLYCINE AMINOTRANSFERASE

Was submitted to the faculty of Graduate Studies, Mahidol University
for the degree of Doctor of Philosophy (Microbiology)
on
February 28, 2014

...
Mr. Hossein Javid
Candidate

...
Assoc. Prof. Nongluksna Sriubolmas, Ph.D.
Chair

.....
Lect. Chartchai Changsen, Ph.D.
Member

.....
Asst. Prof. Suthep Wiyakrutta, Ph.D.
Member

.....
Lect. Nuttawee Niamsiri, Ph.D.
Member

.....
Prof. Vithaya Meevootisom, Ph.D.
Member

.....
Prof. Banchong Mahaisavariya, M.D., Dip Thai Board of Orthopedics
Dean
Faculty of Graduate Studies
Mahidol University

.....
Assoc. Prof. Krongtong Yoovathaworn
Ph.D. (Pharmacology)
Deputy Dean for Policy and Quality Development
Acting Dean
Faculty of Science
Mahidol University

# ACKNOWLEDGMENTS

When I came to SCMI for the first time, I did not have any idea about what I wanted to do until I entered VM-SW laboratory where I met many talented people whom I deeply appreciate for their companionship, succor and challenging me in numerous ways to find my path. First of all, I would like to express my deepest appreciation to my major thesis advisor, mentor and the current head of SCMI, Asst. Prof. Dr. Suthep Wiyakrutta, who stands at the forefront for providing scientific supports and guidance during my Ph.D. study, his knowledge and genuine enthusiasm for research is peerless. I would like to express my profound gratitude to Prof. Dr. Vithaya Meevootisom my thesis co-advisor and the former head of SCMI for helping me to achieve my goals by providing critical suggestions and guidance which greatly enhanced not only the preparation of this dissertation, but also my life in Thailand.

This work would not be progressed without helping, invaluable suggestions and moral support of the respected members of the advisory committee, Dr. Chartchai Changsen and Dr. Nuttawee Niamsiri. I also would like to take this opportunity and sincerely express my abysmal reverence to Mrs. Duangnate Isarangkul Na Adyudhaya and the other members of Molecular Industrial Microbiology (MIM) laboratory (lab room B600 and B601) and my friends and the people who have not been mentioned here for their support and relief as well as to those who made my life to render easily in amazing Thailand.

My special and profound appreciation is for my beloved family. I would like to dedicate this dissertation to Dr. Mohammadreza Javid, my father and my first biology teacher who taught me the first biology lesson in his laboratory when I was six and offered me invaluable moral support during my life and helped me to come to this point where I am obtaining a Ph.D. degree, in which I believe that it would not be the last challenge in my life that I have been raised to face; Mrs. Soudabeh Amiri, my mother who consistently cheered me up with her endless and unconditional love and reminded me that always the bright dawn comes after the darkest moment of night; Mr. Hassan Javid, my brother, who filled my loneliness with his care and humor over these years; Mrs. Mehri Kherad and Mrs. Farangis Dianat, my lovely grandmothers, their cuisine recipes saved my life; my beloved aunt, Mrs. Farkhondeh Javid who through long phone conversations at crucial moments helped me to find the strength back; Mr. Khalil Javid and Dr. Alireza Javid, my respected uncles for their care and supports and my deceased grandfather, Mr. Mohsen Javid, his memory is in my mind trough my life.

Hossein Javid

EFFECTS OF HALOPHILIC PEPTIDE FUSION ON SOLUBILITY AND STABILITY OF D-PHENYLGLYCINE AMINOTRANSFERASE

HOSSEIN JAVID 5236022 SCMI/D

Ph.D. (MICROBIOLOGY)

THESIS ADVISORY COMMITTEE: SUTHEP WIYAKRUTTA, Ph.D. VITHAYA MEEVOOTISOM, Ph.D., CHARTCHAI CHANGSEN, Ph.D., NUTTAWEE NIAMSIRI, Ph.D.

ABSTRACT

D-Phenylglycine aminotransferase (D-PhgAT) from *Pseudomonas stutzeri* ST-201 is useful for enzymatic synthesis of enantiomerically pure D-phenylglycine. However, its low protein solubility prevents its application at high substrate concentrations. With the aim of increasing protein solubility, N-terminus of D-PhgAT was genetically fused with short peptides ($A_1$ α-helix, $A_2$ α-helix, and ALAL which is a hybrid of A1 and A2) from a ferredoxin enzyme of a halophilic archaeon, *Halobacterium salinarum*. The fused enzymes $A_1$-D-PhgAT, $A_2$-D-PhgAT and ALAL-D-PhgAT displayed reduced p*I* and increased in solubility by 6.1-, 5.3-, and 8.1-fold in TEMP pH 7.6 storage, respectively, and 5-, 4.5-, and 5.9-fold in CAPSO pH 9.5 reaction buffers, respectively, compared to the wild-type enzyme (WT-D-PhgAT). In addition, all the fused D-PhgAT displayed a higher enzymatic reaction rate than the WT-D-PhgAT at all concentrations of L-glutamate monosodium salt used. The highest one, 23.82 ± 1.47 mM $h^{-1}$, was that obtained from having ALAL-D-PhgAT reacted with 1500 mM of the substrate. Moreover, the halophilic fusion significantly increased the tolerance of D-PhgAT in the presence of NaCl and KCl, slightly in favor of KCl, where under the same condition at 3.5 M NaCl or KCl all halophilic fused variants showed higher activity than WT-D-PhgAT. In addition a higher thermal stability has been seen in halophilic fused variants as the hydrophobicity (log *p*) of miscible organic solvents increased.

KEY WORDS: D-PHENYLGLYCINE AMINOTRANSFERASE / HALOPHILIC PEPTIDE FUSION / SOLUBILITY / STABILITY

116 pages

# CONTENTS

# CONTENTS (cont.)

# CONTENTS (cont.)

# CONTENTS (cont.)

# CONTENTS (cont.)

# LIST OF TABLES

# LIST OF FIGURES

# LIST OF FIGURES (cont.)

# LIST OF ABBREVIATIONS

| | |
|---|---|
| A | Absorbance |
| AT | Aminotransferase |
| AU | Absorbance unit |
| bp | Base pair |
| BSA | Bovine serum albumin |
| BZF | Benzoylformic acid |
| C | Cysteine |
| °C | Degree Celsius |
| CAPS | N-cyclohexyl-3-aminopropanesulfonic acid |
| CAPSO | 3-(Cyclohexylamino)-2-hydroxy-1-propanesulfonic acid |
| cm | Centimeter |
| D | Aspartic acid |
| D | Dimension |
| D- | Dextro, turning the plane of polarized light to the right |
| DEAE | Diethylaminoethyl |
| DMSO | Dimethyl sulfoxide |
| DNA | Deoxyribonucleic acid |
| dNTP | Deoxyribonucleotide triphosphate |
| D-4-OHPhg | D-4-hydroxyphenylglycine |
| D-Phg | D-phenylglycine |
| D-PhgAT | D-phenylglycine aminotransferase |
| DW | Distilled water |
| ε | Extinction coefficient |
| E | Glutamic acid |
| EC | Enzyme commission |
| *E. coli* | *Escherichia coli* |
| EDTA | Ethylenediamine tetraacetic acid |
| e.g., | Latin phrase exempli gratia; for example |

# LIST OF ABBREVIATIONS (cont.)

| | |
|---|---|
| *et al.* | Latin phrase et alii; and others |
| FPLC | Fast Protein Liquid Chromatography |
| g | Gram |
| *g* | Relative Centrifugal Force (RCF) |
| h | Hour |
| HIC | Hydrophobic Interaction Chromatography |
| *Hm* Fdx | *Halobacterium marismortui* ferredoxin enzyme |
| *Hs* Fdx | *Halobacterium salinarum* ferredoxin enzyme |
| i.e., | Latin phrase id est.; that is |
| IEX | Ion Exchange Chromatography |
| IPTG | β-D-thiogalactopyranoside |
| k | Kilo |
| kb | Kilobase |
| kDa | Kilodalton |
| L | Liter |
| L- | Levo, turning the plate of polarized light to the left |
| λ | Wavelength |
| LB | Luria-Bertani medium |
| M | Molar |
| mg | Milligram |
| min | Minute |
| mL | Milliliter |
| mM | Millimolar |
| Mr | Relative molecular mass |
| MW | Molecular weight |
| nm | Nanometer |
| N | Asparagine |
| OHBZF | 4-Hydroxybenzoylformic acid |
| PCR | Polymerase chain reaction |

# LIST OF ABBREVIATIONS (cont.)

| | |
|---|---|
| PDB | Protein database |
| pH | Power of hydrogen |
| pI | Isoelectric point |
| PIPES | piperazine-N,N′-bis(2-ethanesulfonic acid) |
| pka | Acid dissociation constant |
| PLP | Pyridoxal-5'-phosphate |
| P-OHBZF | Para-hydroxybenzoylformate |
| rpm | Revolutions per minute |
| SDS-PAGE | sodium dodecyl sulfate polyacrylamide gel electrophoresis |
| sec | Second |
| SOC | Super Optimal broth with Catabolite repression |
| sp. | Species |
| TBE | Tris-Borate EDTA |
| TE | Tris-EDTA |
| TEMED | N,N,N',N'-Tetramethylethylenediamine |
| Tm | Melting temperature |
| Tris | 2-Amino-2-hydroxymethyl-propane-1,3-diol |
| OD | Optical Density |
| U | Unit |
| UV | Ultraviolet |
| V | Voltage |
| V | Volume |
| Ver. | Version |
| µg | Microgram |
| µL | Microliter |

# CHAPTER I
# INTRODUCTION

## 1.1 Introduction

First purification and characterization of D-phenylglycine aminotransferase (D-PhgAT; EC 2.6.1.72), a stereo-inverting pyrodoxal-5′-phosphate (PLP) dependent enzyme from *Pseudomonas stutzeri* ST-201 with the ability to catalyze reversible transamination of D-phenylglycine (D-Phg) with α-ketoglutaric acid as an amino group acceptor to form L-glutamate and benzoylformic acid as products (Figure 1.1) was reported in 1997 [1]. Its aminotransferase activity can be inhibited by aminooxyacetic acid. Crystallography and 3D studies revealed homodimer structure of D-PhgAT with a subunit molecular weight of 47.5 kDa and size of 453 residues [2]. Each monomer possesses three domains, namely C-terminus, N-terminus and cofactor binding domain (Figure 1.2).

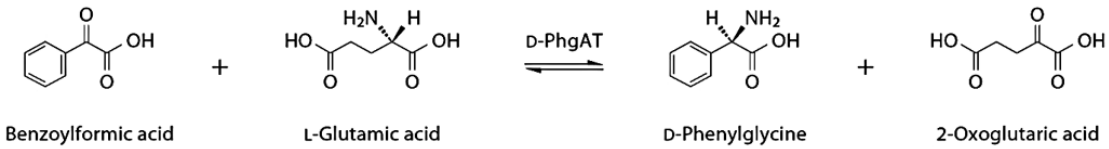


**Figure 1.1** Stereo-inverting and reversible reaction of D-PhgAT which can be used for synthesis of D-Phg from benzoylformic acid and L-glutamate as cheap substrates.

Later D-PhgAT encoding gene, *dpgA*, was successfully cloned by using pET-17b plasmid vector and over-expressed in *Escherichia coli* BL21 (DE3) expression host [3]. Genetically modified $His_6$-Tag version of this enzyme cloned and over-expressed by using pET-11a plasmid vector in *E. coli* Tuner (DE3) pLysS in order to facilitate D-PhgAT purification in one step immobilized metal ion affinity chromatography [4].

Due to its stereo-inverting and reversible properties, D-PhgAT is concerned as an invaluable catalyzer in single-step synthesis of D-Phg and D-4-hydroxyphenylglycine (D-4-OHPhg) that are essential side chain moieties for manufacturing of highly demanded semisynthetic antibiotics pertain to penicillin and cephalosporin families by utilizing a cheap amino group donor, L-glutamic acid. Currently, a two-steps and low reaction rate procedure (due to low solubility of substrates) is applied for production of these side chain moieties by D-hydantoinase and D-carbamoylase enzymes [5]. Application of other D-amino acid aminotransferases for these proposes is restricted as a result of their low activity and merely high specificity toward D-amino acids which are highly expensive. Moreover, using an amino acid racemase to convert L-amino acids to corresponding D-amino acids may baffle aminotransferase activity [6].

Furthermore, as a common predestination, enzymes encounter variety of inactivation, denaturation and precipitation reactions in the course of production, storage and ulterior utilization in industries [7], phenomena which D-PhgAT is not excluded. The issue of plunged in-vitro solubility of D-PhgAT was partially improved up to 5.9 fold via introducing single and double site directed mutations (N439D and Q444E) at highly solvent exposed β-turn residues involved with protein crystal contact with no unfavorable effects on activity and structural conformation of D-PhgAT [8]; however, D-PhgAT is still suffering from precipitation in high concentrated solutions, low solubility and inactivation at presence of high proportions of salts or organic solvents which occasionally, are inevitable in industrial applications.

Various techniques have been reviewed, addressed and successfully practiced in order to increase soluble enzyme stability [9, 10 and 11] in high proportions of salts and organic solvents. In this favor, three major techniques are considered vastly:

a) Screening and isolation of new enzymes, especially from extremophiles which are able to withstand harsh reaction conditions due to extreme factors.

b) Production of stable and durable enzymes through genetically modified mesophilic hosts.

c) Stabilizing of unstable enzymes by employing methods such as protein engineering, chemical modification, immobilization and reaction medium engineering.

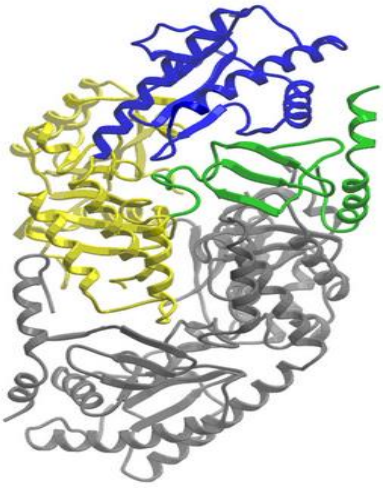

**Figure 1.2** Two subunits of D-PhgAT homodimer (chain A and A′ (gray chain)) are shown in this figure. Each subunit is composed of 3 domains: N-terminal domain (green), cofactor-binding domain (yellow), and C-terminal domain (blue).

Amongst these techniques, protein engineering and genetically modification and manipulation of mesophilic enzymes are highly interested in recent years, which proteins have been stabilized via introducing site directed mutations; however, merely a confined number of mutations propelled to large elation in stability [11]. Furthermore, some microorganisms are living in natural habitats with high salt contents and so referred as halophiles. These microorganisms which are mostly belong to domain archaea display unique adaptation strategies to save their proteins from high ionic strength in their natural habitats. One of the most important adaptation strategies of these microorganisms is manifested in their biased negative amino acid signature through high content of glutamate (E) and aspartate (D) as well as low lysine (K) residues. In addition halophilic proteins show higher number of surficial small hydrophobic and lower number of large hydrophobic residues. These significant amino acid signatures do not only enable halophilic proteins to endure highly ionic ecosystems, but also reduce water activity as key superiority to warrant stability in organic solvents [12]. One halophilic adaptation strategy is seen in ferredoxin enzymes from *Halobacterium marismortui* and *Halobacterium salinarum*, *Hm* Fdx and *Hs* Fdx

respectively, which have been shown to possess a 30 residues length extra N-terminus domain (Figure 1.3), composed of two α-helixes and two loops, 13 residues of them (~44%) are acidic compared with their non-halophilic plant-type homologues [13]. Two proposed halophilic adaptation mechanisms for this enzyme are halophilic substitution and halophilic addition; the former indicates high acidic residues on the surface while the later mentions earning of an extra acidic domain. Insertion or even embedment of a short extra N-terminus domain is considered as a fast halophilic adaptation mechanism for proteins that their genes have been adopted from non-halophilic organisms, then proteins may meet a better chance to remain and evolve in a halophilic host and achieve a proper distribution of surficial negative residues.

It is very interesting to know that it is pragmatic to convert a non-halophilic protein into a halophilic one through methods such as site directed mutagenesis and halophilic addition. In current study, based on learning from nature and combined with protein engineering techniques, we successfully applied and practiced a new approach in increasing solubility and stability of D-PhgAT as model protein in the presence of high proportions of salt and miscible organic solvents as additives in reaction medium through introducing two α-helixes, namely $A_1$ and $A_2$ and a hybrid of these two α-helixes, namely ALAL, from ferredoxin enzyme of a halophilic archaeon, *H. salinarum*, at the N-terminus domain of D-PhgAT.

A)

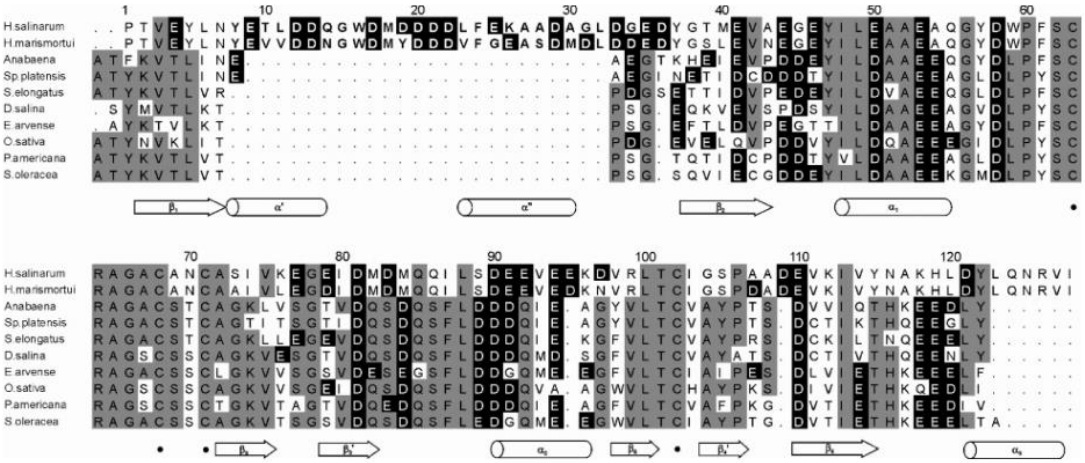


B)

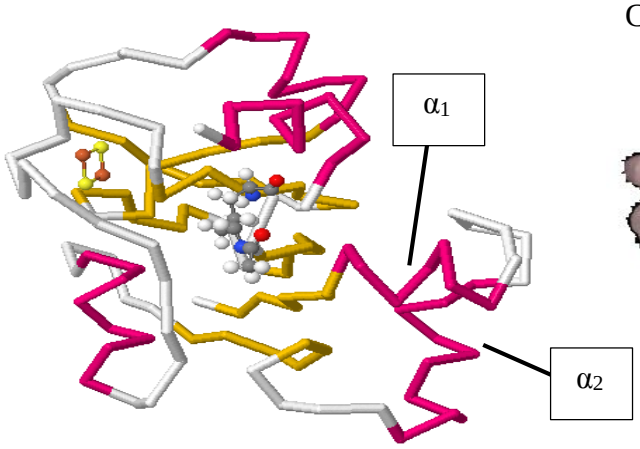


C)

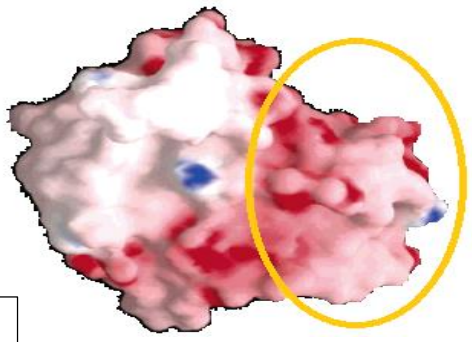

**Figure 1.3** A) Sequence alignments of *Hs* Fdx and its non-halophilic plant-type counterparts, B) Elements of secondary structure of *Hs* Fdx protein and position of $\alpha_1$ and $\alpha_2$ helixes, C) Electrostatic potential distribution on *Hs* Fdx surface where positive and negative charges are shown in blue and red color, respectively [13].

## 1.2 Objectives

Objectives of this study include:

1. Fusion of two α-helixes, namely $A_1$ and $A_2$, and a hybrid of them, ALAL, from ferredoxin enzyme of *H. salinarum* halophilic archaeon (*Hs* Fdx), at the N-terminus domain of D-PhgAT (Figure 1.4) in order to increase solubility and stability of D-PhgAT at the presence of high ionic strength and miscible organic solvents and over-expression of the newly modified recombinant protein.

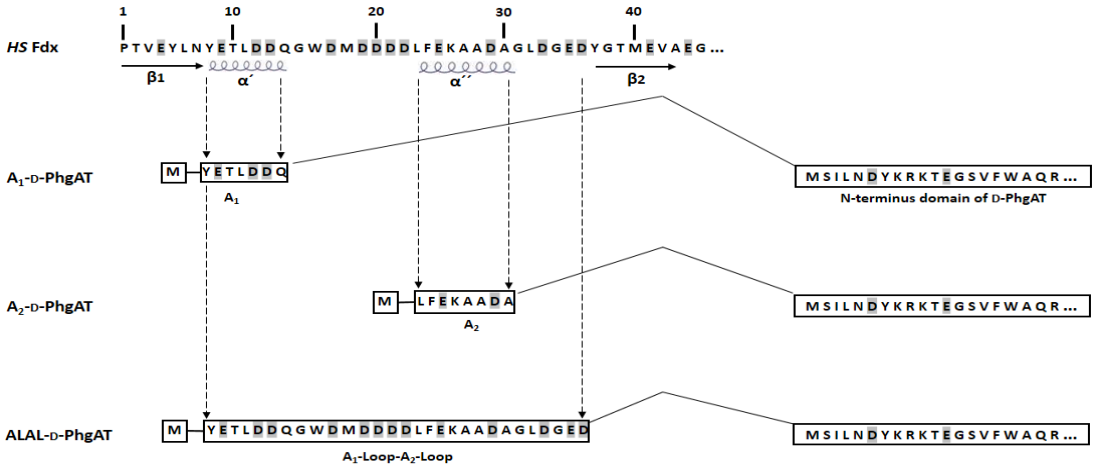


**Figure 1.4** Amino acid sequence diagrams showing the construction of D-PhgAT fusion with halophilic peptides from *Hs* Fdx as indicated with line-connected boxed amino acid sequences. Acidic residues (D and E) in the extra N-terminus domain of *Hs* Fdx are shown in gray highlights. Sequence numbering is given at the top. The start codon methionine residue added and is shown as the first M at the N-terminus of each peptide. Alpha-helixes and beta sheets regions, α′, α″, $\beta_1$ and $\beta_2$ are indicated below the related sequences. Only the first 20 N-terminus residues of D-PhgAT are shown in this figure.

2. Determination of in-vitro stability and solubility of modified D-PhgAT at the presence of different proportions of different inorganic salts and miscible organic solvents compared with non-modified wild type D-PhgAT.

# CHAPTER II
# LITERATURE REVIEW

Immemorial commercial utilization of biocatalysts, e.g., wine making, vinegar and dairy production, bread leavening, medical purposes and etc., has been connoted back to the very early epoch of human history and civilizations e.g., Codex of Hammurabi, ancient Rome, Greece and China [14]. Nowadays due to improved production technologies, engineered enzyme properties and new application fields, global demand for enzymes is expected to be over US$ 3.47 billion annually by 2015 according to a new report by Global Industry Analysts, Inc. [15]. However, due to the high cost of production, purification and storage, the impact of enzymes in applied fields is largely affected.

Intrinsic instability is one of the most critical obstacles which leads to difficulties in production, processing and storage of biocatalysts and is considered as a critical application and economic disadvantages. Another problem that can largely affect many fields in protein researches and industrial applications is related to the low solubility of proteins and high tendency of polypeptides for aggregation. Firstly, biochemical and biophysical studies e.g., structural analysis are suppressed by low solubility. In addition, low solubility and aggregation are major problems in the development of pharmacologically active proteins and peptides in spite of their good therapeutic potential. Many neurodegenerative diseases e.g., Alzheimer's, Parkinson's, and prion diseases are somehow related to the formation of polypeptide aggregates in CNS, therefore barricading polypeptide aggregation is considered as a pragmatic therapeutic strategy in dealing with such diseases [16].

## 2.1 Stability of proteins

During production, storage and applications, enzymes may largely be susceptible to deactivation. General protein denaturation is referred to the unfolding of

the native tertiary structure of a given protein (N) to a highly disordered polypeptide with misalignment key residues, namely unfolded state (U). As a result, denaturation may happen due to the lack of contribution of these key residues in functional and structural stabilizing interactions. Denaturation could be either reversible or irreversible. In reversible denaturation upon excluding of denaturizing agents from reaction medium, denaturation permanently could be revoked, while in case of irreversible denaturation a given protein might loss its activity as a result of chemical changes, highly disordered structures and random coils formation, aggregation and production of inactive monomers [17].

The native structure of a protein is maintained mainly by non-covalent hydrophobic and electrostatic interactions. Hydrophobic interactions affect non-polar groups, while electrostatic interactions exert on charged residues. As a general definition, protein stability refers to the propensity of the protein to retain its native functional folded state against physical, chemical and biological denaturizing agents (Table 2.1) [18]. However, researchers may use different explanation for "protein stability" since this term has been evolved over time to have different meanings. The length of the time that a given protein remains active at a given denaturizing condition or the propensity of a given protein to unfold in the presence of a given denaturizing agent are two examples of different meanings of protein stability. In this regard, the propensity of proteins to retain their native and functional folded states against denaturizing agents is referred to thermodynamic stability, while the length of time that a protein remains active in a given denaturizing condition is referred to kinetic stability [19]. Both thermodynamic and kinetic stability could be illustrated in following equation:

$$N \leftrightarrow U \leftrightarrow I$$

Where $N \rightarrow U$ refers to thermodynamic stability and $N \rightarrow I$ refers to kinetic stability. According to Lumry-Eyring [20], enzyme inactivation is happening at least in a two steps manner: 1) Unfolding of the native structure of enzyme, which could be reversible (thermodynamic inactivation) due to disruption of responsible interactions for maintaining of native structure of protein. 2) Irreversible aggregation and covalent change of enzyme (kinetic inactivation).

While inactivation of most monomeric enzymes firstly starts with changes in their tertiary structures, in multimeric enzymes first inactivation step is subunits dissociation and follow series of reactions e.g., , denaturation of ternary or secondary structures, aggregation, coagulation, chemical decompositions and proteolysis [21]. Compared with monomeric proteins, multimeric enzymes are naturally more stable due to their rigid structures, reduced surficial accessible area and simpler quaternary structures. In multimeric proteins, subunit-subunit multi-interactions increase rigidity as a result of decreased mobility of groups which are involved in interactions, thus extreme thermal stabilization may achieve due to protein oligomerization. However, under certain conditions, these subunit-subunit interactions can be weakened and result to dissociation of subunits and consequent inactivation of enzymes is presumptive. Nowadays the development of methodologies in order to stabilize these complex structures with multiple subunits and cofactors are liable to quest [21]. A deep understanding of the mechanisms of inactivation of enzymes and possibility of reversible reactions could be helpful to control stability, deactivation and catalytic properties of enzymes.

**Table 2.1** Protein denaturizing agents, their targets and end products, modified from [18].

| Denaturizing agents | Target | End product |
|---|---|---|
| **Heat** | Hydrogen bonds | Highly disordered structure and aggregates |
| **Cold** | Hydrophobic bonds and solvate groups | Aggregates and inactive monomers |
| **Mechanical forces** | Solvate groups and void volume | Highly disordered structure and inactive monomers |
| **Radiation** | Functional groups e.g., cysteine and peptide bonds | Highly disordered structure |
| **Proteases** | Peptide bonds | Oligopeptides and amino acids |
| **Acids** | Buried uncharged groups e.g., histidine and peptide groups | Random coil |
| **Alkali** | Buried uncharged groups e.g., tyrosine, cysteine | Random coil |
| **Organic Hydrogen bond formers** | Hydrogen bonds | Random coil |
| **Salts** | Polar and non-polar groups | Highly disordered structure |
| **Solvents** | Non-polar groups | Highly disordered peptide with large helical regions |
| **Surfactants** | Hydrophobic domain (all surfactants) and charged groups (ionic surfactants) | Incompletely disordered structures with large helical regions |
| **Oxidants** | Functional groups e.g., cysteine, methionine and tryptophan. | Inactivated enzyme, disordered structures |
| **Heavy metals** | Functional groups e.g., cysteine and histidine | Inactivated enzyme |
| **Chelating agents** | Cations important for structure or function | Inactivated enzyme |

### 2.1.1 Techniques for stabilization of enzyme

#### 2.1.1.1 Screening for intrinsically stabilized enzymes

Extremophiles are the best choice for this approach with their interesting and unique capability to survive in hostile environments and habitats.

Classification of extremophiles is based on noxious and extreme conditions of their lodgings. Table 2.2 shows some examples of extremophiles and their natural habitats.

**Table 2.2** Some examples of extremophiles and their natural habitats, modified from [22 and 23].

| Factors | Condition | Natural habitat | Example species |
|---|---|---|---|
| **Salt** | > 6% | Salterns, salt brines | *Halobacterium* sp., *Haloferax* sp. |
| **pH** | pH below 5 | acidic mine drainage | *Thiobacillus* sp. |
| | pH above 9 | Soda lakes | *Bacillus* sp. |
| **Temperature** | -2.5 – 0 °C | Arctic and Antarctica | *Flavobacterium* sp. |
| | 0 – 4 °C | Marine environments | *Pseudomonas* sp. |
| | 65 – 95 °C | Hydrothermal springs | *Thermus* spp. |
| | >100 – 121 °C | Black smokers | *Thermococcus barophilus* |
| **Pressure** | 500 - 1034 atm | Marine trenches | *Moritella yayanosii* |
| **Radiation** | 3 – 5 M rad [1] | Nuclear plants | *Deinococcus radiodurans* |
| **Hyperacceleration (extreme gravity)** | Up to 403627 *g* [2] | In vitro, useful for astrobiology studies | *Paracoccus denitrificans* |

These organisms are subjected to immense studies in recent decades and considered as promising sources of highly stable enzymes known as “extremozymes”. The main character of extremozymes and so called extreme proteins is their stability and function under very precluding and detrimental conditions where other proteins cannot withstand. Due to these outstanding properties, extremozymes are considered as excellent biocatalysts in some biotechnological and industrial processes which demand harsh conditions, e.g., high or low temperature, extreme pH and high ionic strength [24]. Table 2.3 shows some recent examples of extremophilic enzymes and the related producing organisms.

[1] Lethal dose for *Homo sapiens* is 0.0001 M rad
[2] *g* force for planet Earth is 1

**Table 2.3** Shows some recent examples of extremophilic enzymes and the related producing organisms, optimal temperature and pH and stability, modified from [25].

| Microorganisms | Extremoenzyme | $T_{opt}$ / °C | $pH_{opt}$ | Stability |
|---|---|---|---|---|
| **Hyperthermophiles** | | | | |
| *Alicyclobacillus acidocaldarius* | Endoglucanase (CelB) | 80 | 4.0 | Stable at pH=1–7, retains 60% activity after 1 h at 80 °C |
| *Methanococcus jannaschii* | α-Amylase | 120 | 5-8 | Stable against denaturants |
| *Pyrobaculum calidifontis* | Carboxylesterase | 90 | 7.0 | ½ life: 2 h at 100 °C |
| *Pyrococcus furiosus* | Chitinase a and b | 90-95 | 6.0 | NA |
| *Pyrodictium abyssi* | Xylanase | 105 | 6.0 | ½ life: 100 min at 105 °C |
| *Rhodothermus marinus* | Amylase | 85 | 6.5 | ½ life: 3 h at 85 °C |
| | Pullulanase | 80 | 6.5-7 | 30 min at 85 °C |
| | α-L-Arabinofuranosidase | 85 | 5.5-7 | 8.3 h at 85 °C |
| | β-Mannanase | 85 | 5-6.5 | 45.3 h at 85 °C |
| *Sulfolobus solfataricus* | Xylanase | 100 | 7.0 | ½ life: 47 min at 90 °C |
| | α-Glucosidase | 120 | 4.5 | Highly thermostable (whole cells used) |
| | Trehalosyl ransglucoylase | 75 | 5.0 | Stable at pH=4.5–11 after 2 h at 80 °C |
| *Sulfolobus shibatae* | α-Glucosidase | 98 | 5.5 | Retained 67% activity after 5 h at 80 °C |
| *Thermococcus litoralis* | L-Aminoacylase | 85 | 8.0 | ½ life: 25 h at 70 °C, 1.7 h at 85 °C |
| *Ralstonia* sp. A-471 | Chitinase | 70 | 5.0 | NA |
| *Thermococcus chitonophagus* | Chitinase | 70 | 7.0 | ½ life: 1 h at 120 °C |
| *Thermoplasma acidophilum* | Glucoamylases | 90 | 2.0 | ½ life: 24 h at 90 °C |
| *Picrophilus torridus* | Glucoamylases | 90 | 2.0 | 24 h at 90 °C |
| *Picrophilus oshimae* | Glucoamylases | 90 | 2.0 | 20 h at 90 °C |
| **Psychrophiles / psychrotolerant** | | | | |
| *Acinetobacter* sp. strain no. 6 | Novel esterase | 50 | 7.8 | Lost 75 % activity at 40 °C in 30 min |
| | Lipase | 20 | 7.0 | ½ life: 30 min at 50 °C |
| *Arthrobacter* sp. C2-2 | β-Galactosidase | 40 | 7.5 | ½ life: 8 min at 50 °C, stable after 4 h at 40 °C |
| *Arthrobacter* sp. strain TAD20 | Chitinase | NA | NA | NA |
| *Bacillus, Clostridium, Actinomycetes* | α-Amylase | NA | NA | NA |
| *Cytophaga, Flexibacter, Bacteroides* | β-Galactosidase | NA | NA | NA |

NA: not available

**Table 2.3** Shows some recent examples of extremophilic enzymes and the related producing organisms, optimal temperature and pH and stability, modified from [25], Cont.

| Microorganisms | Extremoenzyme | $T_{opt}$ / °C | $pH_{opt}$ | Stability |
|---|---|---|---|---|
| *Pedobacter cryoconitis* sp. nov | Oxidase, catalase, | NA | NA | NA |
| | protease, amylase, | NA | NA | NA |
| | β-glucosidase, | NA | NA | NA |
| | β-galactosidase, | NA | NA | NA |
| | β-lactamase | NA | NA | NA |
| *Clostridium* strain PXYL1 | Filter paper cellulase | 20 | 5–6 | ½ life: 30 min at 40 °C |
| | Endocellulase | 20 | 5–6 | |
| | Xylanase | 20 | 5–6 | |
| *Cystofilobasidium larimarini* | Polygalacturonase | 40 | 5.0 | The enzymes were very |
| *Cystofilobasidium capitatum* | Polygalacturonase | 40 | 5.0 | unstable at 30–40 °C |
| *Cryptococcus macerans* | Polygalacturonase | 50 | 4.0 | |
| *Cryptococcus aquaticus* | Polygalacturonase | 50 | 4.0 | |
| *Cryptococcus adeliae* | Xylanase | 45–50 | 5.0 | ½ life: 78 min at 35 °C |
| *Cryptococcus cylindricus* | Pectinase | NA | NA | NA |
| *Mrakia frigida* | Pectinase | NA | NA | NA |
| *Cystofilobasidium capitatum* | Pectinase | NA | NA | NA |
| *Flavobacterium psychrophilum* | Metalloprotease | 24 | 6.5 | Lost all activity after 5 min at 40 °C |
| *Pseudoalteromonas haloplanktis* | Cellulase | NA | NA | NA |
| | Xylanase (family 8) | 25 | 5–8 | ½ life: 1.9 min at 55 °C |
| *Psychrobacter* sp. Ant300 | Esterase | 5–25 | 7–9 | 16 min at 40 °C |
| *sychrobacter okhotskensis* sp. nov | Lipase | NA | NA | NA |
| *Pseudomonas* strain DY-A | Alkaline protease | 40 | 10 | NA |
| *Bacillus* spp. | Subtilisin | 40–45 | 10–11 | Thermolabile |
| **Thermoalkaliphiles / alkaliphiles** | | | | |
| *Alkalimonas amylolytica* | Amylase | NA | NA | NA |
| *Streptomyces* sp. | Endocellulase | 50 | 8.0 | Retained 95 % activity at 50 °C for 30 min |
| *Bacillus firmus* | Xylanase | 70 | 5–9 | Retained 70 % activity after 16 h at 62 °C |
| *Bacillus halodurans* | Amylase | 55–65 | 10 | NA |
| | Pullulanase | 55–65 | 10 | NA |
| *Bacillus subtilis* | α-Amylase | 52–55 | 9.0 | Lost 60 % activity after 10 |
| *Bacillus* isolate KSM-K38 | α-Amylase | 55–60 | 8–9 | min at 95 °C, Resistant to chelating and oxidants reagents |
| *Nesterenkonia* sp. AL-20 | Alkaline protease | 74 | 11 | Highly stable against $H_2O_2$ |
| *Bacillus pumilus* | Alkaline protease | 50–60 | 11.5 | NA |
| *Arthrobacter ramosus* | Alkaline protease | 65 | 11 | NA |
| *Bacillus alcalophilus* | Alkaline protease | 65 | 10 | NA |

**Table 2.3** Shows some recent examples of extremophilic enzymes and the related producing organisms, optimal temperature and pH and stability, modified from [25], Cont.

| Microorganisms | Extremoenzyme | $T_{opt}$ / °C | $pH_{opt}$ | Stability |
|---|---|---|---|---|
| *Nocardiopsis* sp. | Keratinase | 70–75 | 11-12 | Stable below 60 °C for 10 min and pH=8 |
| *Pseudomonas* sp. LBA34 | Lipase | NA | NA | NA |
| *Halomonas* sp. LBB1 | Lipase | NA | NA | NA |
| *Bacillus* sp. | Azoreductase | 80 | 8–9 | NA |
| | Catalase-peroxidase | 60 | 8.0 | ½ life: 20 h at pH=9 and 60 °C |
| *Thermus brockianus* | Catalase | 90 | 8.0 | ½ life: 3h at 90°C |
| *Bacillus alcalophillus* | Pectate lyase | 45 | 9-10 | NA |
| *Thermomonospora* | Endocellulase | 50 | 5.0 | ½ life: 3 h at 70 °C |
| **Halophiles** | | | | |
| *Halothermothrix orenii* | α-Amylase | 65 | 7.5 | Tolerates up to 25 % NaCl, |
| *Bacillus dipsosauri* | α-Amylase | 60 | 6.5 | Optimum at 5 % |
| *Haloferax mediterranei* | α-Amylase | 50-60 | 7-8 | Stable at 2–4 M NaCl, Optimum at 3 M |
| *Halobacillus* sp. strain MA-2 | Amylase | 50 | 7.5-8.5 | Maximum stable at 5 % NaCl |
| Halophilic bacterium, CL8 | Xylanase 1 | 60 | 6.0 | Stable 7 min at 60 °C, Optimum at 4 M NaCl |
| | Xylanase 2 | 65 | 6.0 | Stable 192 min at 60 °C, Optimum at 4 M NaCl |
| *Halorhabdus utahensis* | β-Xylanase | 55-70 | NA | Optimum at 5–15 % NaCl |
| | β-Xylosidase | 65 | NA | Optimum at 5 % NaCl |
| *Pseudoalteromonas* sp. strain CP76 | Protease CPI | 55 | 8.5 | Tolerates 0–4 M NaCl, |

NA: not available

#### 2.1.1.2 Production of stable enzymes by genetically modified organisms

One major problem in isolation of extremophiles and production of extremozymes is their fastidious and slow growing nature. Due to this difficulty a more convenient approach is cloning of extremozymes genes from extremophiles and expression of them in mesophilic hosts which is a great advantage in production of extremozymes. For instance, a *p*-nitrobenzyl esterase has been evolved by random mutagenesis and direct evolution which showed 16 folds higher catalytic efficiency compared to wild type loracarbef nucleus *p*-nitrobenzyl ester [26].

#### 2.1.1.3 Protein engineering and modification of existing mesophilic enzymes

In the past few decades, there have been reports of proteins being stabilized by introducing mutations. These include reports ranging from mutations of small enzymes e.g., T4 lysozyme [27] and barnase [28] to protein designing and directed evolution. Many strategies for protein stabilization have been proposed e.g., entropic stabilization by introducing prolines or disulfide bridges that have been reported to manifest reasonable success rates. Comparative studies in direct evolution have shown that mutational strategies lead to high stability. Changing the amino acid sequence in a very limited number can significantly contribute to increase stability. For example, thermostability is a result of minor differences in amino acid sequences that confer a more rigid conformation or a higher number of hydrophobic interactions [29]. PST-01 protease has very similar amino acid sequence to that of the thermolysin (33% primary structural homology). The only difference is the presence of disulfide bonds in PS-T01 protease which is absent in thermolysin. Interestingly, PST-01 protease manifests similar thermostability to that of the thermolysin but its organic solvent stability is much higher [30]. Despite these achievements no general strategies for converting mesophilic enzymes into extremozymes enzymes have been emerged yet.

#### 2.1.1.4 Chemical modification of enzymes

The interesting feature of chemical stabilization of protein macromolecules, unlike the other available methods for redesigning of enzymes structures and functions, is not only limited to the abundance of 20 amino acids but also permit unlimited alterations of amino acid side chain structures. One approach of chemical modification could be done with derivatives of amino acids, acylated proteins, alkylated proteins and proteins with miscellaneous substituents. For example one of the general approaches to thermostabilization is the replacement of lysine or histidine residues with arginine that results in enhanced intramolecular or inter-subunit salt bridges. This can be done by chemically amidation and guanidination e.g., acetamidination that can significantly exalt the enzymes thermostabilization [18]. Fatty acids and amphipathic polymers e.g., PEG can be applied in order to increase stability of enzyme under conditions of elevated temperature, alkaline pH and

presence of anionic surfactants [31]. One example of this approach is modification of subtilisin with octanoic acid and palmitic acid with increasing in stabilization about 15-fold at 45 °C and 2.5-fold at 65 °C. A copolymer of PEG and maleic anhydride (PM) led to increasing in stability of lipase from *P. fluorescens* that is used in conversion of lauryl alcohol to lauryl stearate in trichloroethane as solvent. Some merits of using PEG or PM for modification of enzymes are reverse hydrolysis, high efficiency in catalysis of hydrophobic substrates as well as stereospecific synthesis in hydrophobic media [32]. Cross-linking is another approach in chemical modification. Agents that generally used for this modification are glutaraldehyde, diimidates, disulfonylchlorides and etc. Ribonuclease cross-linking with dimethylsuberimidate enhanced its rigidity and consequently its thermostabilization [18]. Temperature, pH and organic solvent stability of penicillin acylase increased as a result of increasing of rigidity of this enzyme via modifying of its amine groups with glutaraldehyde [33]. Grafting of enzymes with some biological molecules e.g., glycoproteins is shown to increase enzymes stability against proteolysis, heat, storage and chemical denaturants, which is assumed to be due to the carbohydrate domain of glycoproteins. For example, glycosylated bovine pancreatic protease, α-chymotrypsin, was noticeably resistant to thermal inactivation after 3 h incubation at 50 °C compared to unmodified native control which was largely suffered in this condition [34].

#### 2.1.1.5 Immobilization

One of the most used and preferred strategies to improve stability of an enzyme is immobilization on solid carriers which is helpful to achieve enhanced operation control, more convenience recovery of products with minor contamination by catalysts, reduced inhibition by products and flexibility of reactor design. In this case stability is the result of molecular rigidity which is introduced by attachment of enzyme to a rigid support and formation of a protected microenvironment [35]. Currently four main practical methods of immobilization are used widely: (a) adsorption, (b) covalent binding, (c) entrapment and (d) membrane confinement. A suitable immobilization method for any enzyme could be selected according to enzyme topology, active site orientation, reaction medium compatibility, operational cost and stability of enzymes. For example, highly activated glyoxyl agarose beads have been applied for immobilization of catechol 2,3-dioxygenase

enzyme from *Bacillus stearothermophilus* with 700-fold increase in stabilization factor compared with free enzyme [36]. In some cases, it is necessary to genetically modify the surface of a given protein to create proper groups in order to enhance interaction with the immobilization support. For example surface of a cysteine-free protease from *B. stearothermophilus* was modified via site-directed mutagenesis to introduce cysteine residues in different positions. This mutant enzyme then was immobilized via sulfhydryl groups of cysteine residues on an activated Thiol-Sepharose. It was shown that binding of this enzyme via engineered cysteine residues at the positions between residues 56 and 69 noticeably increased thermal stability at 75 °C [37]. In another study, His tagged D-phenylglycine aminotransferase enzyme with a cysteine residue at C-terminus was successfully expressed in *E. coli* and then immobilized on Eupergit C 250 L resin. Soluble and immobilized enzyme showed similar activity based on effect of pH but higher thermal and storage stability was detected in case of immobilization [4]. Immobilization also can enhance stability of a given protein in organic solvents. For example, immobilization of α-chymotrypsin to polyacrylamide gel protects this enzyme from irreversible inactivation by both miscible (acetone, butanol, and DMF) and immiscible (heptane and cyclohexane) organic solvents at elevated temperatures up to 70 °C [38]. A fused protein consisting of a cellulose-binding domain (CBD) and horseradish peroxidase (HRP) was immobilized on cellulose beads showed 6 folds increase its half-life in aqueous-organic medium and enhanced stability in increasing concentrations of acetone (0 – 92%). There was a general decrease in activity of soluble enzyme as the solvent concentration in the mixture increased but the immobilized enzyme was, at all times, more active than the soluble enzyme [39].

#### 2.1.1.6 Addition of additives

One of the most used methods of enzyme stabilization is addition of additives, as a good approach toward enhancing enzyme storage stability. However due to incompatibility with the reaction system, some of these stabilizing additives may interfere with the final application of the enzyme. In addition, the concentrations required for stabilization may be unfavorable or economically unsuitable. Despite these unmerited properties, most of enzyme formulations are stabilized using additives, as it remains the oldest and most reliable stabilization

methods applicable in the enzyme marketing [40]. These additives can be categorized in following groups:

**1) Ligands as additives:** Binding of substrates and other ligands may lead to stabilization, increase in lability or may have no effect at all. In one study stabilization of lactate dehydrogenase was achieved via addition of substrates NAD, NADH and lactate [41]. Stabilization of enzyme by its both substrate and cofactor are also reported. Glucose-6-phosphate dehydrogenase was stabilized by its substrate glucose-6-phosphate and cofactor $NADP^{+}$ under both thermal and ultrasonic inactivation conditions [42].

**2) Salts as additives:** Two categories in study of stability upon adding salts are specific ion effects with concentrations less than 0.1 M and non-specific ion effects with concentrations more than 0.1 M. Thermolysin, a thermostable zinc protease from *B. stearothermophilus*, has four $Ca^{+2}$ ligands for asparagine and glutamine carboxyl groups. Bridging function of $Ca^{+2}$ have been shown to increase rigidity of this biomolecule leading to a higher stability. The main disadvantages of stabilization via divalent cations e.g., $Ca^{+2}$ is highly specificity of this method, so it is impossible to use this method as a general stabilization strategy. In case of non-specific ion effects, ions bind to charged groups of protein or dipoles and this could lead to salting out effect and consequently results in compaction and rigidity and increasing of the enzyme`s stability [40].

**3) Other possible additives:** Addition of sugars and polyols to solutions of a given enzyme can strengthen the hydrophobic interactions between non-polar amino acid residues. This can increase rigidity of protein and consequently elevates protein`s resistance to thermal deactivation. Stabilization effect of such compounds seems to be due to their positive effect on the medium`s water activity and a decrease in the possibility of microbial contamination. Some additives e.g., sorbitol, trehalose and glycerol have been reported to improve thermal stability and resistance against proteolysis of α-amylase of *B. licheniformis* and *B. amyloliquefaciens* [43]. In another experiment, lactate dehydrogenase has been protected from freeze–thawing damages by using solutes of very dissimilar chemical classes e.g., sugars, polyols, amino acids, methylamines, and salts. Preferentially exclusion of these solutes from contact with the protein surface is thought to be responsible for their cryoprotective behavior

[44 and 45]. Miscellaneous additive such as Tween 20 has been shown to be effectively stabilizing β-amylase in concentration of 0.05% (v/v); however, the stabilization mechanism is not fully understood. Addition of 0.02% (w/v) Triton X-100 to porcine pancreatic amylase was shown to stabilize this enzyme over a period of 3 h. It seems that stabilization occurs due to the binding of these miscellaneous additives to the protein and gives it an optimally folded and compact structure that gives enhanced stability and activity [46].

## 2.2 Solubility of proteins

Protein solubility is an important pre-requisite for many aspects of protein studies and industrial applications. Acquiring soluble proteins in sufficiently high concentrations has been considered as a major experimental challenge for decades [47]. Based on the physical definition of solubility of solutes in a given solvent, protein solubility could be defined as the amount of a protein that is completely dissolved in a solvent e.g., water, storage or reaction buffers under specific conditions and compositions of solvent e.g., pH and ingredients of medium; physical environmental factors e.g., temperature and pressure as well as the instinct properties of the given protein e.g., p*I* and hydrophobicity.

Different types of low protein solubility could be classified as low in-vitro and in-vivo protein solubility. The former one involves proteins that are expressed, purified, and folded at room temperature, but cannot be sufficiently and highly concentrated for further structural studies, general biochemical studies, pharmaceutical or industrial applications. The later one is a very common type of low protein solubility involves low solubility of recombinant proteins upon over-expression in an expression host. This type of problem is manifested by aggregation of over-expressed proteins in cells of expression hosts as formation of inclusion bodies that consequently results in low native protein yield [48].

Despite many motivating progresses in increasing protein solubility, many heterologously expressed proteins are insoluble and often solubilization is a trial and error process with relatively low success rate. Some of these progresses could be categorized in improving of protein solubility during heterologous expression e.g.,

weak promoters and low-temperature or modification of growth media, co-expression of proteins with molecular chaperons and fusion of proteins with solubility enhancing tags [47].

### 2.2.1 Techniques for increasing solubility of proteins

#### 2.2.1.1. Addition of additives

Additives have been developed to control protein properties such as folding, stability and aggregation. Some additives stabilize native fold, while the others destabilize or denature the protein structure. Addition of additives is one of the most successfully used strategies for increasing solubility of a given protein. For example 50 mM L-arginine and L-glutamic acid have been used successfully to significantly increase protein solubility of several proteins. The proposed possible mechanism is the interaction of charged free amino acids with the opposite charges located on the surface of the protein, while the hydrophobic parts of the free amino acids will interact with adjacent exposed hydrophobic surface of the protein and mask it [49].

#### 2.2.1.2 Fusion of soluble peptide tags

The other possible technique for increasing protein solubility can be achieved via fusion of soluble peptides or proteins to a target protein of interest. The solubility of amino acids range widely, from a few score micromolar to several hundred millimolar, which presents a primitive technical hurdle, among many others, for the construction of a solubility propensity scale, because such a wide range of values is difficult to measure accurately with a single protocol. Peptide sequences consisting of a single amino acid type (poly-amino-acid peptides) can be useful in partly overcoming this problem, because they tend to amplify the adhesive, aggregation, polymerization, and solubility properties of the amino acids. For example, fusion of the acidic tail of synuclein (ATS) peptide [50] to three different therapeutic proteins (human growth hormone, granulocyte colony-stimulating factor, and human leptin), significantly increased their solubility. The solubilizing effect of the ATS peptide is thought to be attributed to the nine acidic residues in this 22-residues peptide [51]. Recently, fusion of charged amino acids (short poly-Lys or

poly-Arg tags) to a bovine pancreatic trypsin inhibitor (BPTI) variant improved protein solubility by over six-fold [52].

#### 2.2.1.3 Genetically modification of surficial residues

Another strategy to increase solubility of protein is modification of residues on surface of protein, e.g., hydrophobic to hydrophilic mutations. This approach mainly is achievable via site-directed mutagenesis and replacement of surface hydrophobic residues with hydrophilic ones. This technique can be used successfully for proteins with known structure, otherwise it might be problematic. Other unmerited view of this approach is mutation of a buried hydrophobic residue to a hydrophilic residue since the solubility of the folded protein may not be affected. In addition conformational stability of the protein is prone to change upon exposure of buried hydrophilic residues to the solvent accessible surface area of protein [48]. Recently, fusion of short charged amino acids (short poly-Lys or poly-Arg tags) to a bovine pancreatic trypsin inhibitor (BPTI) variant, improved protein solubility by over six-fold [52].

In one study, sequence and structure alignments between human and murine leptin proteins led to identifying positions for hydrophobic to hydrophilic mutations that consequently increased human leptin solubility successfully. In another study N439D, Q444E double mutations were successfully applied on D-PhgAT enzyme in order to increase its in-vitro solubility [8], suggesting that this method should be usable to increase solubility of those proteins with available structural information.

## 2.3 Understanding effects of salts on protein stability

At late 19$^{th}$ century, Franz Hofmeister found that egg white proteins precipitate in high concentration of some salts. The solubility of these proteins was strongly dependent not only on the concentration, but also on the type (nature) of the salt used for the experiment. He described the salting-out and salting-in properties of some used salts in the so-called Hofmeister series (Figure 2.1). In this ranking, ions are classified as chaotropes and kosmotropes. The former group has destabilizing effect (salting-in) on proteins while later group has stabilizing effect (salting-out)

General phenomenology of kosmotropic/chaotropic nature of a solute maybe explained by two physical properties of solvent, e.g., water, namely ordered and disordered states [53]. One unique property of an aqueous medium is the ability of water to form strong inter-molecular hydrogen-bonded network, which could be extended and highly ordered in pure water (Figure 2.2).

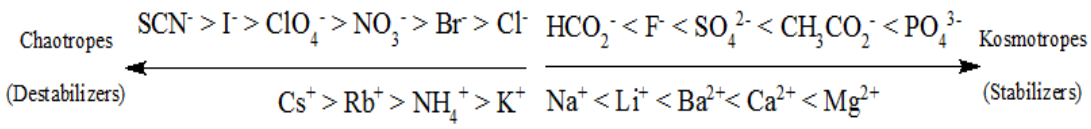


**Figure 2.1** Comparison of ion properties in the Hofmeister series.

Kosmotropic co-solvents interact with water molecules more than protein particles with non-polar surface, which leads to “preferential exclusion” from solvation shell of hydrophobic molecules. Hydrophobic effect of surficial non-polar amino acids is believed to be the major key of protein stabilization and folding driving force that protects and buries hydrophobic amino acids in the core of protein. As a consequence, proteins are pushed together to minimize exposed surface, results in stabilization but at the expense of protein flexibility, aggregation and precipitation. At the increased ionic strength, the protein stability raised but at the same time protein became more rigid. The catalytic activity of the enzyme strongly depends on structural flexibility. In highly saline conditions, halophilic proteins have to overcome many problems, e.g., they have to prevent aggregation and precipitation effects of salting-out by competing with salt ions for binding of water molecules. In addition protein flexibility, somehow, must be maintained at suitable levels for proper catalytic activity [54].

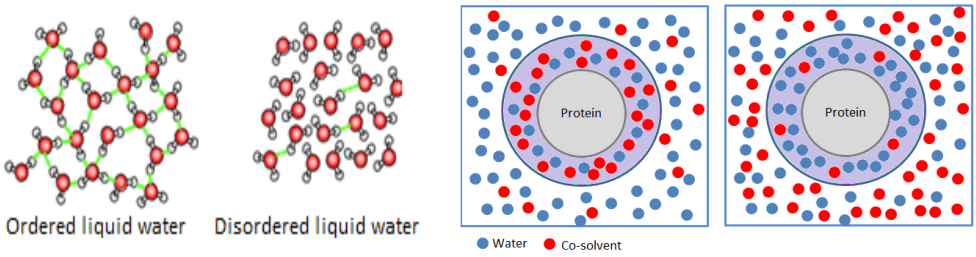


**Figure 2.2** Ordered and disordered structure of water (left panel), preferential phenomena in mixture of water and hydrophobic solute in the presence of chaotropic and kosmotropic co-solvents (right panel) [54].

In the presence of chaotropic co-solvents, disruption of water structure is energetically unfavorable. Thus the co-solvent molecules are pushed away from bulk water to shell region and even binding to protein, known as "preferential binding". Under this situation, smaller number of water molecules remains in the shell region and in contact with protein surface leading to weaker interaction between protein and water. These results in an increase in solvent accessible surface and consequently destabilization of hydrophobic aggregates, unfolding and denaturation of protein and lose of function.

## 2.4 Understanding the effects of low-water environments and organic solvents on protein stability

Halophilic microorganisms should be able to tackle long-term dryness and desiccations in their natural habitats. Isolation of a 250 million year old halotolerant bacterium from ancient salt crystals shows that halophilic organisms are able to survive in very little amount of water available in fluid inclusions in salt crystals [55]. In one study, the effect of dryness on the thermodynamic stability of halophilic malate dehydrogenase *Haloarcula marismortui* (*Hm* MDH) and its non-halophilic homologue from pig heart has been examined [56] Non-halophilic protein destabilized very fast but halophilic enzyme was resistance to desiccation. In fact in dry salt crystals and in saturated salt solution (~6 M NaCl), 90% and 15% of enzyme activity, respectively, have been recovered after 1 h incubation at 60 °C.

Adaptation to low water activity makes halophilic proteins resistant to desiccation. At room temperature $a_w$ values of saturated NaCl (~6 M) and KCl (~4.8 M) solutions are 0.75 and 0.84 respectively. It was assumed that at $a_w$ under 0.6, life is not possible, however, recently some forms of life have been observed in environments containing 5 M magnesium chloride [57]. Since halophilic proteins are evolved to be functional at low $a_w$; they are supposed to be stable and catalytically active in net organic solvents or in a water-organic solvent mixture as the reaction media. It may come to the mind that enzymes and other proteins denature and lose their native structure and activity when used in pure organic solvents. Actually this idea came from testing enzyme activity in aqueous-organic mixtures not in net organic solvents and it may be tempting to suppose that if proteins lose their native structure and activity in the former media, they may also suffer the same fate in the later media; and this has been shown to be wrong. The reason is that water acts as a molecular lubricant [58] thus, proteins are rigid in the absence of this lubricant. In aqueous-organic mixtures, both propensity [59] and conformational flexibility (due to water) are favorable for protein denaturation; while in pure non-aqueous solvents a greater propensity for denaturation of proteins is available, but the required flexibility for this process is absent.

In fact in organic solvents due to lack of involved water in hydrogen bonds, reduced dielectric constant and increased strong intra-protein electrostatic interactions, protein molecules are rigid and consequently enzyme activity drops. In this case introducing a small amount of water to enzyme non-aqueous reaction medium can raise enzyme activity. It is also reported that some organic solvents such as glycerol and ethylene glycerol (compatible solutes) are able to enhance enzyme activity because of multiple hydrogen bonds formation and mimic the water effect [59]. Some other reports emphasis enhanced enzyme activity in crown ethers and cyclodextrins. Introducing of organic chemicals such as dimethylformamide into the reaction mixture can make halophilic enzyme more stable in low salt conditions and also can prevent the corrosive effect of high NaCl concentrations .

Some of the most important benefits of using non-aqueous media include: limiting microbial contamination of reaction media and bioreactors, improving of enzyme thermodynamic stability, preventing unfavorable aqua-induced reactions such

as polymerization and hydrolysis, shifting of thermodynamic equilibrium of reactions that are not favorable in aqua and providing a medium for solubilization of hydrophobic substrates. The latter is in special important when poorly soluble or even insoluble compounds are desired to be used in pharmaceutical and fine chemical industries for the synthesis of chiral synthons and some intermediates [60].

In addition to water, enzyme activity in net organic solvents also depends on many other factors, for instance, pH memory. Since pH is an aqueous parameter, it has no meaning in net organic solvent. In fact the catalytic activity of the enzyme in organic solvent is a function of the pH in their last aqueous media; therefore after introducing into the next organic media, a given lyophilized enzyme keeps ionized state of its ionogenic (amino) groups. So, if the enzyme has been lyophilized from aqueous media with optimal pH, its activity in organic solvents can be much enhanced [61].

## 2.5 Lessons from nature: Salt tolerant proteins in halophiles

As previously mentioned in section 2.1.1.1, one of the techniques in finding stabilized proteins is screening of intrinsically stabilized proteins in extremophilic microorganisms. Since these microorganisms not only survive in their precluding habitats, but also cell divide and reproduce, they have been evolved to manifest different protein adaptation in a time line of millions of years of evolution. Amongst these microorganisms, halophiles with the ability to survive in high salt concentrations and in habitats with low water activity are considered as a good source for enzymes with high feasibility to cope with high ionic strength and presence of organic solvents. Some of these adaptation strategies are common amongst most of halophiles while some others are special for certain halophilic proteins.

### 2.5.1 Some of common salt-adaptation strategies of halophilic proteins and their amino acid signature

Many differences show up when halophilic and non-halophilic proteins are compared. One common feature of their constitutive proteins is biased negatively charged residues especially on their surface which manifest their low p*I* value

*Halobacterium salinarum*, which is the first extreme halophile with fully revealed proteome sequence, possesses an average theoretical p*I* value of 5.1. 2D-gel electrophoresis (Figure 2.3) confirmed that most of its cytoplasmic proteins have acidic properties and are resolvable in pH 3.5-5.5 [62].

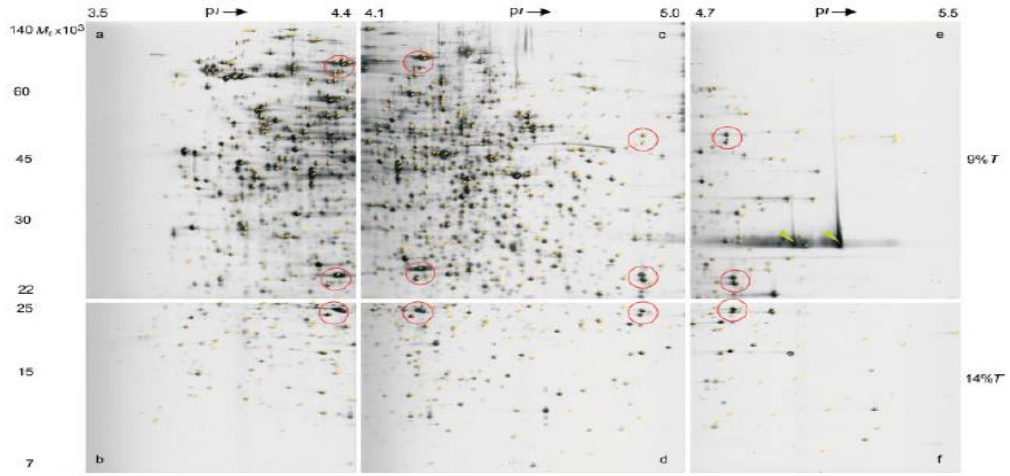


**Figure 2.3** 2-D reference map of *H. salinarum* proteome. The cytosolic proteins were separated on overlapping zoom gels, covering the p*I* range from 3.5–5.5 and stained with silver nitrate [62].

It has been shown that increased acidic residues (glutamic acid and aspartic acid) and decreased number of lysine residue on the surface of halophilic proteins are responsible for negative charge of the proteome and subsequently low p*I* value. In addition alanine, glycine and valine (small hydrophobic residues) are seen in higher numbers, but isoleucine, leucine, phenylalanine and methionine (large hydrophobic residues) are decreased. In some cases, threonine and serine (polar uncharged residues) are increased too. High numbers of aspartate and glutamate residues on the surface of protein which decrease protein's solvent-accessible area, was found to be the main mechanisms of haloadaptation [63].

Interestingly, a large number of extreme halophiles show high genomic G + C content around 60-70%. Some studies have shown a relationship between G + C content and frequency of amino acids. In one study to reveal the effect of nucleotide composition on amino acid composition, amino acid content has been

compared to dinucleotide sequences of the genome. The results revealed that the aspartic acid content of halophiles increased by three fold compared with non-halophiles. Consequently, in order to maintain the high G + C content (68%) of the genome, the frequency of alanine increased and that of the lysine decreased as the result of the "Dragging effect" from the need to increase aspartic acid. This seems to be the principal strategy that is used by halophiles to adapt their total proteomes to their favorable habitats [64]. Moreover, any single protein in halophiles must further be adjusted according to their specific tertiary structures by appropriate amino acid substitutions.

### 2.5.2 Specific salt-adaptation strategy halophilic 2Fe-2S ferredoxins

Monomeric halophilic 2Fe-2S ferredoxins from *H. marismortui* (*Hm* Fdx) and *H. salinarum* (*Hs* Fdx), have been shown to have two iron-sulphur clusters and, similar to other halophilic proteins, high surface acidic residues [65]. In addition, compared to non-halophilic counterparts, *Hm* Fdx and *Hs* Fdx possesses an extra N-terminus domain (two α-helixes) of 30 residues, 13 of which (~44%) are acidic (Figure 1.3). Two proposed halophilic adaptation mechanisms for these enzymes are halophilic substitution and halophilic addition; the former indicates high acidic residues on the surface (common adaptation) while the later mentions earning of an extra acidic domain.

Compared to wild-types of this enzymes variants, strains with mutation in *Hs* Fdx extra N-terminus domains defect in the reconstitution of iron-sulfur cluster. At least 2 M NaCl is required for reconstitution of iron-sulfur cluster in wild-type enzyme, whereas, the mutant enzyme is able to reconstitute in the absence of salt. These findings mention that extra N-terminal acidic domain is necessary for folding and stability of protein in the presence of salt [13]. Another study has shown that in low salt conditions, addition of polylysine could be effective in stabilizing of *Hs* Fdx [65], most likely because of salt bridges formation between polylysine and carboxyl groups on the protein surface and enhanced hydrophobic interactions. Insertion or even replacement of a short extra N-terminus domain is considered to be a fast halophilic adaptation mechanism for proteins that their genes have been adopted from

non-halophilic organisms, then proteins may acquire a better chance to stay and evolve in a halophilic host to acquire proper distribution of negative residues on their surface.

As previously mentioned in sections 2.1.1 and 2.1.2, techniques to increase stability and solubility of proteins could be categorized in three major groups e.g., A) Screening and isolation of enzymes from extremophiles, B) Protein engineering and genetically modification of mesophilic enzymes and C) Stabilization of proteins by methods such as chemical modification, immobilizing and medium engineering via introducing additives into storage or reaction media. Amongst these techniques, protein engineering and genetically modification of mesophilic enzymes are in center of interest in the past 20 years, in which proteins been stabilized by introducing mutations, however, only a limited number of mutations could lead to large increase in stability.

Here, based on the learning from nature, we introduce a new approach in protein engineering technique by fusion of two α-helixes and a hybrid of them from ferredoxin enzyme of halophilic archaeon, *Halobacterium salinarum*, into N-terminus domain of D-PhgAT protein to increase its solubility and stability in high salt concentrations and in the presence of organic solvent systems.

# CHAPTER III
# MATERIALS AND METHODS

## 3.1 Materials

### 3.1.1 Chemicals and reagents

All chemicals and reagents used in the current study were of analytical and molecular biology grade and obtained from Merck (Germany), Fisher Scientific (USA), Fluka (Switzerland), Sigma (Switzerland), GE Healthcare (Sweden), UBS (USA) and BD (France).

### 3.1.2 Instruments

The following instruments were used in current study: ÄKTA purifier (GE Healthcare, Uppsala, Sweden), Biofuge® *pico* Heraeus (Kendor, Germany), Centrifuge 5417R (Eppendorf, Germany), DarkReader™ (Clare Chemical Research, Dolores, USA), Ettan™ IPGphor™ (Amersham Bioscience, USA), FSIM-SPO 16 incubator shaker (Labcon, USA), Gene Amp® PCR System (Applied Biosystems, USA), Hελios α spectrophotometer (Spectronic Unicam, UK ), Innova®40 incubator shaker (New Brunswick Scientific, USA ), Libror AGE-220 balance (Shimadzu Co., Japan), Master cycler (Eppendorf, Germany), NanoDrop® ND-100 spectrophotometer (Thermo Scientific, USA), Mini-protein II Dual Slab Cell (BIO-RAD, USA), Rotina 380R refrigerated centrifuge (Hettich, UK), SevenEasy™ pH Meter S20 (Mettler Taledo, Switzerland), Sorvall® RC 5C Plus refrigerated centrifuge (Sorvall, USA), Sub-Cell GT MINI (BIO-RAD, USA), Thermomixer comfort (Eppendorf, Germany), TR-403 balance (Denver Instrument Company, Germany).

### 3.1.3 Soft wares and computer programs

The following scientific licensed or open source soft wares were used in the current study: ACD/ChemSketch (Ver 12.01), BioEdit (Ver. 7.0.5.3), ChemStation

for LC 3D systems (Ver B.04.01), Graphpad Prism 5 for windows (Ver. 5.04), EndNote X7 (Bld 7072), Plasm (Ver. 2.0.4.29), SeqCalc (Ver. 1.0), Unicorn controller (Ver. 5.11) and Vision Pro™ (Ver. 2.02) and Microsoft Office Professional plus 2013 package (Ver. 15.0.4420.1017).

### 3.1.4 Bacterial strains, plasmids, oligonucleotides and primers

Plasmid pET-17b carrying *dpgA* gene (PDB: 2CY8) was obtained from a previous study [3] and was used for construction of plasmid to be used in the current study. Optimized oligonucleotide sequences of $A_1$, $A_2$ and ALAL for expression in *E. coli* host were obtained from amino acid sequences of halophilic archaeon *Halobacterium salinarum* ferredoxin enzyme (*Hs* Fdx; PDB: 1E02_A) and ordered to synthesize by 1st base company (Thailand, Bangkok). *E. coli* XL-10 Gold (Stratagene) was used as cloning host while *E. coli* Tuner (DE3) pLysS (Novagen) was used as expression host. Plasmids and oligonucleotides were kept at -20 °C in sterile deionized water until use. *E. coli* strains were grown in Difco™ LB medium to $OD_{600}$ of 0.8 and kept at -80 °C with 15% (v/v) glycerol.

## 3.2 Methods

### 3.2.1 Construction of plasmids

In this study, plasmid pET-17b containing *dpgA* gene from previous study was used for fusion of $\alpha_1$ and $\alpha_2$ α-helixes ($A_1$ and $A_2$) and a hybrid of $\alpha_1$ and $\alpha_2$ and two loops between them (ALAL) at N-terminus of D-PhgAT protein. Amino acid sequences of these inserts obtained from ferredoxin enzyme of halophilic archaeon, *Halobacterium salinarum* are shown in Figure 1.3. Overall plan for plasmid construction is illustrated in Figure 3.1.

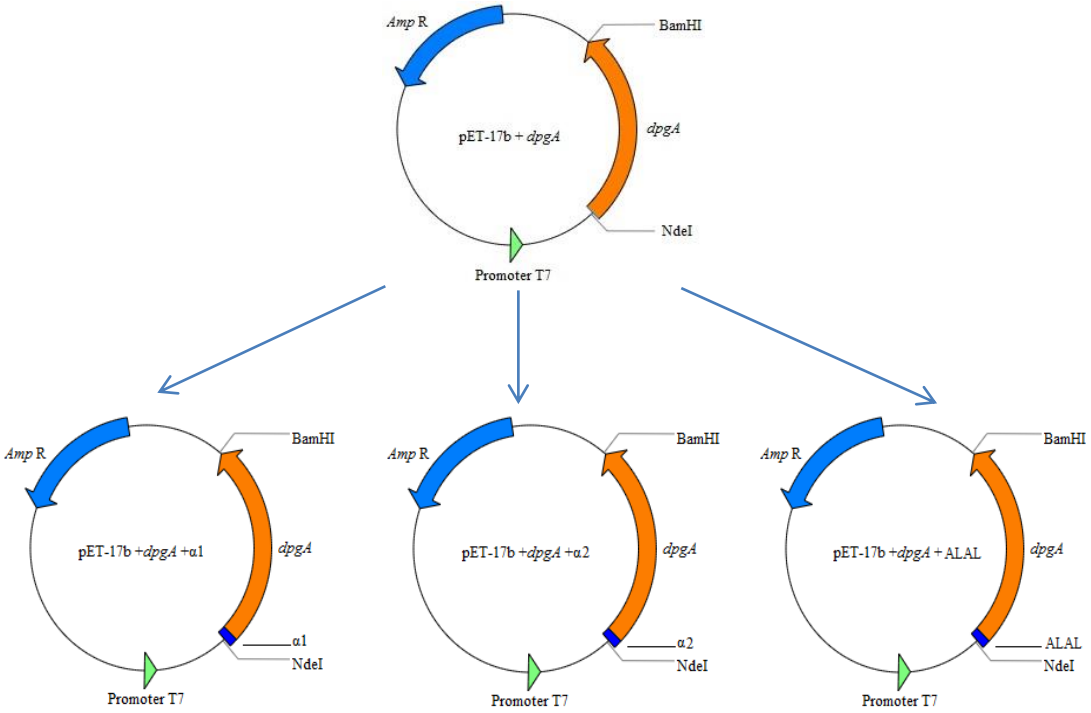


**Figure 3.1** Overall plan for plasmid construction and cloning of α1, α2 and ALAL inserts into pET-17b plasmid which carried *dpgA* gene.

### 3.2.1.1 Extraction of plasmid pET-17b carrying *dpgA* gene for ligation of $A_1$ and $A_2$ inserts

Plasmid pET-17b carrying *dpgA* gene was extracted from *E. coli* tuner (DE3) pLysS by QIAprep® Spin Miniprep Kit (QIAGEN) as follow according to the provided protocol by manufacturer: 5 mL of overnight culture of aforementioned strain of *E. coli* in Difco™ L.B medium contained 100 µg/mL ampicillin and 34 µg/mL chloramphenicol at 37 °C and 200 rpm, was centrifuged in 1.5 mL micro-centrifuge tubes at 13,000 rpm (16,060 *g*) for 1 min by using a desktop micro-centrifuge (Biofuge® *pico* Heraeus). Bacterial cell pellet then was re-suspended in 250 µL of buffer P1 (Re-suspension buffer, Appendix 10.1) containing RNase-A enzyme, then 250 µL of buffer P2 (Lysis buffer, Appendix 10.2) was added and mixed thoroughly followed by adding 350 µL of buffer N3 (neutralizing buffer, Appendix 10.3) and mixed immediately by inverting the tube 2-3 times and then centrifuged at 13,000 rpm (16,060 *g*) for 10 min. Supernatant then was applied to QIAprep spin column and centrifuged at 13,000 rpm (16,060 *g*) for 1 min, flow-through was

discarded. 500 µL of buffer PB (binding buffer) was added to the spin column and centrifuged at 13,000 rpm (16,060 g) for 1 min followed by discarding the flow-through. 750 µL of PE buffer (washing buffer) was added to spin column and centrifuged for 1 min at 13,000 rpm (16,060 *g*), flow-through was discarded and the spin column was centrifuged again for an additional 1 min to remove any residual washing buffer. To elute the plasmid DNA the spin column was placed in a clean sterile 1.5 mL micro-centrifuge tube and then 50 µL of 70 °C pre-heated sterile deionized water was added to the center of spin column. The spin column then was incubated for 5 min at room temperature followed by centrifugation for 1 min at 13,000 rpm (16,060 *g*). Eluted plasmid DNA was checked for purity and concentration by using a NanoDrop® ND-1000 spectrophotometer and then kept at -20 °C until use.

#### 3.2.1.2 Determination of concentration and purity of plasmid DNA

DNA concentration was determined by UV absorbance at wavelength of $260_{nm}$ ($A_{260}$) by using a NanoDrop® ND-1000 spectrophotometer. The ratio of absorbance at wavelengths $260_{nm}$ and $280_{nm}$ ($A_{260}/A_{280}$) indicates DNA purity that should be in the range between 1.8 and 2.0. Plasmid DNA was kept at -20 °C until use.

#### 3.2.1.3 Digestion of plasmids with restriction enzyme, *Nde*I

Single digestion of plasmids was performed by *Nde*I restriction enzyme (New England Biolabs) at 5′ end of *dpgA* gene. Generally, 1 µg of plasmid DNA, 5 µL 10X buffer 4, 10 units of *Nde*I restriction enzyme and sterile deionized water to a final volume of 50 µL were mixed together in a 1.5 mL micro-centrifuge tubes and gently finger taped and then was incubated at 37 °C in order to 3 h for full digestion. After incubation, restriction enzyme was inactivated by heating the reaction mixture at 65 °C for 20 min. Digested plasmids were subjected to dephosphorylation by Antarctic phosphatase at 5′ ends as is described in 3.2.1.4.

#### 3.2.1.4 Dephosphorylation of digested plasmid vector

Self-ligation of plasmid was nullified by 5′ dephosphorylation of plasmid with Antarctic phosphatase enzyme (New England BioLabs). Appropriate amount of 10X Antarctic phosphatase buffer was added to digest plasmid to a final

concentration of 1X followed by adding 5 units of Antarctic phosphatase enzyme and incubation at 37 °C for 1 h. The restriction enzyme was inactivated by heating at 65 °C for 5 min. Digested and dephosphorylated plasmid was run on agarose gel, stained with CYBR® Gold nucleic acid gel stain (Invitrogen), visualized with blue light DarkReader™ trans-illuminator (Clare Chemical Research) and purified by GFX™ PCR DNA and Gel Band Purification Kit (GE healthcare, UK).

**3.2.1.5 Agarose gel electrophoresis**

One percent of low melting temperature agarose (V*i*vant*i*s biochemical) was prepared in 0.5X TBE buffer (Appendix 2.2). Firstly, 5 µL of DNA samples were mixed with 1 µL of 6X DNA loading buffer (Fermentas) and then loaded into wells of 1% agarose in a BIO-RAD Mini-sub Cell GT electrophoresis cell. Electrophoresis was performed at 100 V by using an EC 135-90 Electrophoresis power supply for 1 h.

**3.2.1.6 Visualization of DNA bands in agarose gel**

After electrophoresis accomplished agarose gel was agitated in 0.5X TBE buffer containing 1X CYBR® Gold nucleic acid gel stain (Invitrogen) for 30 min with slow agitation (35 rpm) at room temperature. Blue light was used to illustrate DNA bands by using a DR-46B dark reader transilluminator (Clare chemical research).

**3.2.1.7 Purification of DNA bands**

Correct bands were cut by using a sharp sterile scalpel blade and transferred to sterile 1.5 ml micro-centrifuge tubes and used as material for purification of plasmid DNA by using GFX™ PCR DNA and Gel Band Purification Kit (GE healthcare, UK) according to manufacturer manual. Then 10 µL of buffer 1 (capture buffer) per each 10 mg of agarose slice was added to the tube and mixed by inverting and followed by incubation at 60 °C until agarose completely dissolved. Then sample-capture buffer mixture was loaded into GFX column followed by incubation for 1 min at room temperature. Centrifugation performed at 13,000 rpm (16,060 *g*) for 30 sec and flow-through was discarded. Then 500 µL of buffer 2 (washing buffer) was added to the GFX column and centrifuged for 30 sec at 13,000 rpm (16,060 *g*). Elution of DNA was performed by adding 50 µL of 70 °C pre-heated sterile deionized water to the center of the column. The GFX column was incubated at

room temperature for 5 min followed by centrifugation for 1 min at 13,000 rpm (16,060 *g*). DNA concentration was determined by using NanoDrop® ND-1000 spectrophotometer as previously described (Section 3.2.1.2). The purified DNA was used for ligation or kept at -20 °C until use.

**3.2.1.8 Extraction of plasmid pET-17b carrying *dpgA* gene for ligation of ALAL insert**

Plasmid pET-17b carrying *dpgA* gene was extracted from *E. coli* tuner (DE3) pLysS carrying the *dpgA* gene by QIAprep® Spin Miniprep Kit (QIAGEN) as described before (Section 3.2.1.1). Extracted plasmids were subjected to digestion with *Nde*I restriction enzyme as described before (Section 3.2.1.3). The only difference is using of NEB buffer 2 instead of NEB buffer 4. *Nde*I is supplied with NEB buffer 4, but also has 100 percent activity in NEB buffer 2. The reason for this substitution of buffers is the next step of preparation of plasmid vectors for ALAL ligation that end-filling of vectors with T4 DNA polymerase is incumbent. T4 DNA polymerase has 100 percent activity in NEB buffer 2 and in the presence of BSA. So in order to minimize one step of purification of DNA after digestion, NEB buffer 2 was used instead of NEB buffer 4.

**3.2.1.9 End-filling of *Nde*I digested plasmid pET-17b for ligation of ALAL insert**

After digestion of plasmid pET-17b with *Nde*I restriction enzyme and heat inactivation at 65 °C, digested DNA was cooled down in room temperature for 30 min and then was kept on ice for the next step that is end-filling with T4 DNA polymerase (New England BioLabs) in order to prepare blunt-end vector. To achieve end-filling of vector, BSA was added to the reaction mixture to the final concentration of 100 µg/mL and then dNTP mix was added to 100 µM final concentrations followed by adding 1 unit of T4 DNA polymerase per microgram of DNA. The reaction mixture was incubated exactly at 12 °C for exactly 15 min. The temperature of the reaction maintained at 12 °C by using Gene Amp® PCR System 9700 (Applied Biosystems). To stop the reaction, EDTA was added to a final concentration of 10 mM and followed by heating at 75 °C for 20 min. The DNA was loaded on 0.5% agarose gel and electrophoresed for 1 h as described above (Section 3.2.1.5). DNA bands were illustrated by CYBR® Gold nucleic acid gel stain (Section

3.2.1.6) and correct band was cut and purified by GFX$^{TM}$ PCR DNA and Gel Band Purification Kit to remove EDTA (Section 3.2.1.7). Then purified DNA was subjected to dephosphorylation as described above (Section 3.2.14). Digested, end-filled and dephosphorylated vector was used as material for ligation with ALAL insert.

### 3.2.2 Preparation of inserts

Sequences of $A_1$ and $A_2$ and ALAL DNA inserts used in this study were obtained from amino acid sequence of *Halobacterium salinarum* ferredoxin enzyme and optimized with online codon optimizer software [66] then ordered to synthesize by 1$^{st}$ base company, Thailand. $A_1$ and $A_2$ oligonucleotides were ordered and synthesized as single stranded DNA with 5′-phosphate modification and compatible sticky ends for ligation with *Nde*I digested vectors. $A_1$ and $A_2$ double stranded DNA inserts were made according to annealing protocol (New England Biolabs) as describe in section 3.2.2.1. ALAL DNA was ordered and synthesized as half-length single stranded sequence with 5′-phosphate modification and 18 overlapping complementary nucleotides. Then a complete set of ALAL double stranded insert was made by a single step extension with *pfu* DNA polymerase as described in section 3.2.2.2.

#### 3.2.2.1 Annealing protocol for preparation of $A_1$ and $A_2$ inserts

Annealing protocol for preparation of $A_1$ and $A_2$ inserts was performed by using a gradient PCR machine (Mastercycler gradient, Eppendorf). Equal amounts of each complementary sequence of $A_1$ or $A_2$ were added to sterile deionized water to a final volume of 100 µL in a 500 µL PCR tube. Then this mixture was heated up to 95 °C for 2 min, followed by a ramp cooling down to 25 °C over a period of 46 min (~ 1.5 °C per min). The resulted double stranded DNA inserts were kept on ice until used in ligation.

#### 3.2.2.2 Single step extension of ALAL insert with *pfu* DNA polymerase

As previously described, ALAL insert was synthesized as two half-length sequences with a short 18 nucleotides complementary sequence. Double stranded and full length ALAL sequence was synthesized via a single step extension (one cycle) by *Pfu* DNA polymerase (Table 3.2 and Figure 3.3). The products were

run on 1.7% agarose and DNA bands were illustrated by CYBR® Gold nucleic acid gel stain (Section 3.2.1.6). The correct band was cut and purified by GFX™ PCR DNA and Gel Band Purification Kit (Section 3.2.1.7). The DNA concentration determined by using a NanoDrop® ND-1000 spectrophotometer as previously described (Section 3.2.1.2) and used for ligation or kept at -20 °C until use.

**Table 3.1** Oligonucleotides used in the current study to prepare inserts.

| **Oligonucleotides name** | **Sequence (5′→ 3′)** |
|---|---|
| **$A_1$ Sense** | P~T**ATG**GGCTACGAAACCCTGGACGACCAGGG |
| **$A_1$ Anti-sense** | P~TACCCTGGTCGTCCAGGGTTTCGTAGCCCA |
| **$A_2$ Sense** | P~T**ATG**GGCCTGTTCGAAAAAGCGGCGGACGCGGG |
| **$A_2$ Anti-sense** | P~TACCCGCGTCCGCCGCTTTTTCGAACAGGCCCA |
| **ALAL Upper strand** | P~**TG**GGCTACGAAACCCTGGACGACCAGGGTTGGGACATGGACGACGACGACCTGTTC |
| **ALAL Lower strand** | P~CCGTCTTCACCGTCCAGACCCGCGTCCGCCGCTTTTTCGAACAGGTCGTCGTCGTC |

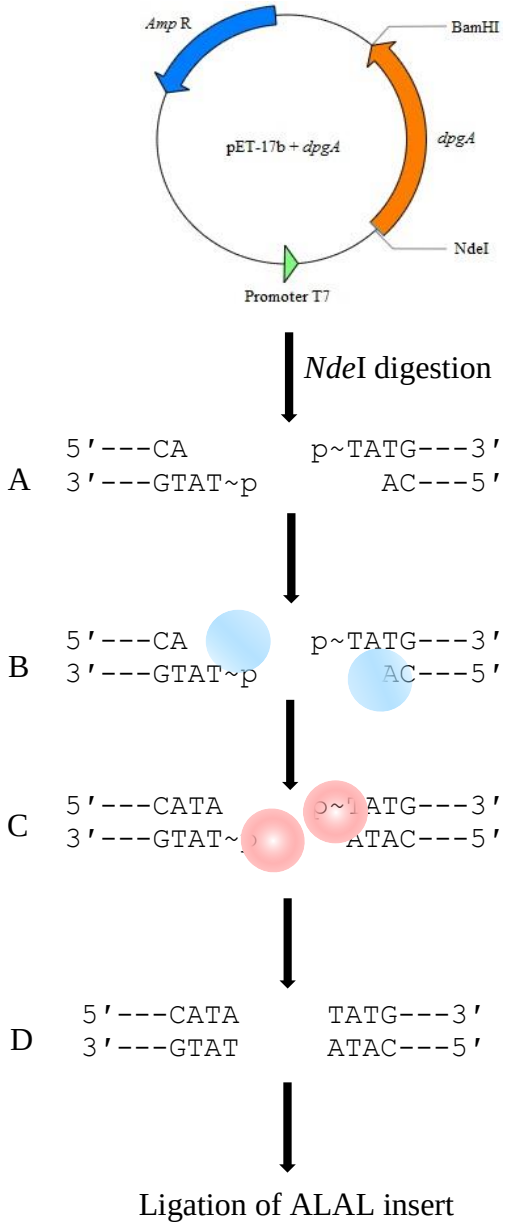


**Figure 3.2** Steps in preparation of plasmid vector of ligation of ALAL inserts. Plasmid digestion by *Nde*I (A), end-filling of digested plasmid by T4 DNA polymerase (B), dephosphorylation of plasmid by Antarctic phosphatase (C), resulting blunt ended and dephosphorylated plasmid (D) was used for ligation of ALAL inserts with T4 DNA ligase.

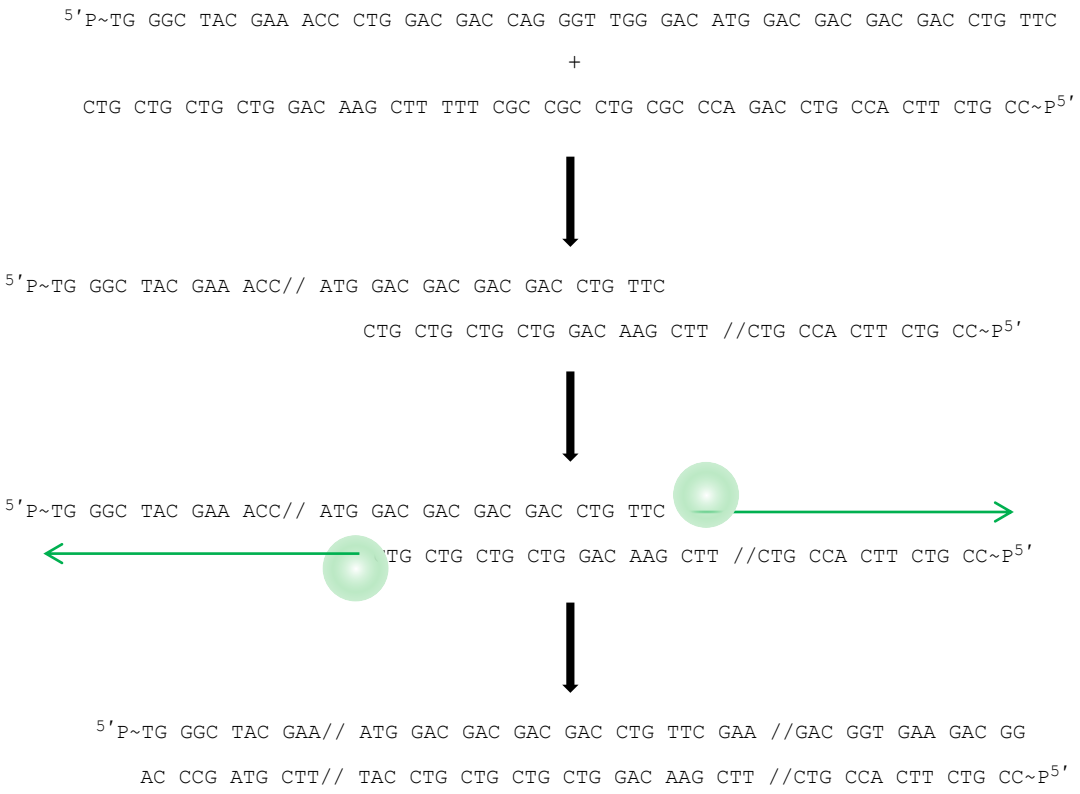


**Figure 3.3** Steps in preparation of ALAL insert. ALAL insert synthesized as two half-length ss DNA (upper and lower strands) with 18 nucleotides length overlapping complementary regions (blue) and 5′ phosphate modifications. Then one step extension by *pfu* DNA polymerase (green circles) was used to synthesize the full-length ds ALAL insert. Newly synthesized sequences are shown in green color. The resulted double stranded ALAL insert then was used for ligation.

### 3.2.3 Ligation

Ligation of $A_1$ and $A_2$ inserts into vectors was performed in 1:1 and for ALAL in 1:3 of vector-insert molar ratio. The amount of insert was calculated for ligation with 100 ng of vector by the following equation:

$$\text{ng of insert} = \frac{\text{ng of vector} \times \text{kb size of insert}}{\text{kb size of vector} \times \text{molar ratio of (insert / vector)}}$$

Appropriate amounts of vector, insert DNA, T4 ligase 10X buffer, 1 unit of T4 ligase enzyme (New England BioLabs) and nuclease free sterilized water mixed together to 20 µL final reaction mixture volume. The reaction mixture was incubated at 16 °C for 16 h. After incubation was finished, the reaction mixture was chilled on ice and 5 µL of ligation products was used for transformation of 100 µL competent cells by the heat shock method (Section 3.2.4.2).

**Table 3.2** Conditions for single step extension with *pfu* DNA polymerase for preparation of ALAL insert.

| **Steps** | | **ALAL** |
|---|---|---|
| **Initial denaturation** | | 95 °C – 2 min |
| **1 Cycle** | **Denaturation** | 95 °C – 30 sec |
| | **Annealing** | 51 °C – 1 min |
| | **Extension** | 72 °C – 5 min |
| **Final extension** | | 72 °C – 5 min |
| **Store** | | 4 °C – ∞ |

### 3.2.4 Transformation of cloning host

*E. coli* XL-10 Gold was used as cloning host in this study. Transformation of cloning host was performed via calcium chloride and heat sock method.

#### 3.2.4.1 Preparation of competent cells of *E. coli* XL-10 Gold as cloning host

Competent cells were prepared by calcium chloride method [67]. Briefly, 20 µL of preserved glycerol stock of *E. coli* XL-10 Gold at -80 °C was added into 80 mL of S.O.C broth medium (Appendix 1.3) in 500 mL baffled flask (Bellco® Biotechnology) and was incubated at 37 °C for 1 h without shaking. Then the flask was shaken at 200 rpm, 37 °C for 2-3 h until $O.D_{600}$ of 0.2-0.4 was achieved. Then cells were harvested by centrifugation at 4 °C and 10,000 rpm (13,147 *g*) for 30 min by using a Sorvall® RC 5C Plus centrifuge. The cell pellet was re-suspend in 40 mL of filter sterilized cold TB ($CaCl_2$) solution (Appendix 3.1) and then was incubated on ice for 25 min followed by a centrifugation step as mentioned above. Again, the cell pellet was re-suspended in 4 mL of cold TB ($CaCl_2$) solution. Cells

were used immediately or kept at 4 °C up to 74 h for later use. During preparation of competent cells, cold chain was maintained by using cold solutions and equipment e.g. pipette tips, tubes and etc.

#### 3.2.4.2 Transformation of competent *E. coli* XL-10 Gold

Transformation of competent cells was modified and performed by the heat shock method as described previously [67]. Briefly, 5 µL of ligation products was added to 100 µL of competent cells followed by adding 1 µL of 40% DMSO (Appendix 3.2) in 1.5 mL micro-centrifuge tube and incubating on ice for 50 min. Then heat shock was applied by incubating tubes exactly at 42 °C and exactly for 90 sec followed by incubation on ice for 5 min. Then 400 µL of sterilized ice cold S.O.C broth (Appendix 1.3) was added to tubes followed by incubation at 37 °C, 200 rpm for 1 h. Tubes then were centrifuged at 5,000 rpm (2,700 *g*) for 1 min and cell pellet was re-suspended in 100 µL S.O.C broth and then was transferred and spread on at 37 °C pre-heated low salt L.B. agar (Appendix 1.2) plates supplied with 100 µg/mL ampicillin and incubated at 37 °C for 14-16 h. After incubation, each transformed colony was selected, picked by sterilized tooth pick and grown on new L.B. agar (Appendix 1.1) plates supplied with 100 µg/mL ampicillin and incubated at 37 °C overnight. Then colonies were checked for correct insertion and orientation by colony PCR method.

### 3.2.5 Detection of correct clones by colony PCR method

Colony PCR method was used to select correct insertion and orientation of each insert. Approximately half of a colony was picked with sterilized tooth pick and was pasted at the bottom of a 200 µL PCR tube. Then 20 µL of nuclease free sterile deionized water was added to each tube and mixed thoroughly by vortexing and followed by heating at 95 °C for 5 min then cooled down at room temperature for 30 min followed by centrifugation at 13,000 rpm (16,060 *g*) for 10 min. Then 2 µL of supernatant was used as template in PCR reaction. Generally, the reaction mixture was set up on ice in a 25 µL final volume with gently pipetting up and down of the PCR reaction components (all from New England BioLabs) as follow: 10X standard *Taq* reaction buffer to final concentration of 1X, dNTPs to final concentration of 200 µM each, forward and reverse primers (Table 3.3) to final concentration of 0.2 µM each,

2 µL of DNA template, 125 µL *Taq* DNA polymerase and nuclease free sterile deionized water. Primers were designed to amplify 106 bp, 117 bp and 172 bp length nucleotide for $A_1$, $A_2$ and ALAL sequences, respectively, from both insert and *dpgA* gene (Figure 3.4). PCR conditions for each insert are shown in (Table 3.4). Extracted plasmid from correct colonies then was sent for sequencing by T7 promoter primer to confirm correct inserts (Section 3.2.6).

### 3.2.6 DNA sequencing

Plasmids from colonies with the correct orientation and inserts (detected by colony PCR) were extracted by QIAprep® Spin Miniprep Kit (QIAGEN) as previously described (Section 3.2.1.1) and used as materials for DNA sequencing at BioDesign Co., Ltd., Thailand, with T7 promoter primer (5′-AATACGACTCACTATAGG) to confirm the correct inserts. After confirmation, correct plasmids with the correct inserts were used for transformation of the expression host, *E. coli* Tuner (DE3) pLysS.

### 3.2.7 Transformation of expression host

*E. coli* Tuner (DE3) pLysS was used as expression host in the current study. Transformation of expression host was performed by calcium chloride and heat sock method. Preparation and transformation of expression host, *E. coli* Tuner (DE3) pLysS, were performed by the same method as previously described for transformation of cloning host competent cells, *E. coli* XL-10 Gold, (Section 3.2.4.1 and 3.2.4.2). Correct transformants were selected and confirmed by colony PCR as described previously (Section 3.2.5) and then were used for expression of recombinant proteins.

### 3.2.8 Expression of recombinant proteins

A 250 µL volume of overnight pre-culture of *E. coli* Tuner (DE3) pLysS containing different variants of *dpgA* gene were inoculated in 250 mL L.B. broth (Appendix 1.1) in 1000 mL baffled flask (Bellco® Biotechnology) supplied with 100 µg/mL ampicillin and 34 µg/mL chloramphenicol. Flasks then were incubated at 37 °C, 200 rpm until $OD_{600}$ ~0.6 was reached. IPTG was added to final concentration

of 0.4 mM. Then cold expression of proteins was performed by incubation at 20 °C with slow shaking at 100 rpm for 16 h. After incubation, cells were harvested at 10,000 rpm (13,147 *g*) and 4 °C for 40 min by using a Sorvall®RC 5C Plus centrifuge, followed by re-suspension of the cell pellet in 9X volume lysis buffer (Appendix 5.1) and used as material for preparation of clarified cell lysate by sonication.

**Table 3.3** Primers used in the current study; amplification of ALAL was performed with the same set of primers used to amplify $A_1$ insert.

| Primer | Sequence 5` → 3` |
|---|---|
| **$A_1$ Forward** | TATGGGCTACGAAACCCTGGACGACCAGGG |
| **$A_1$ Reverse** | CATGACCGACCGAGCGCGTTGTG |
| **$A_2$ Forward** | GGCCTGTTCGAAAAAGCGGCG |
| **$A_2$ Reverse** | GGTTACGCCGTCGGGCATGA |

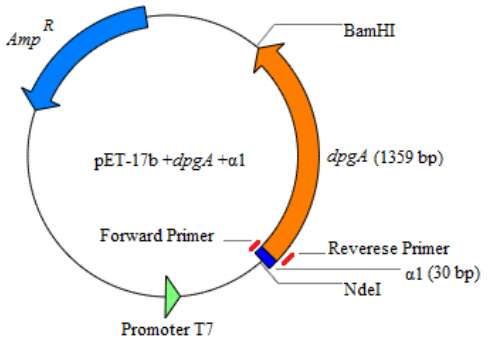


**Figure 3.4** Schematic position of primers used to amplify $A_1$ insert and a short region of *dpgA* gene in pET-17b vector. The same strategy was used for other inserts and vectors.

**Table 3.4** Conditions of colony PCR for each of inserts and the length of PCR products.

| Steps | | $A_1$ | $A_2$ | ALAL |
|---|---|---|---|---|
| **Pre-heat** | | 95 °C – 2 min | 95 °C – 2 min | 95 °C – 2 min |
| | **Denaturation** | 95 °C – 20 sec | 95 °C – 20 sec | 95 °C – 20 sec |
| **30 Cycles** | **Annealing** | 63 °C – 20 sec | 60 °C – 20 sec | 63 °C – 20 sec |
| | **Extension** | 72 °C – 20 sec | 72 °C – 20 sec | 72 °C – 20 sec |
| **Final extension** | | 72 °C – 5 min | 72 °C – 5 min | 72 °C – 5 min |
| **Store** | | 4 °C – ∞ | 4 °C – ∞ | 4 °C – ∞ |
| **Product length (bp)** | | 106 | 117 | 172 |

### 3.2.9 Preparation of clarified cell lysate

In order to prepare cell lysate, cell pellets from previous step were re-suspended in 9X volume of lysis buffer (Appendix 5.1) and were incubated on ice for 20 min. Cell disruption performed on ice in 20 cycles of 10 sec burst and 10 sec cooling intervals by ultra-sonication in Vibra-Cell™ SONICS instrument. Clarified cell lysate was acquired by centrifugation of cell lysate at 4 °C and 12,000 rpm (17,210 *g*) for 20 min by using a Sorvall®RC 5C Plus centrifuge. Clarified cell lysate then was used to determine protein concentration, enzyme activity and purification of different variants of recombinant D-PhgAT enzyme.

### 3.2.10 Purification of different variants of recombinant D-PhgAT protein

Purification of different variants of recombinant D-PhgAT proteins was performed as follow.

#### 3.2.10.1 Fractional ammonium sulfate precipitation

In fractional ammonium sulfate precipitation, proteins in clarified cell lysate were subjected to precipitation by ammonium sulfate at 25%-45% saturation as previously described [3]. First, finely ground ammonium sulfate powder was gradually added to clarified cell lysate up to 25% saturation while stirring in a beaker on ice bath for 1 h in order to even precipitation. Then the protein precipitate mixture was removed by centrifugation at 12,000 rpm (17,210 *g*) by using a

Sorvall®RC 5C Plus centrifuge for 45 min at 4 °C. Then supernatant was collected and used for further precipitation steps with ammonium sulfate until 45% saturation was reached. Stirring of the mixture was continued for 1 h on ice bath. Then precipitated protein mixture containing D-PhgAT was collected by centrifugation as mentioned above. This protein pellet was kept at -20 °C until use in the next step of purification.

**3.2.10.2 Hydrophobic interaction chromatography (HIC)**

In the next step of purification, precipitated protein mixture pellet from fractional ammonium sulfate precipitation was applied to different chromatography columns connected to an ÄKTA purifier FPLC (Fast Protein Liquid Chromatograph). The first used column was Phenyl Sepharose 6 Fast Flow (Amersham Pharmacia Biotech) for hydrophobic interaction chromatography [47]. The resin was packed in a XK16/40 glass chromatography column (Amersham Pharmacia Biotech) with 14 mL of bed volume and was pre-equilibrated with 20 mM TEMP buffer pH 7.6 containing 1 M ammonium sulfate (Appendix 5.3). Precipitated protein mixture pellet from the previous step was dissolved in 5 mL of pre-equilibration buffer and then loaded into the column by using a 5 mL static loop at 1 mL/min flow rate. Then unbounded proteins were washed out with 2 beds volume of the same buffer at 2 mL/min flow rate. The elution of bound proteins was performed by a linear descending gradient from 1 - 0 M ammonium sulfate in four bed volume. Eluted proteins were collected in 3 mL volume fractions by Frac-950 automated fraction collector (GE Healthcare). D-PhgAT activity in each fraction was determined by spectrophotometric method (Section 3.2.11.3). Active fractions were pooled and concentrated by Amicon® 50 kDa cut off centrifugal device at 4 °C and 4,000 rpm (3,095 *g*) by Rotina® 380R centrifuge. Then pooled fractions were desalted several times by adding 10 mL of 20 mM TEMP buffer pH 7.6 (Appendix 5.2) to the Amicon® 50 kDa cut off centrifugal device followed by centrifugation as mentioned above. Pooled, desalted and concentrated protein samples were applied in the next step of purification.

**3.2.10.3 Anion exchange chromatography (IEX)**

Pooled, desalted and concentrated active fractions from the previous step was applied via static loop at a flow rate of 1 mL/min onto the second chromatography column, DEAE Sepharose™ FF IEX column (GE Healthcare),

connected to an ÄKTA purifier FPLC. The resin was packed in XK16/40 glass chromatography column (Amersham Pharmacia Biotech) with 25 mL bed volume which was pre-equilibrated with 20 mM TEMP buffer pH 7.6. The unbound proteins were washed out with 1 bed volume of the same buffer at 2 mL/min flow rate. Elution of bound proteins was performed by applying 8 bed volume of a linear ascending gradient of NaCl in 20 mM TEMP buffer pH 7.6 from 0 to 1 M at 2 mL/min flow rate. Eluted proteins were collected in 3 mL volume fractions by Frac-950 automated fraction collector (GE Healthcare). D-PhgAT activity and purity of each fraction were determined by spectrophotometric (Section 3.2.11.3) and SDS-PAGE (Section 3.2.11.2) methods, respectively, then active fractions were pooled, desalted and concentrated by Amicon® 50 kDa cut off centrifugal device (Millipore®) as mentioned in Section 3.2.10.2. Purified protein was kept in Protein LoBind 1.5 mL micro-centrifuge tubes (Eppendorf) at 4 °C until proceed in further experiments.

### 3.2.11 Characterization of purified protein variants

#### 3.2.11.1 D-PhgAT concentration assay

Solutions of different variants of D-PhgAT Protein were applied on a NanoDrop® ND-1000 spectrophotometer (Thermo Scientific, USA) to determine protein concentration at $280_{nm}$. Since determination of protein concentration by this method inevitably based on the molar absorption coefficient of each variant of protein at $280_{nm}$ ($\varepsilon_{280}$); therefore, $\varepsilon_{280}$ of each variant should be calculated in advance. The following equation was used for $\varepsilon_{280}$ determination:

$$\varepsilon_{280} = (5500 \times n_W) + (1490 \times n_Y) + (125 \times n_{S\text{-}S})$$

Where *n* is numbers of tryptophan (W), tyrosine (Y) and disulfide bond formation by cysteine (s-s). Molar absorption coefficients for different variant of D-PhgAT used in this experiment are shown in table 3.5.

**Table 3.5** Molar absorption coefficients for different variants of D-PhgAT used in this experiment.

| Protein variants | $n_W$ | $n_Y$ | $n_{S\text{-}S}$ | $\varepsilon_{280}$ $M^{-1}$ $cm^{-1}$ |
|---|---|---|---|---|
| **D-PhgAT** | 5 | 7 | 2 | 38180 |
| **$A_1$-D-PhgAT** | 5 | 8 | 2 | 39670 |
| **$A_2$-D-PhgAT** | 5 | 7 | 2 | 38180 |
| **ALAL-D-PhgAT** | 6 | 8 | 2 | 54170 |

#### 3.2.11.2 Sodium dodecyl sulfate-polyacrylamide gel electrophoresis (SDS-PAGE)

SDS-PAGE analysis was performed by electrophoresis of protein samples in 4% and 12% stacking and separating gels, respectively. A 16 µL volume of protein samples were mixed and dissolved in 4 µL of 5X sample loading buffer (Appendix 7.3). After being heated at 99 °C for 5 min and briefly centrifugation, the mixture was loaded into the wells of the stacking polyacrylamide gel. A 5 µL volume of protein molecular weight marker was loaded into the first well of stacking gel. Electrophoresis was performed in a Mini-Protein II Dual Slab Cell electrophoresis chamber (1 mm spacer) at a constant 100 V until the bromophenol blue dye of sample loading buffer reached the end of the separating gel. Visualization of protein bands was performed by 30 min slow agitation (35 rpm) of gel in coomassie blue staining solution (Appendix 8). Then gel was distained by destaining solutions I (Appendix 8.2) for 1 h and destaining solutions II (Appendix 8.3) until clear background appeared. Gels were stored in sterile deionized water until being analyzed.

#### 3.2.11.3 D-PhgAT activity assay

D-PhgAT activity was assayed by using a method based on formation of p-Hydroxybenzoylformic acid (p-OHBZF) upon transamination of 4-Hydroxy-D-phenylglycine (D-4-OHPhg) as substrate with α-ketoglutaric acid monosodium salt as an amino acceptor. p-OHBZF was monitored by using Heλios α spectrophotometer (Spectronic Unicam, Cambridge, UK) at $340_{nm}$ and 37 °C for 180 sec. The reaction mixture, in 1 mL, contained 20 µL of enzyme solution, 10 mM D-4-OHPhg, 10 mM α-ketoglutarate, 50 mM CAPSO buffer pH 9.5, 5 µM PLP and 5 µM

EDTA. The molar absorption of $24\times10^3$ $M^{-1}cm^{-1}$ was used for calculation of generated p-OHBZF in 1 min. One unit of D-PhgAT was defined as the amount of enzyme used for transamination of 1 µmol of D-4-OHPhg to 1 µmol p-OHBZF per 1 min at 37 °C.

#### 3.2.11.4 Determination of the effects of substrate concentrations on D-PhgAT activity

For this experiment, modified from [68], production of D-phenylglycine in the reverse reaction of D-PhgAT was assayed by HPLC method. The reaction mixture, in 1 mL final volume, contained 100 mM CAPSO buffer pH 9.5, 50 mM benzoylformic acid pH 7, 25 µM PLP, 25 mM EDTA and different concentrations of L-glutamic acid monosodium salt pH 9.5 (GMS) and 10 µL of enzyme solution (1 unit). The mixture was incubated at 37 °C for 1 h; while at 20 min intervals, 50 µL aliquots of reaction mixture were inactivated and diluted simultaneously in 150 µL of 85 °C pre-heated distilled water and left standing for 2 min. Then, 20 µL of diluted solution was injected into Spherisorb ODS2 column (250 × 46 mm, Waters, Milford, USA) which was connected to HPLC 1100 series system (Hewlett Packard, USA) and analyzed at $254_{nm}$. Isocratic 50 mM ammonium acetate buffer pH 5.5 containing 10% methanol was used as mobile phase at 1.2 mL / min flow rate. The concentrations of products were evaluated in compare with standard solutions.

#### 3.2.11.5 Determination of pH effect on enzyme activity

To determine the effect of pH on enzyme activity at a range from 5.0 to 11.0, 50 mM of following buffers were used: citrate buffer (pH 5.0-6.0), PIPES buffer (pH 6.0-7.5), Tris-HCl buffer (pH 7.5-8.5), CAPSO buffer (pH 8.5-10.0) and CAPS buffer (pH 10.0-11.0). D-PhgAT activity was measured at 37 °C by using the spectrophotometric method as mentioned in section 3.2.11.3.

### 3.2.12 Determination of isoelectric point (p*I*) value

#### 3.2.12.1 Determination of theoretical p*I* value

Theoretical p*I* values of different variants of D-PhgAT were calculated by submitting protein sequences into open source SeqCalc software (Ver. 1.0) in FASTA format [69].

#### 3.2.12.2 Determination of experimental p*I* value

Seven cm Immobilline™ DryStrips, pH 3-10 NL (GE Healthcare) was used to determine isoelectric point values of different variants of D-PhgAT. Rehydration of the strips was performed for 13 h in ceramic IPGphor strip holder (GE Healthcare) by 125µL rehydration solution (Appendix 9.1) containing 100 µg of the protein sample. The first dimension of isoelectric focusing (IEF) was performed according to protocol 28-9537-55 AA provided by the manufacturer as illustrated in table 3.6 by an Ettan™ IPGphor™ II isoelectric focusing system (GE Healthcare). Then the strips were equilibrated in 5 mL of equilibration solution (Appendix 9.2) for 15 min at room temperature just prior to the second dimension. The second dimension, vertical SDS-PAGE, was performed in a Mini-Protein II Dual Slab Cell electrophoresis chamber. Each strip, after equilibration, was placed on top of 12.5% acrylamide gel (1.5 mm spacer) in vertical slab. A 15 µL volume of protein marker was positioned adjacent to the strip by using a piece of sterilized whatman filter paper. The strip was sealed with 0.5% of low melting point agarose gel (V*i*vant*i*s biochemical) containing trace amount of bromophenol blue dye (a few grains). Electrophoresis was performed at 100 V until the dye reached to the bottom of the gel. Protein bands were visualized as described in section 3.2.11.2.

**Table 3.6** Steps and conditions for first dimension of isoelectric focusing (IEF).

| Step | Step voltage mode | Voltage (V) | Step duration (h:min) | Volt-hours (kVh) |
|---|---|---|---|---|
| **1** | Step and hold | 300 | 0:30 | 0.2 |
| **2** | Gradient | 1000 | 0:30 | 0.3 |
| **3** | Gradient | 5000 | 1:30 | 4.5 |
| **4** | Step and hold | 5000 | 0:30 | 3.0 |
| **Total** | - | - | 3:00 | 8.0 |

### 3.2.13 Determination of in-vitro protein solubility

In-vitro protein solubility was determined in triplicates at 25 °C in storage buffer of enzyme (20 mM TEMP buffer, pH 7.6), and reaction buffer of enzyme (50 mM CAPSO, pH 9.5) by a concentration method as previously described [70] and modified [8]. In this method a 30 K MWCO centrifugal device (Microcon® Ultrcel YM-30) was used to concentrate the enzyme solution at 4,000 rpm (1,700 *g*) and 25 °C with interval quantification of protein concentration by NanoDrop® ND-1000 at

$280_{nm}$ as explained in section 3.2.11.1 until no further concentration was observed. During this experiment, membrane blockage was avoided by interval agitation of protein solution followed by centrifugation at 13,000 rpm (14,000 *g*) for 15 min.

### 3.2.14 Effect of different concentrations of salts and miscible organic solvents on pH value of CAPSO pH 9.5

Hydrogen power (pH) of a given buffered enzyme solution may subject to change upon addition of salt or organic solvent. This shifting in buffer`s pH may significantly affect enzyme solubility, activity and stability; therefore in order to investigate the effect of salts and organic solvent on proteins, firstly, it is necessary to investigate the effect of salts and organic solvents on the pH value of the buffer. A stock aqueous 0.85 mM solution of thymol blue (Fluka analytical) was used as pH indicator in the current study with second transition, yellow to blue at pH 8.0 – 9.6, p$k_{aq}$= 8.9 (Figure 3.5) as described in the next sections.

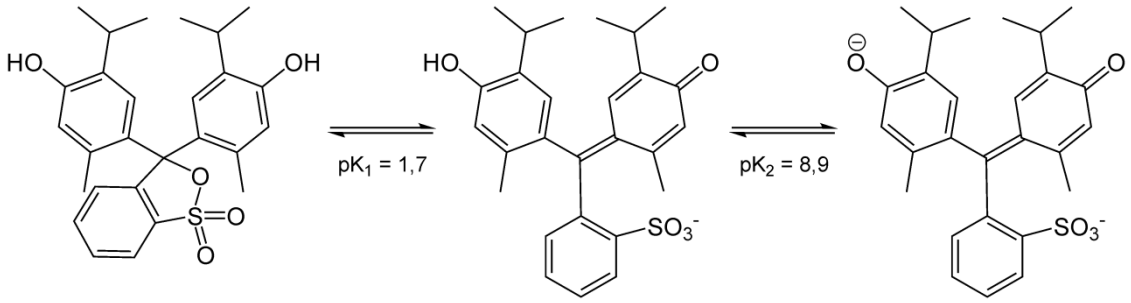


**Figure 3.5** Chemical structure of thymol blue pH indicator.

#### 3.2.14.1 Plotting standard curve of absorbance of thymol blue dye complexes as a function of pH

A 100 µL of 10X CAPSO buffer (500 mM) with different pH values (7.5 – 10.1) was mixed with 40 µL of 0.85 mM stock solution of thymol blue and distilled water to a final volume of 1000 µL (50 mM and 0.35 µM final concentration of CAPSO buffer and thymol blue, respectively) and mixed thoroughly. Then absorption spectrum of the resulted dye complexes was determined from $400_{nm}$ to $750_{nm}$ by using a scan mode of a Heλios α spectrophotometer. The peak

absorption was detected at $595_{nm}$ and used to plot the standard curve of absorption as a function of pH.

#### 3.2.14.2 Investigation of effect of different concentrations of salts on pH value of D-PhgAT reaction buffers

A 100 µL volume of 10X CAPSO buffer pH 9.5 (500 mM) was mixed with 40 µL of 0.85 mM stock solution of thymol blue, different amount of 5 M NaCl or 4 M KCl solutions and deionized water were mixed together to 1X final concentration of CAPSO buffer pH 9.5 (50 mM) containing different concentrations of NaCl and KCl and 0.35 µM thymol blue (Table3.7). Scan mode of Heλios α spectrophotometer was used to determine the absorption spectrum of the dye complexes in the range of $400_{nm}$ to $750_{nm}$. The peak absorbance at $595_{nm}$ was used to determine the pH of the solution by using previously plotted standard curve (Section 3.2.14.1). Then change of pH of CAPSO buffer pH 9.5 (Δ pH) in the presence of different salts concentration was calculated and recorded and was used in preparation of CAPSO buffer with different pH in the next steps of the experiment.

#### 3.2.14.3 Investigation of effect of different concentrations organic solvents on pH values of D-PhgAT reaction buffer

To determine the effect of different concentration of different organic solvents on pH value of CAPSO buffer, similar to section 3.2.14.2, A 100 µL volume of 10X CAPSO buffer pH 9.5 (500 mM), 40 µL of 0.85 mM stock solution of thymol blue, different amount of absolute miscible organic solvents (DMF, acetone and isopropanol) and deionized water were mixed together to 1X final concentration of CAPSO buffer pH 9.5 (50 mM) containing different proportions of different miscible organic solvents and 0.35 µM thymol blue (Table 3.8). Scan mode of Heλios α spectrophotometer was used to determine the absorption spectrum of dye complexes in the range of $400_{nm}$ to $750_{nm}$. The peak absorbance at $595_{nm}$ was used to determine the pH of the solution by using previously plotted standard curve (Section 3.2.14.1). Then change of pH of CAPSO buffer pH 9.5 (Δ pH) in the presence of different proportions of different miscible organic solvents was calculated and recorded and was used in preparation of CAPSO buffer with different pH in the next steps of the experiment.

### 3.2.15 D-PhgAT activity assay in different proportions of NaCl and KCl

D-PhgAT activity was determined by monitoring and recording of p-OHBZF formation upon transamination of D-4-OHPhg with 2-oxoglutarate as an amino acceptor by rate mode of Heλios α spectrophotometer at $340_{nm}$ for 180 sec immediately after adding and mixing of 20 µL of enzyme solution into 980 µL of reaction mixture containing different concentrations of inorganic salts (NaCl and KCl). The pH of CAPSO buffer was calculated according to result of experiment in section 3.2.14.2.

### 3.2.16 D-PhgAT activity assay in different proportions of different miscible organic solvents

Enzyme activity was determined by monitoring and recording of the formation of p-OHBZF upon transamination of D-4-OHPhg with 2-oxoglutarate as an amino acceptor by using Heλios α spectrophotometer at 340 nm for 180 sec immediately after mixing 20 µL of enzyme solution into 980 µL of reaction mixture containing different proportions of different miscible organic solvents (DMF, acetone and isopropanol). The pH of CAPSO buffer was calculated according to the results of experiment in section 3.2.14.3.

### 3.2.17 Effect of different organic solvents on thermal stability of different variants of D-phgAT

First 10 µL of each enzyme solution in TEMP buffer pH 7.6 was dried in a vacuum centrifuge at 25 °C until completely dried. Then 10 µL of TEMP buffer pH 7.6 (as control) or 10 µL of different miscible organic solvents (DMF, acetone and isopropanol) were added to each tube and then incubated at different temperatures (25, 40, 60 °C) for 1 h. Organic solvents were removed by drying the sample in a vacuum centrifuge at 25 °C and then 10 µL of TEMP buffer pH 7.6 was added to each tube. Tubes were incubated on ice for 1 h then remained activity of each D-PhgAT variant was assayed (Section 3.2.11.3).

**Table 3.7** Different amount of NaCl (A), KCl (B), 10X CAPSO pH 9.5, thymol blue and water used in the reaction mixture for determining the effect of salts on the pH of CAPSO buffer.

A)

| Final concentration (M) | 10X CAPSO pH 9.5 (µL) | Thymol blue, 0.85 mM stock (µL) | Salt, 5 M stock (µL) | Water (µL) |
|---|---|---|---|---|
| **0.5** | 100 | 40 | 100 | 760 |
| **1.0** | 100 | 40 | 200 | 660 |
| **1.5** | 100 | 40 | 300 | 560 |
| **2.0** | 100 | 40 | 400 | 460 |
| **2.5** | 100 | 40 | 500 | 360 |
| **3.0** | 100 | 40 | 600 | 260 |
| **3.5** | 100 | 40 | 700 | 160 |

B)

| Final concentration (M) | 10X CAPSO pH 9.5 (µL) | Thymol blue, 0.85 mM stock (µL) | Salt, 4 M stock (µL) | Water (µL) |
|---|---|---|---|---|
| **0.5** | 100 | 40 | 125 | 735 |
| **1.0** | 100 | 40 | 250 | 610 |
| **1.5** | 100 | 40 | 325 | 535 |
| **2.0** | 100 | 40 | 500 | 360 |
| **2.5** | 100 | 40 | 625 | 235 |
| **3.0** | 100 | 40 | 750 | 110 |

**Table 3.8** Different amount of absolute miscible organic solvents, 10X CAPSO pH 9.5, thymol blue and water used in the reaction mixture for determining the effect of miscible organic solvents on the pH of CAPSO buffer.

| Final concentration (%) | 10X CAPSO pH 9.5 (µL) | Thymol blue, 0.85 mM stock (µL) | Organic solvent (µL) | Water (µL) |
|---|---|---|---|---|
| **10** | 100 | 40 | 100 | 760 |
| **20** | 100 | 40 | 200 | 660 |
| **30** | 100 | 40 | 300 | 560 |
| **40** | 100 | 40 | 400 | 460 |
| **50** | 100 | 40 | 500 | 360 |

### 3.2.18 Statistical analysis

All experiments were carried out in triplicate (n = 3). Analysis of variance was used to interpret data. Means and standard deviations are shown in graphs.

# CHAPTER IV
# RESULTS

## 4.1 Construction of plasmids

Extracted pET-17b DNA plasmid carrying *dpgA* gene in section 3.2.1.1 was subjected to digestion with *Nde*I restriction enzyme followed by a dephosphorylation step with Antarctic phosphatase and then was run on agarose gel as mentioned in section 3.2.1.5. Visualization of DNA bands was performed by CYBR® Gold nucleic acid gel stain (Invitrogen) as described in section 3.2.1.6 and compared with GeneRuler™ 1 kb DNA Ladder (Fermentase). Figure 4.1 shows the DNA band of digested and dephosphorylated pET-17b DNA plasmid on stained agarose gel. Size of digested pET-17b DNA carrying *dpgA* gene is 4689 bp. DNA band then was cut with a sharp and clean surgical scalpel blade and used as material for purification with GFX™ PCR DNA and Gel Band Purification Kit (GE healthcare, UK) according to manufacturer manual (Section 3.2.1.7). In case of insertion of ALAL insert, plasmid was extracted, digested with *Nde*I restriction enzyme and end-filled with T4 DNA polymerase as described in sections 3.2.1.8 and 3.2.1.9. Preparations of $A_1$ and $A_2$ inserts was achieved as described in sections 3.2.2.1 by annealing protocol while a complete ALAL insert was generate by a single step extension of two overlapping oligonucleotides with *pfu* DNA polymerase as mentioned in section 3.2.2.2. Then prepared plasmid vector and inserts were used in ligation reaction with T4 ligase as described in section 3.2.3.

## 4.2 Preparation and transformation of competent *E. coli* XL-10 Gold as cloning host

Competent *E. coli* XL-10 Gold competent cells were prepared by calcium chloride method as described in section 3.2.4.1 then transformation of these competent cells with ligation products (plasmids containing *dpgA* gene and fused $A_1$,

$A_2$ and ALAL sequences) was performed by heat shock method as described in section 3.2.4.2. Transformants were selected on L.B. agar medium containing 100 µg/mL ampicillin. Colonies then picked up and checked by colony PCR method to select correct insertion and orientation.

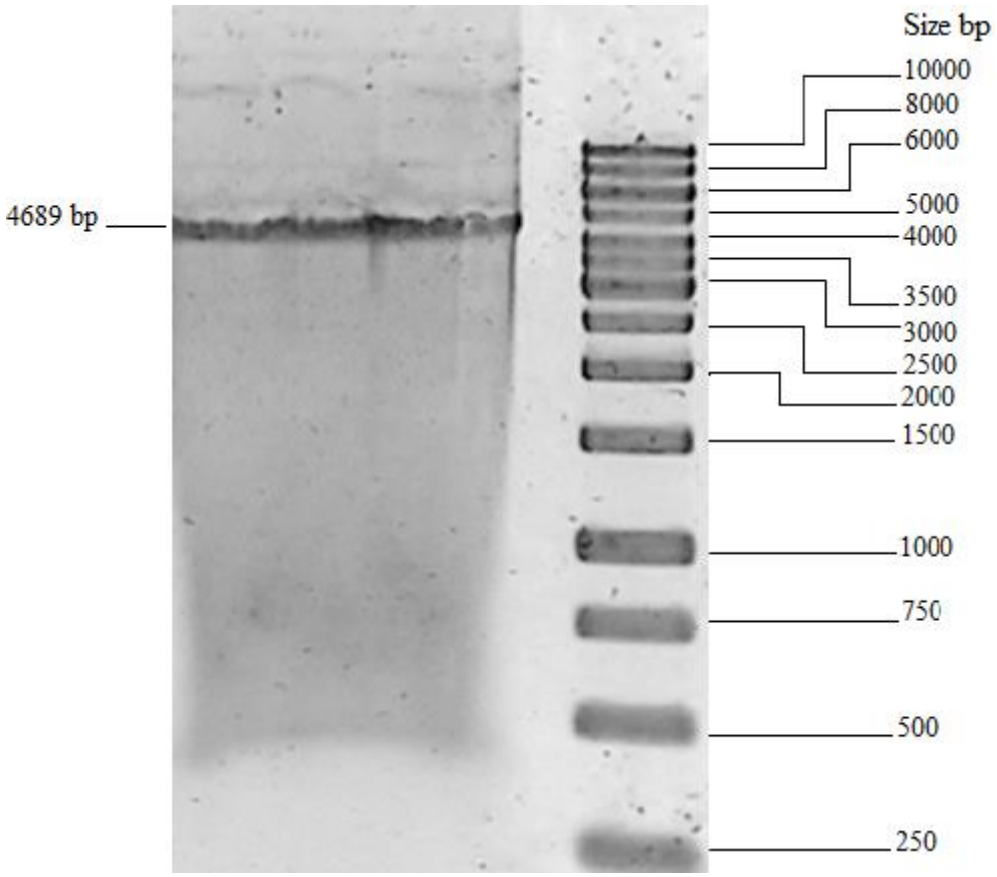


**Figure 4.1** DNA band of digested and dephosphorylated pET-17b on stained agarose gel. The size of digested pET-17b with *dpgA* gene is 4689 bp.

## 4.3 Detection of correct insertion and orientation by colony PCR

Detection of correct clones with correct orientation was performed by colony PCR method as described in section 3.2.5 by using sets of primers as shown in figure 3.3 and PCR condition as shown in table 2.4. PCR products were run on agarose gel and visualized as described in section 3.2.16. The products size of $A_1$, $A_2$

and ALAL are 106 bp, 117 bp and 172 bp, respectively. Figure 4.2 shows positive results of colony PCR of $A_2$ insert.

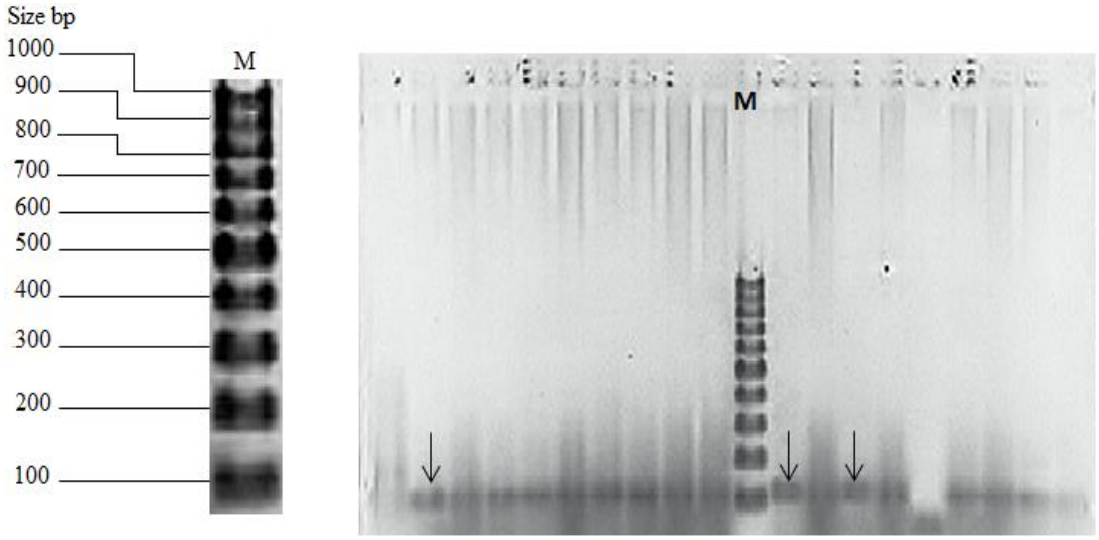


**Figure 4.2** Positive results of colony PCR of $A_2$ insert; correct bands are indicated by arrows, M indicates 100 bp ladder marker.

## 4.4 DNA sequencing and nucleotide sequences of constructed plasmids

Positive results of colony PCR method with correct inserts and orientation were used as materials for DNA sequencing by BioDesign Co., Ltd., Thailand by using T7 promoter vector specific primer (5′-AATACGACTCACTATAGG). The nucleotide sequencing results are shown in figures 4.3 - 4.5.

## 4.5 Transformation of *E. coli* tuner (DE3) pLysS and expression of recombinant proteins

*E. coli* tuner (DE3) pLysS which contains pLysS plasmid with chloramphenicol antibiotic resistance gene was transformed with pET-17b plasmids containing *dpgA* gene with $A_1$, $A_2$ or ALAL fused sequences at N-terminus domain by

same heat shock method as described in section 3.2.4.2. L.B agar medium supplied with 100 µg/mL ampicillin and 34 µg/mL chloramphenicol was used to select transformants. Each selected transformants was subjected to another colony PCR test as described in section 3.2.5. After correct transformation was confirmed, recombinant proteins were expressed by the method described in section 3.2.8. Cell pellets and clarified cell lysate were prepared by methods as mentioned in section 3.2.9. Expression of the recombinant protein was checked by SDS-PAGE analysis and activity of D-PhgAT in clarified cell lysate was determined by spectrophotometric method as described in section 3.2.11.3. The result of SDS-PAGE analysis and activity assay are shown in figure 4.6 and figure 4.7, respectively.

>1391 bp pET-17b-$A_1$-D-PhgAT sequence

***ATG***GGCTACG AAACCCTGGA CGACCAGGGA TGTCGATCCT TAACGACTAC AAACGTAAGA 60
CAGAAGGCTC AGTATTTTGG GCACAACGCG CTCGGTCGGT CATGCCCGAC GGCGTAACCG 120
CAGACACCCG AGTATTTGAC CCACACGGCC TTTTCATTAG TGACGCCCAA GGCGTTCACA 180
AGACCGATGT AGACGGCAAT GTGTACCTAG ACTTTTTTGG CGGGCACGGA GCCCTCGTAC 240
TAGGTCATGG CCATCCTCGG GTTAACGCAG CCATCGCCGA AGCTCTTAGC CATGGCGTCC 300
AGTACGCGGC CAGCCACCCA CTGGAAGTGC GATGGGCAGA ACGCATCGTG GCCGCATTTC 360
CCTCAATTCG TAAACTGCGC TTCACCGGAA GCGGCACCGA AACTACGCTG CTGGCTTTGC 420
GGGTAGCTCG TGCCTTCACG GGCCGCCGCA TGATACTGCG CATCGCCACT CATTATCATG 480
GCTGGCACGA TTTTTCCGCA TCTGGTTATA ACAGCCATTT CGATGGCCAG CCGGCGCCGG 540
GCGTGCTACC TGAAATTGCG AAGAATACTT TGCTGATTCG CCCTGATGAT ATTGAAGGCA 600
TGCGAGAAGT TTTCGCGCAG CATGGCAGCG ACATTGCAGC ATTCATTGCC GAACCTGTGG 660
GTTCGCACTT TGGCGTCACT CCAGTGAGCG ATAGCTTTCT ACGCGAAGGC GCAGAATTGG 720
CTCGGCAATA CGGTGCCCTG TTCATCCTAG ACGAAGTAAT TTCTGGTTTC CGGGTCGGGA 780
ATCACGGAAT GCAGGCGCTC CTTGATGTTC AGCCGGATCT CACCTGCCTG GCTAAGGCCA 840
GCGCAGGCGG GCTTCCCGGT GGCATCTTGG GCGGGCGCGA AGATGTCATG GGAGTTCTCA 900
GCCGAGGCAG TGATCGCAAG GTACTACATC AGGGTACTTT TACCGGCAAC CCGATTACTG 960
CGGCAGCGGC GATCGCAGCC ATCGACACCA TCCTTGAAGA CGATGTTTGC GCGAAGATCA 1020
ATGACCTTGG TCAATTCGCC AGGGAGGCGA TGAATCATCT ATTTGCCCGC AAGGGACTGA 1080
ACTGGCTGGC CTATGGTCGC TTCTCAGGCT TCCACCTGAT GCCGGGGCTG CCACCTAATA 1140
CAACCGACAC CGGCTCCATA ACCCGAGCTG AAGTCGCACG CCCCGATGTG AAGATGATCG 1200
CAGCAATGCG CATGGCATTG ATATTGGAAG GTGTGGATAT CGGCGGGCGC GGGTCAGTTT 1260
TCCTGTCAGC ACAGCATGAA CGCGAACATG TTGAGCATCT GGTGACAACC TTTGATCGCG 1320
TATTAGACCG CCTGGCGGAC GAAAACCTGT TGTCTTGGCA ACCAACTAAT TTGTCTGGAA 1380
ACCAATCA***TA A*** 1391

**Figure 4.3** Nucleotide sequencing result of $A_1$ insert and *dpgA* gene, totally 1391 bp. $A_1$ insert is shown underlined, start and stop codons are shown in italic bold.

>1394 bp pET-17b-$A_2$-D-PhgAT sequence

***ATG***GGCCTGT TCGAAAAAGC GGCGGACGCG GGATGTCGAT CCTTAACGAC TACAAACGTA 60
AGACAGAAGG CTCAGTATTT TGGGCACAAC GCGCTCGGTC GGTCATGCCC GACGGCGTAA 120
CCGCAGACAC CCGAGTATTT GACCCACACG GCCTTTTCAT TAGTGACGCC CAAGGCGTTC 180
ACAAGACCGA TGTAGACGGC AATGTGTACC TAGACTTTTT TGGCGGGCAC GGAGCCCTCG 240
TACTAGGTCA TGGCCATCCT CGGGTTAACG CAGCCATCGC CGAAGCTCTT AGCCATGGCG 300
TCCAGTACGC GGCCAGCCAC CCACTGGAAG TGCGATGGGC AGAACGCATC GTGGCCGCAT 360
TTCCCTCAAT TCGTAAACTG CGCTTCACCG GAAGCGGCAC CGAAACTACG CTGCTGGCTT 420
TGCGGGTAGC TCGTGCCTTC ACGGGCCGCC GCATGATACT GCGCATCGCC ACTCATTATC 480
ATGGCTGGCA CGATTTTTCC GCATCTGGTT ATAACAGCCA TTTCGATGGC CAGCCGGCGC 540
CGGGCGTGCT ACCTGAAATT GCGAAGAATA CTTTGCTGAT TCGCCCTGAT GATATTGAAG 600
GCATGCGAGA AGTTTTCGCG CAGCATGGCA GCGACATTGC AGCATTCATT GCCGAACCTG 660
TGGGTTCGCA CTTTGGCGTC ACTCCAGTGA GCGATAGCTT TCTACGCGAA GGCGCAGAAT 720
TGGCTCGGCA ATACGGTGCC CTGTTCATCC TAGACGAAGT AATTTCTGGT TTCCGGGTCG 780
GGAATCACGG AATGCAGGCG CTCCTTGATG TTCAGCCGGA TCTCACCTGC CTGGCTAAGG 840
CCAGCGCAGG CGGGCTTCCC GGTGGCATCT TGGGCGGGCG CGAAGATGTC ATGGGAGTTC 900
TCAGCCGAGG CAGTGATCGC AAGGTACTAC ATCAGGGTAC TTTTACCGGC AACCCGATTA 960
CTGCGGCAGC GGCGATCGCA GCCATCGACA CCATCCTTGA AGACGATGTT TGCGCGAAGA 1020
TCAATGACCT TGGTCAATTC GCCAGGGAGG CGATGAATCA TCTATTTGCC CGCAAGGGAC 1080
TGAACTGGCT GGCCTATGGT CGCTTCTCAG GCTTCCACCT GATGCCGGGG CTGCCACCTA 1140
ATACAACCGA CACCGGCTCC ATAACCCGAG CTGAAGTCGC ACGCCCCGAT GTGAAGATGA 1200
TCGCAGCAAT GCGCATGGCA TTGATATTGG AAGGTGTGGA TATCGGCGGG CGCGGGTCAG 1260
TTTTCCTGTC AGCACAGCAT GAACGCGAAC ATGTTGAGCA TCTGGTGACA ACCTTTGATC 1320
GCGTATTAGA CCGCCTGGCG GACGAAAACC TGTTGTCTTG GCAACCAACT AATTTGTCTG 1380
GAAACCAATC A***TAA*** 1394

**Figure 4.4** Nucleotide sequencing result of $A_2$ insert and *dpgA* gene, totally 1394 bp. $A_2$ insert is shown underlined, start and stop codons are shown in italic bold.

>1458 bp pET-17b-ALAL-D-PhgAT sequence

***ATG***GGCTACG AAACCCTGGA CGACCAGGGT TGGGACATGG ACGACGACGA CCTGTTCGAA 60

AAAGCGGCGG ACGCGGGTCT GGACGGTGAA GACGGTATGT CGATCCTTAA CGACTACAAA 120

CGTAAGACAG AAGGCTCAGT ATTTTGGGCA CAACGCGCTC GGTCGGTCAT GCCCGACGGC 180

GTAACCGCAG ACACCCGAGT ATTTGACCCA CACGGCCTTT TCATTAGTGA CGCCCAAGGC 240

GTTCACAAGA CCGATGTAGA CGGCAATGTG TACCTAGACT TTTTTGGCGG GCACGGAGCC 300

CTCGTACTAG GTCATGGCCA TCCTCGGGTT AACGCAGCCA TCGCCGAAGC TCTTAGCCAT 360

GGCGTCCAGT ACGCGGCCAG CCACCCACTG GAAGTGCGAT GGGCAGAACG CATCGTGGCC 420

GCATTTCCCT CAATTCGTAA ACTGCGCTTC ACCGGAAGCG GCACCGAAAC TACGCTGCTG 480

GCTTTGCGGG TAGCTCGTGC CTTCACGGGC CGCCGCATGA TACTGCGCAT CGCCACTCAT 540

TATCATGGCT GGCACGATTT TTCCGCATCT GGTTATAACA GCCATTTCGA TGGCCAGCCG 600

GCGCCGGGCG TGCTACCTGA AATTGCGAAG AATACTTTGC TGATTCGCCC TGATGATATT 660

GAAGGCATGC GAGAAGTTTT CGCGCAGCAT GGCAGCGACA TTGCAGCATT CATTGCCGAA 720

CCTGTGGGTT CGCACTTTGG CGTCACTCCA GTGAGCGATA GCTTTCTACG CGAAGGCGCA 780

GAATTGGCTC GGCAATACGG TGCCCTGTTC ATCCTAGACG AAGTAATTTC TGGTTTCCGG 840

GTCGGGAATC ACGGAATGCA GGCGCTCCTT GATGTTCAGC CGGATCTCAC CTGCCTGGCT 900

AAGGCCAGCG CAGGCGGGCT TCCCGGTGGC ATCTTGGGCG GGCGCGAAGA TGTCATGGGA 960

GTTCTCAGCC GAGGCAGTGA TCGCAAGGTA CTACATCAGG GTACTTTTAC CGGCAACCCG 1020

ATTACTGCGG CAGCGGCGAT CGCAGCCATC GACACCATCC TTGAAGACGA TGTTTGCGCG 1080

AAGATCAATG ACCTTGGTCA ATTCGCCAGG GAGGCGATGA ATCATCTATT TGCCCGCAAG 1140

GGACTGAACT GGCTGGCCTA TGGTCGCTTC TCAGGCTTCC ACCTGATGCC GGGGCTGCCA 1200

CCTAATACAA CCGACACCGG CTCCATAACC CGAGCTGAAG TCGCACGCCC CGATGTGAAG 1260

ATGATCGCAG CAATGCGCAT GGCATTGATA TTGGAAGGTG TGGATATCGG CGGGCGCGGG 1320

TCAGTTTTCC TGTCAGCACA GCATGAACGC GAACATGTTG AGCATCTGGT GACAACCTTT 1380

GATCGCGTAT TAGACCGCCT GGCGGACGAA AACCTGTTGT CTTGGCAACC AACTAATTTG 1440

TCTGGAAACC AATCA***TAA*** 1458

**Figure 4.5** Nucleotide sequencing result of ALAL insert and *dpgA* gene, totally 1458 bp. ALAL insert is shown underlined, start and stop codons are shown in italic bold.

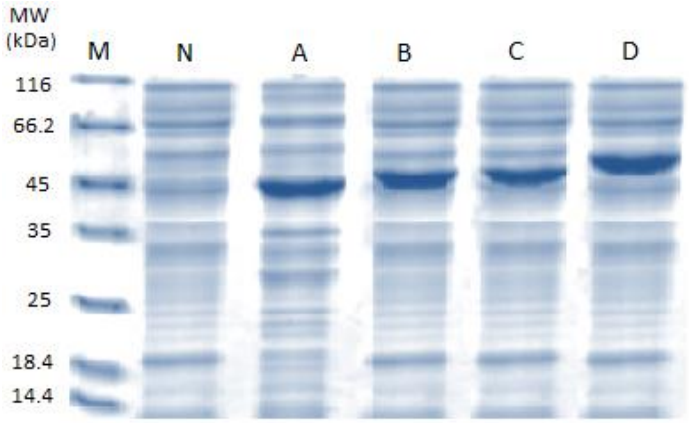


**Figure 4.6** SDS-PAGE profiles of different variants of D-PhgAT protein. M: protein molecular weight marker, N: negative control, A: wild type D-PhgAT, B: $A_1$-D-PhgAT, C: $A_2$-D-PhgAT and D: ALAL-D-PhgAT. The results indicate expression of different variants of D-PhgAT.

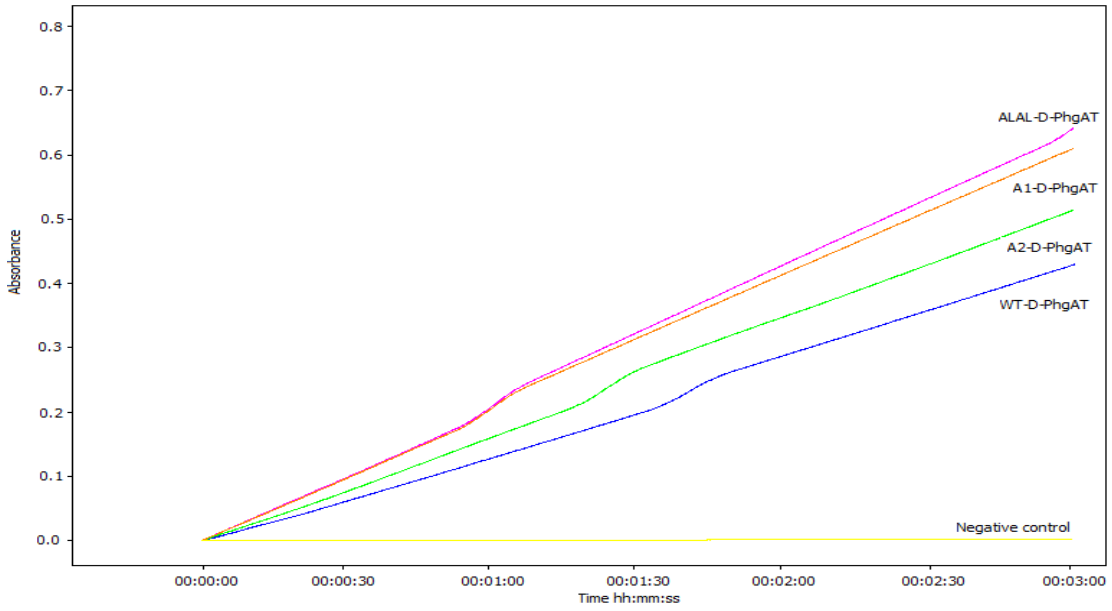


**Figure 4.7** Activity profiles of clarified cell lysate of different variants of D-PhgAT. All variants show activity indicating correct expression and folding of D-PhgAT variants.

## 4.6 Purification of different variants of D-PhgAT

The clarified cell lysates of *E. coli* tuner (DE3) pLysS expressing different variants of D-PhgAT were subjected to 25 - 45% stepwise fractional ammonium sulfate precipitation. Protein precipitate then was collected by centrifugation and used as material for Hydrophobic Interaction Chromatography (HIC) purification.

### 4.6.1 Hydrophobic Interaction Chromatography (HIC)

Protein pellets from 25 - 45% stepwise fractional ammonium sulfate precipitation were dissolved in TEMP buffer pH 7.6 containing 1 M ammonium sulfate and applied on Sepharose 6 Fast Flow Hydrophobic Interaction Chromatography (HIC) pre-equilibrated with the TEMP buffer pH 7.6 containing 1 M ammonium sulfate. After washing out of unbound proteins, D-PhgAT protein variants were eluted by a descending gradient concentration of ammonium sulfate from 1 M to 0 M. The presence of D-PhgAT in each fraction and the purity of each fraction were checked by SDS-PAGE while the activity of each fraction was assayed by spectrophotometric method. Active fractions were pooled and concentrated with 50 kDa centrifugal filter device for the next step of purification. Figures 4.8 – 4.15 show chromatogram patterns and SDS-PAGE analysis of different variants of D-PhgAT with ~ 45 kDa protein bands after purification with HIC column.

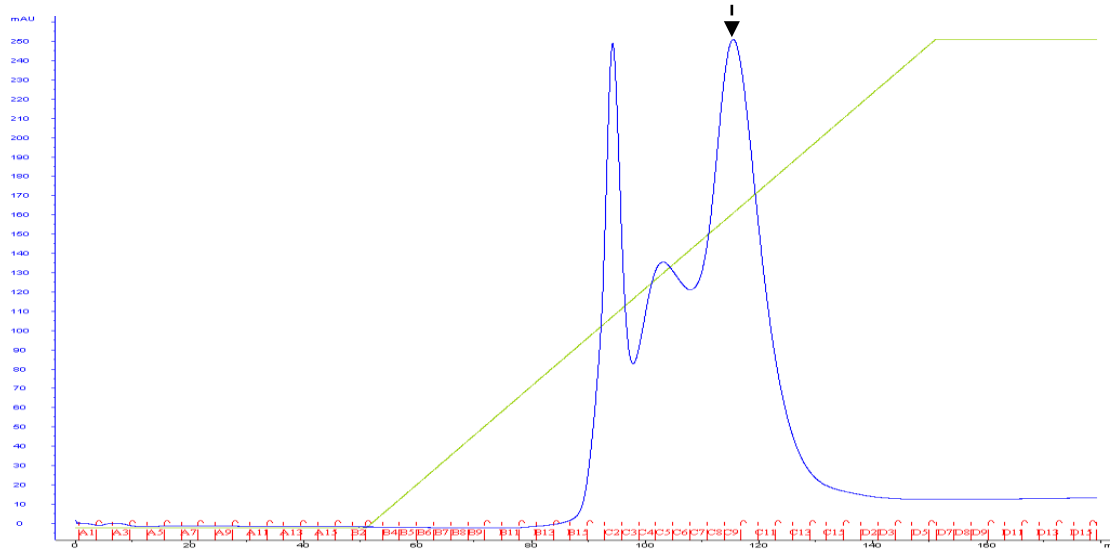

**Figure 4.8** Purification chromatogram of WT-D-PhgAT in HIC column. Active fractions were detected in 3$^{th}$ peak (indicated by arrow).

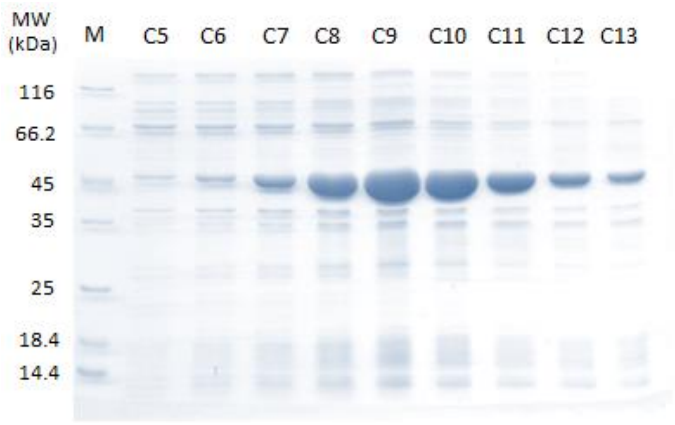


**Figure 4.9** SDS-PAGE result of WT-D-PhgAT eluted active fractions (B5-B13) of the 3$^{th}$ peak.

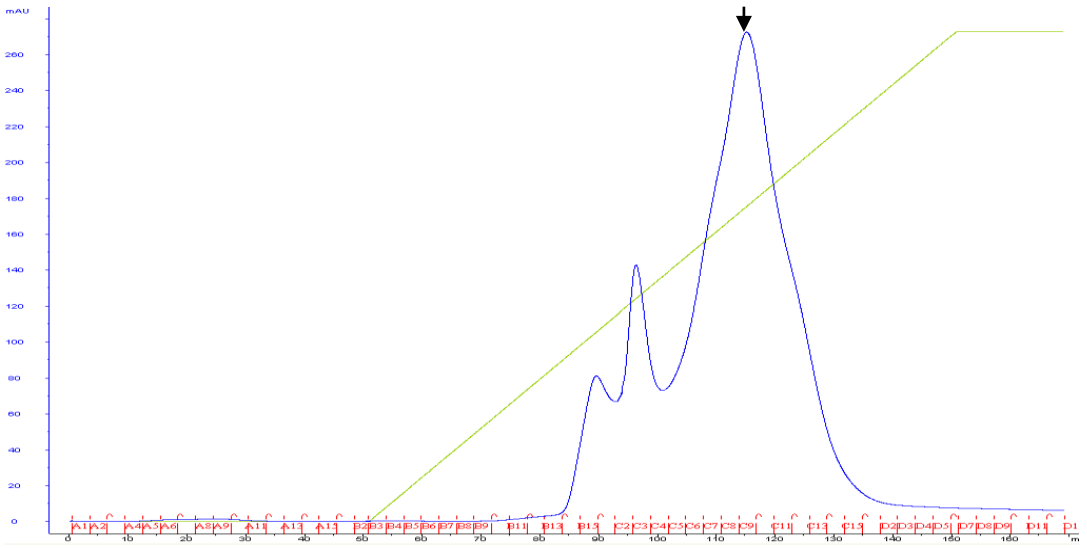

**Figure 4.10** Purification chromatogram of $A_1$-D-PhgAT in HIC column. Active fractions were detected in 3$^{th}$ peak (indicated by arrow).

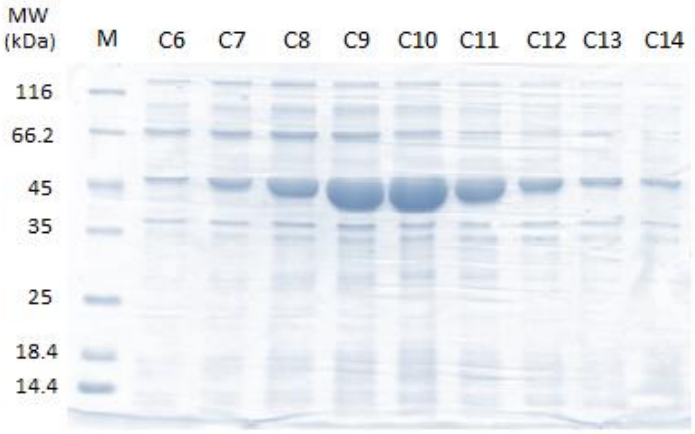


**Figure 4.11** SDS-PAGE result of $A_1$-D-PhgAT eluted active fractions (B10-C3) of the 3$^{th}$ peak.

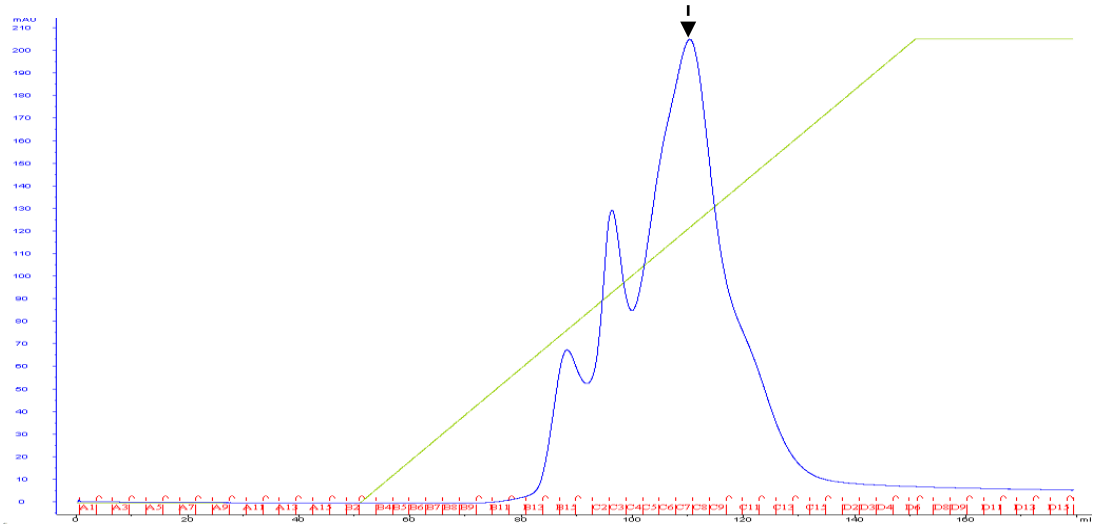

**Figure 4.12** Purification chromatogram of $A_2$-D-PhgAT in HIC column. Active fractions were detected in 3$^{th}$ peak (indicated by arrow).

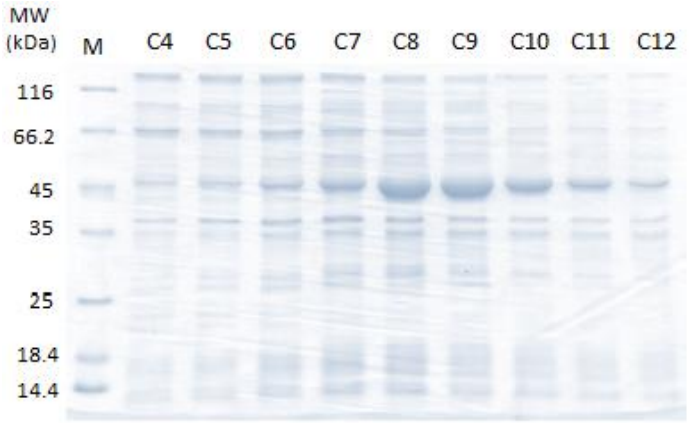


**Figure 4.13** SDS-PAGE result of $A_2$-D-PhgAT eluted active fractions (D13-E6) of the 3$^{th}$ peak.

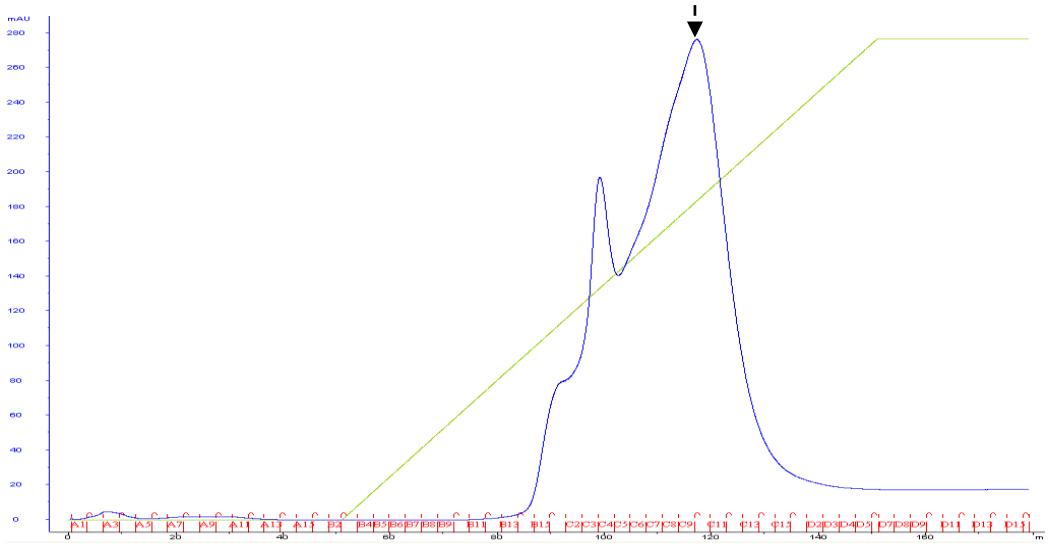

**Figure 4.14** Purification chromatogram of ALAL-D-PhgAT in HIC column. Active fractions were detected in 3$^{th}$ peak (indicated by arrow).

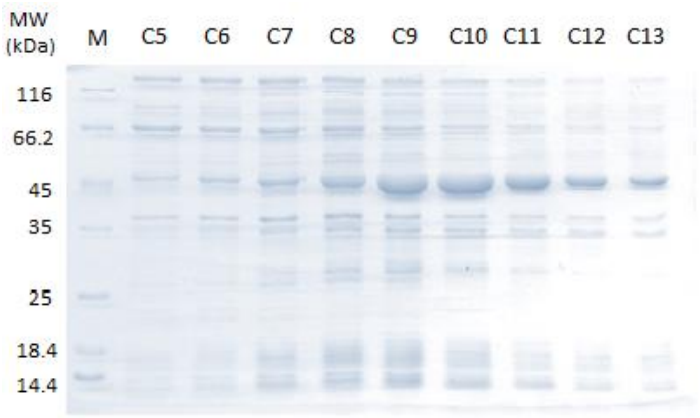


**Figure 4.15** SDS-PAGE result of ALAL-D-PhgAT eluted active fractions (B10-C3) of the 3$^{th}$ peak.

### 4.6.2 Anion exchange chromatography (IEX)

In this step of purification, active, pooled, desalted and concentrated fractions from HIC chromatography column were applied on DEAE Ion Exchange Chromatography (IEX) column pre-equilibrated with TEMP buffer pH 7.6. Proteins were eluted by an ascending gradient of 0 M to 1 M NaCl in TEMP buffer pH 7.6. Fractions were collected, pooled and concentrated with a 50 kDa centrifugal filter device. Purity and activity were checked by SDS-PAGE and D-PhgAT spectrophotometric activity assay. Active fractions were pooled and concentrated with 50 kDa centrifugal filter device. Figures 4.16 – 4.23 show chromatogram patterns and SDS-PAGE analysis of different variants of D-PhgAT with ~ 45 kDa protein bands after purification with IEX column. Table 4.1 shows the purification details of different variants of recombinant D-PhgAT. Purified proteins were kept on ice in 4 °C refrigerator until used in further experiments.

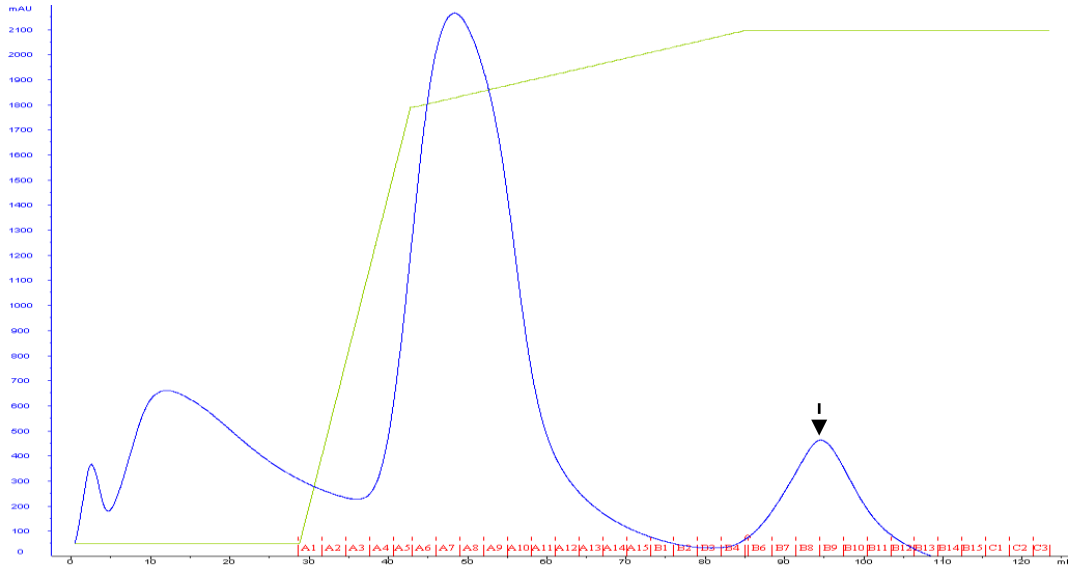

**Figure 4.16** Purification chromatogram of WT-D-PhgAT in IEX column. Active fractions were detected in 3$^{th}$ peak (indicated by arrow).

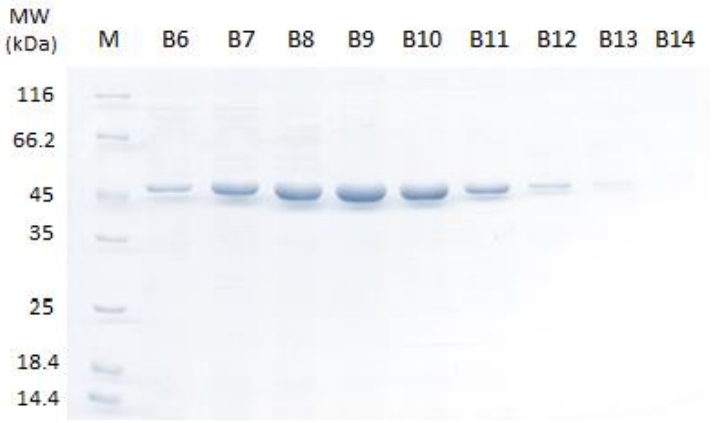


**Figure 4.17** SDS-PAGE result of WT-D-PhgAT eluted active fractions (C6-C14) of the 3$^{th}$ peak.

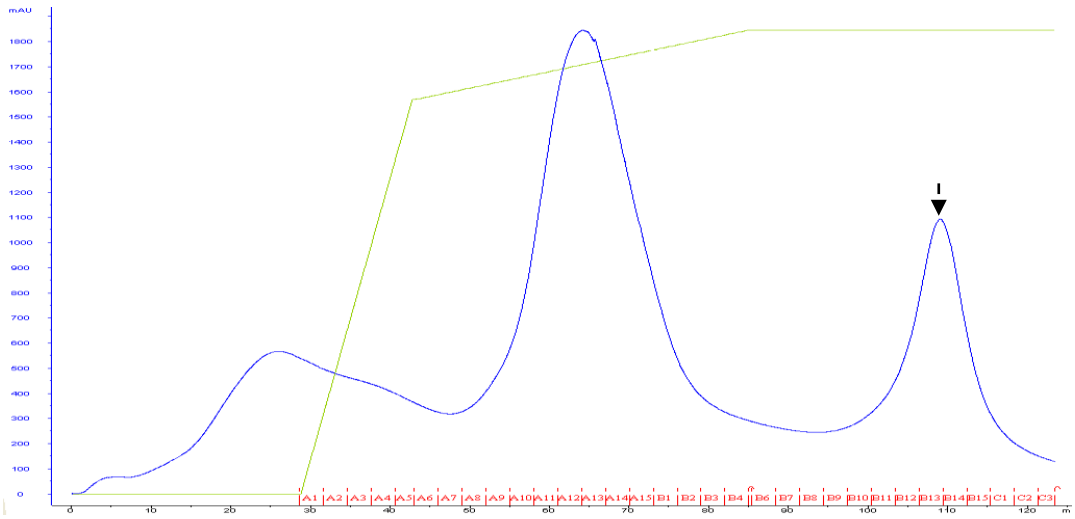

**Figure 4.18** Purification chromatogram of $A_1$-D-PhgAT in IEX column. Active fractions were detected in 3$^{th}$ peak (indicated by arrow).

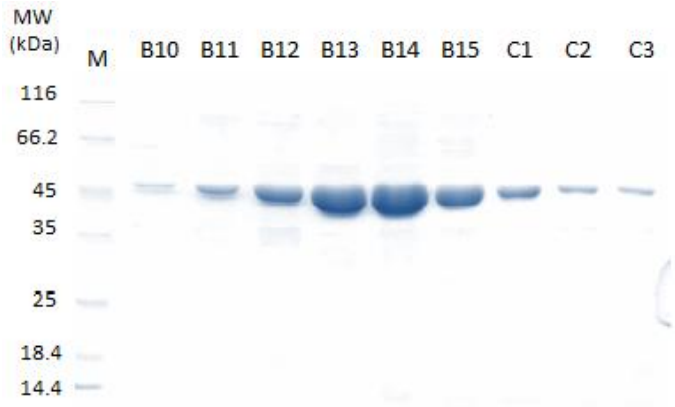


**Figure 4.19** SDS-PAGE result of $A_1$-D-PhgAT eluted active fractions (C5-C13) of the 3$^{th}$ peak.

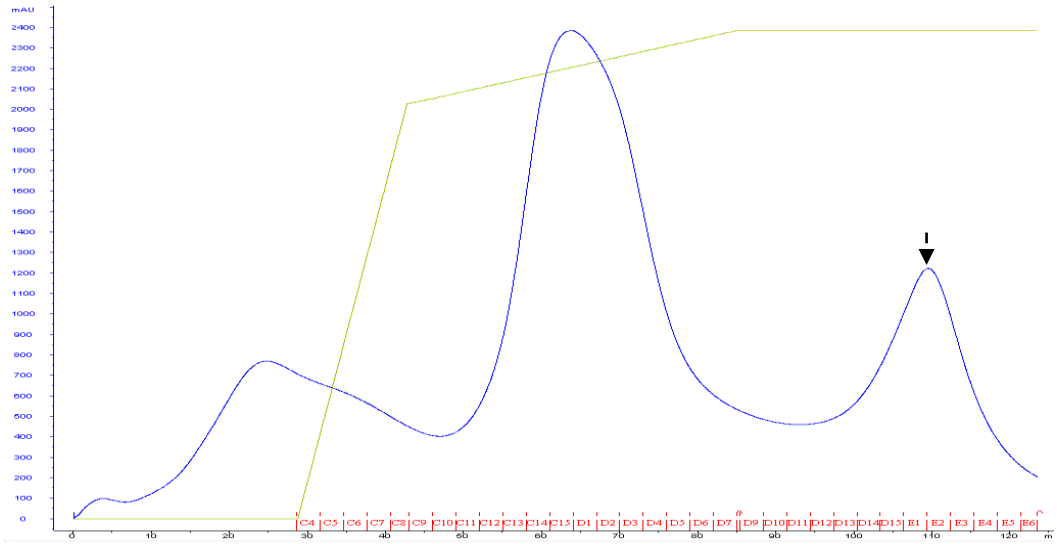

**Figure 4.20** Purification chromatogram of $A_2$-D-PhgAT in IEX column. Active fractions were detected in 3$^{th}$ peak (indicated by arrow).


**Figure 4.21** SDS-PAGE result of $A_2$-D-PhgAT eluted active fractions (C3-C11) of the 3$^{th}$ peak.

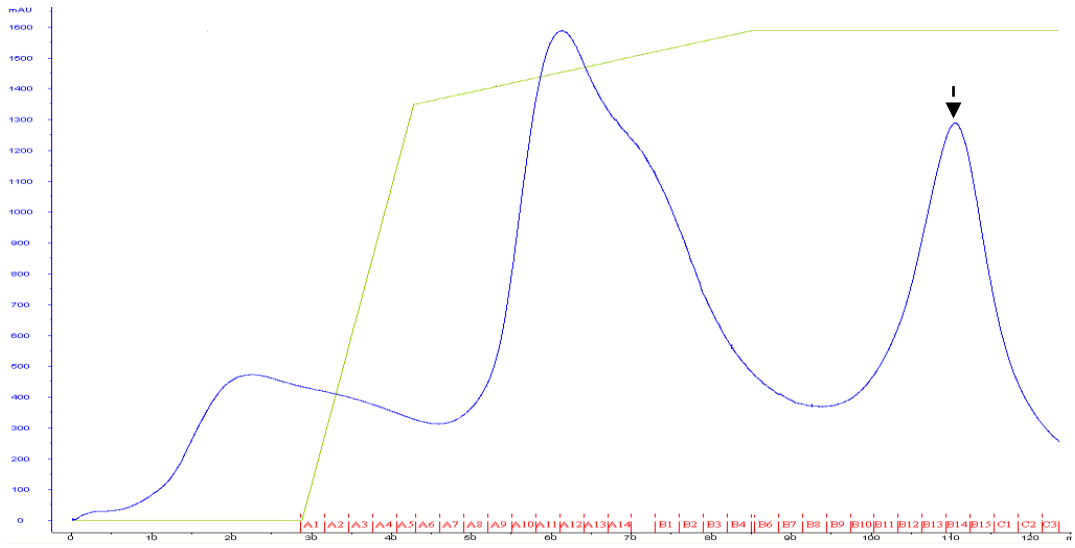

**Figure 4.22** Purification chromatogram of ALAL-D-PhgAT in IEX column. Active fractions were detected in 3$^{th}$ peak (indicated by arrow).

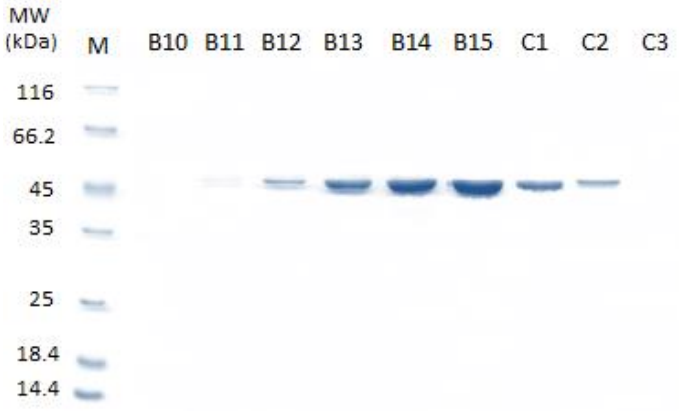


**Figure 4.23** SDS-PAGE result of ALAL-D-PhgAT eluted active fractions (C4-C12) of the 3$^{th}$ peak.

**Table 4.1** Purification table of different variants of D-PhgAT

| Purification steps | Protein variants | Total protein (mg) | Total activity (U) | Specific activity (U/mg) | Purification fold | Yield (%) |
|---|---|---|---|---|---|---|
| **Clarified cell lysate** | D-PhgAT | 92.56 | 474.20 | 5.12 | 1 | 100 |
| | $A_1$-D-PhgAT | 89.30 | 446.50 | 5.00 | 1 | 100 |
| | $A_2$-D-PhgAT | 91.20 | 460.56 | 5.05 | 1 | 100 |
| | ALAL-D-PhgAT | 93.12 | 485.15 | 5.21 | 1 | 100 |
| **$(NH_4)_2SO_4$ precipitation** | D-PhgAT | 29.85 | 285.60 | 9.57 | 1.86 | 60.22 |
| | $A_1$-D-PhgAT | 30.58 | 302.74 | 9.90 | 1.98 | 67.80 |
| | $A_2$-D-PhgAT | 30.70 | 297.48 | 9.69 | 1.91 | 64.57 |
| | ALAL-D-PhgAT | 32.33 | 321.68 | 9.95 | 1.90 | 66.30 |
| **Phenyl Sepharose 6 FF (HIC)** | D-PhgAT | 5.53 | 187.85 | 33.97 | 6.63 | 39.61 |
| | $A_1$-D-PhgAT | 5.56 | 198.15 | 35.64 | 7.12 | 44.37 |
| | $A_2$-D-PhgAT | 5.59 | 191.73 | 34.30 | 6.79 | 41.62 |
| | ALAL-D-PhgAT | 5.63 | 201.66 | 35.82 | 6.87 | 41.56 |
| **DEAE Sepharose FF (IEX)** | D-PhgAT | 1.58 | 136.24 | 86.23 | 16.84 | 28.73 |
| | $A_1$-D-PhgAT | 1.64 | 142.15 | 86.98 | 17.39 | 31.83 |
| | $A_2$-D-PhgAT | 1.61 | 155.70 | 86.71 | 17.17 | 33.80 |
| | ALAL-D-PhgAT | 1.68 | 146.78 | 87.37 | 16.76 | 30.25 |

## 4.7 Determination of pH effect on activity of different variants of D-PhgAT

After purification of proteins, determination of effects of different pH ranges on activity was performed according to method described in section 3.9.6. Figure 4.23 shows the effect of different pH ranges on relative activity of different variants of D-PhgAT. All variants of D-PhgAT with halophilic peptide fusion showed relatively low transamination activity at acidic and neutral pH while the activity of all variants gradually enhanced as pH shift toward alkaline condition progressed until the maximum activity was observed at CAPSO buffer pH 9.5. On the contrary at slightly elevated pH toward 10, enzyme activity diminished markedly and no significant activity was observed at pH 11. Our results aligned with the previous results [1] and attest no remarkable change in optimal pH upon halophilic peptide fusion compared WT- D-PhgAT.

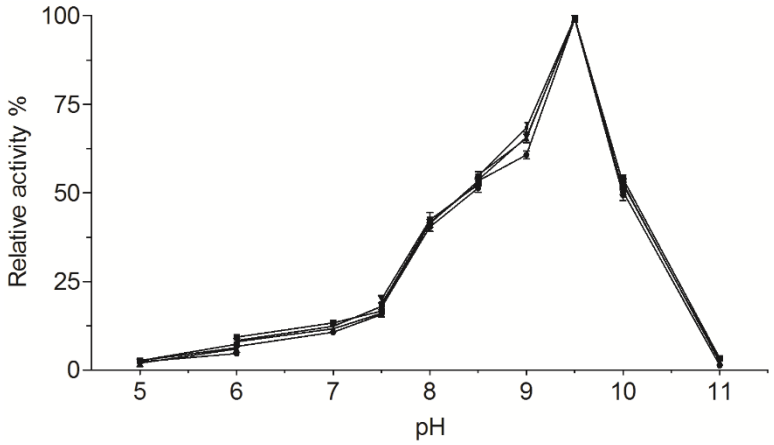


**Figure 4.24** Relative Activity of different variants of D-PhgAT in different pH related to that of wild type D-PhgAT. WT-D-PhgAT (●), $A_1$-D-PhgAT (▲), $A_2$-D-PhgAT (▼) and ALAL-D-PhgAT (■). Bars represent the standard deviation (n = 3).

## 4.8 Effects of halophilic peptide fusion on isoelectric point (p*I*) of different variants of D-PhgAT

Theoretical and experimental isoelectric points (p*I*) of different variants of D-PhgAT were determined by procedures described in section 3.2.12. Figure 4.25 shows the migration distance comparison of different variant of D-PhgAT as a function of their p*I* and table 4.2 shows calculated p*I* of these variants. Figure 4.26 shows reference curve that was used for calculation of experimental p*I*. Isoelectric point value of WT-D-PhgAT was reported to be 6.68 in previuos study [8]. In the current study p*I* value of D-PhgAT was largely reduced to 5.53, 5.76 and 5.28 by fusion of $A_1$, $A_2$ and ALAL halophilic peptides, respectively.

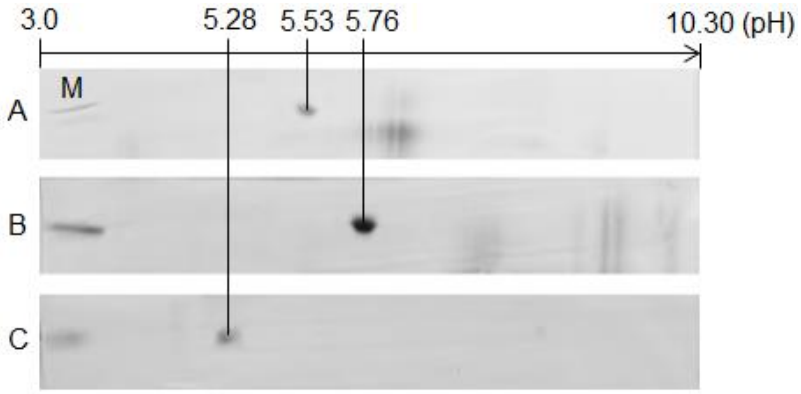


**Figure 4.25** Position of different variants of D-PhgAT after being focused on 7 cm Immobiline$^{TM}$ DryStrips pH 3-10 NL. A) $A_1$-D-PhgAT, B) $A_2$-D-PhgAT and C) ALAL-D-PhgAT. M indicates 45 kDa marker.

**Table 4.2** Experimental and calculated p*I* value of different variants of D-PhgAT. Experimental p*I* of D-PhgAT has been reported before [8].

| **D-PhgAT variants** | **Calculate p*I*** | **Experimental p*I*** |
|---|---|---|
| **WT-D-PhgAT** | 6.04 | 6.68 |
| **$A_1$-D-PhgAT** | 5.84 | 5.53 |
| **$A_2$-D-PhgAT** | 5.97 | 5.76 |
| **ALAL-D-PhgAT** | 5.39 | 5.28 |

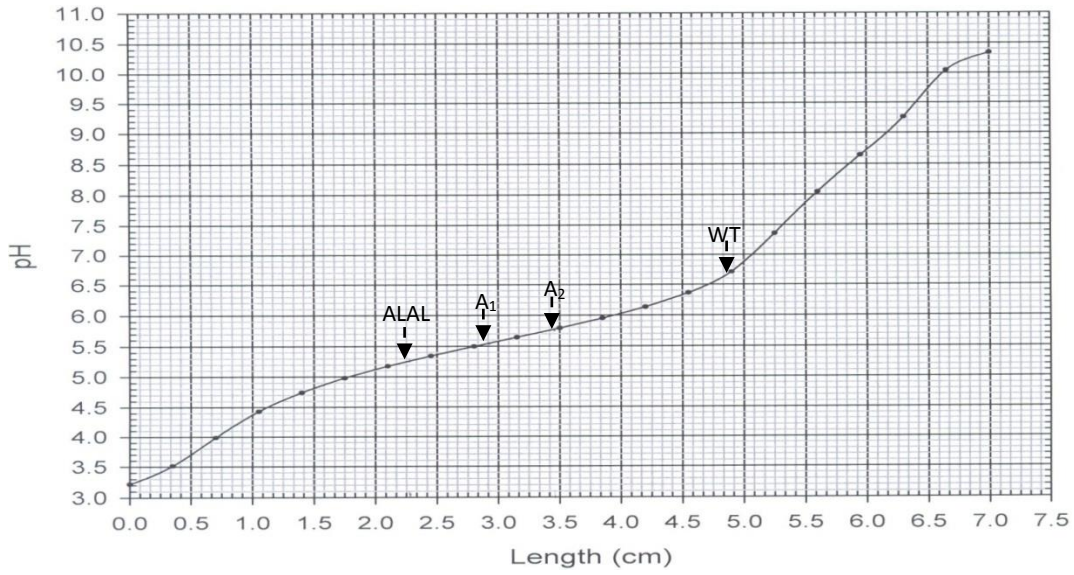


**Figure 4.26** The reference curve used for determination of p*I* value by using 7 cm Immobiline™ DryStrips pH 3-10 NL.

## 4.9 Effects of halophilic peptide fusion on solubility of D-PhgAT

The in-vitro solubility of D-PhgAT variants were determined at 25 °C in 20 mM TEMP pH 7.6 (storage) and 50 mM CAPSO pH 9.5 (reaction) buffers by concentration method as described in section 3.2.13 with a Microcon® YM-30 centrifugal device with 30 kDa membranes was used to concentrate the enzyme solution at 4000 rpm (1700 *g*) with interval quantification of protein concentration by NanoDrop® ND-1000 at $280_{nm}$ as explained in section 3.2.11.1, until no further concentration was observed. As it was expected and shown in Table 4.3, fusion of highly negative charged halophilic peptides at N-terminus domain of D-PhgAT increased the solubility of $A_1$-D-PhgAT, $A_2$-D-PhgAT and ALAL-D-PhgAT 6.1-, 5.3-, and 8.1-fold, respectively in TEMP pH 7.6 and 5-, 4.5-, and 5.9-fold in CAPSO pH 9.5 buffers compared to WT- D-PhgAT.

**Table 4.3** Summary of the solubility properties of different variants of D-PhgAT in 20 mM TEMP pH 7.6 storage and 50 mM CAPSO pH 9.5 reaction buffers (n = 3).

| Protein variants | Solubility mg/mL (solubility fold) | |
|---|---|---|
| | **20 mM TEMP pH 7.6** | **50 mM CAPSO pH 9.5** |
| WT-D-PhgAT | 6.0 ± 0.4 (1) | 12 ± 0.1 (1) |
| $A_1$-D-PhgAT | 37.0 ± 0.3 (6.1) | 61 ± 0.2 (5) |
| $A_2$-D-PhgAT | 32.0 ± 0.3(5.3) | 54 ± 0.4 (4.5) |
| ALAL-D-PhgAT | 49.0 ± 0.1 (8.1) | 71 ± 0.4 (5.9) |

## 4.10 Effects of substrate concentration on catalytic performance of D-PhgAT

Effects of various concentrations of MSG salt as a substrate on the reverse activity of D-PhgAT to produce D-Phg was determined by the HPLC method. Increasing concentrations of MSG salt in the reaction mixture resulted in proportional increase in activity of D-PhgAT and its variants up to a certain value for each but beyond that the activity start to drop (Figure 4.27). The highest reaction rate for WT-D-PhgAT was 12.56 ± 1.16 mM $h^{-1}$ with 1250 mM of MSG and those for $A_1$-D-PhgAT, $A_2$-D-PhgAT and ALAL-D-PhgAT were 17.81 ± 0.67, 20.17 ± 1.1 and 23.82 ± 1.47 mM $h^{-1}$, respectively, with 1500 mM of MSG. At higher concentrations than 1250 mM for WT-D-PhgAT and 1500 mM for the halophilic fused variants the reaction rates diminished gradually. Surprisingly, the activity of $A_2$-D-PhgAT was higher than that of the $A_1$-D-PhgAT at all MSG concentrations which has higher solubility compared with $A_2$-D-PhgAT. The reason for this incoherence is yet to be investigated.

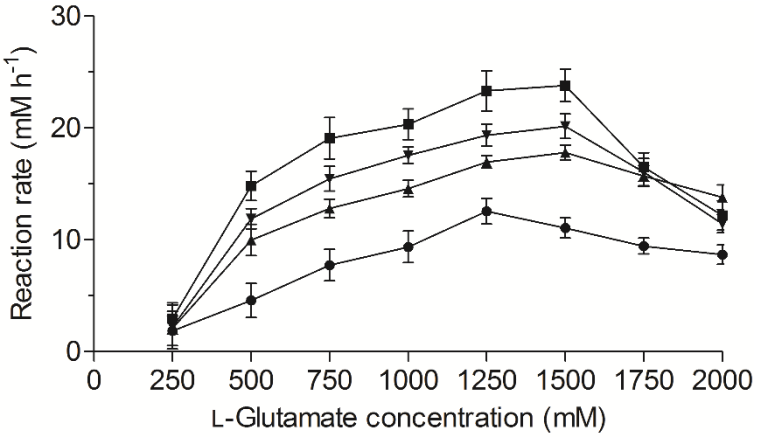


**Figure 4.27** Effect of different concentrations of L-Glutamate monosodium salt as substrate on reaction rate of WT-D-PhgAT (●), $A_1$-D-PhgAT (▲), $A_2$-D-PhgAT (▼) and ALAL-D-PhgAT (■) at 50 mM benzoylformic acid. Bars represent the standard deviation (n=3).

## 4.11 Effect of different concentrations of salts and miscible organic solvents on pH value of CAPSO pH 9.5

It is well documented that upon addition of salt or organic solvents into an enzyme solution, pH of this buffered solution may subject to change, a phenomenon that can significantly impress enzyme solubility, activity and stability [71, 72]. Therefore in order to verify the effect of salts and organic solvents on proteins, interrogation of the effect of salts and organic solvents on pH value of the enzyme buffer solution is irrevocable. In current study thymol blue was used as pH indicator with second transition, yellow to blue at pH 8.0 – 9.6, $pk_{aq}$= 8.9 in absence or presence of different proportions of salts and miscible organic solvents as described in section 3.2.14. Figure 4.28 shows maximum absorbance peak ($\lambda_{Max}$) of 50 mM CAPSO buffer with various pH values at $595_{nm}$ and used to plot reference curve (Figure 4.29) of absorbance against pH. Then different proportion of miscible organic solvents (Figures 4.30 – 4.32) or salts (Figure 4.33 – 4.34) involved into CAPSO buffer pH 9.5 in order to detect pH change. As it is shown in Table 4.4 pH was reduced as proportion of miscible organic solvents increased while in case of

inorganic salts, pH increased slightly as salts concentration increased (Table 4.5). To vanquish this hazardous pH change, CAPSO buffer with various pH used in experiments to keep pH at 9.5.

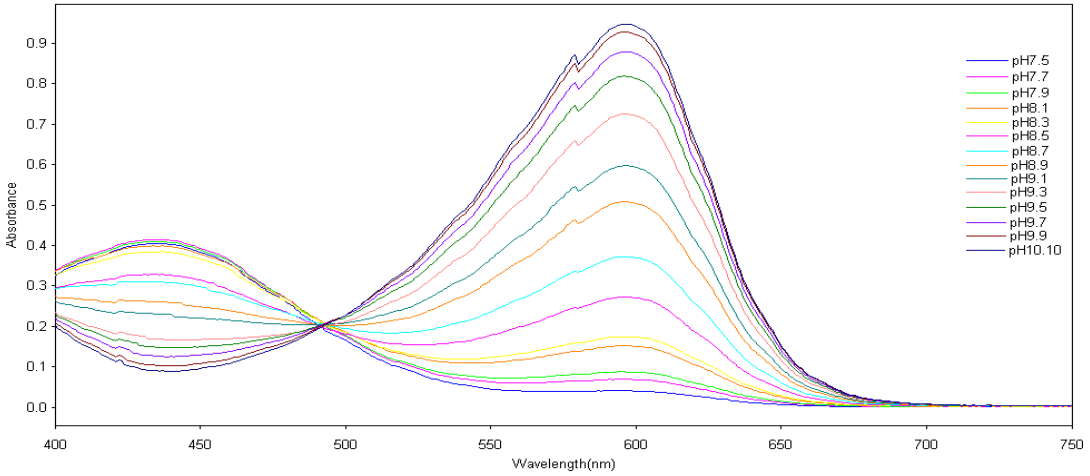


**Figure 4.28** Shows spectrogram of 50 mM CAPSO buffer with various pH values (7.5 – 10.1) in different wave lengths ($400_{nm}$ – $750_{nm}$). Isosbestic point absorbance ($\lambda_{iso}$) and maximum absorbance peak ($\lambda_{Max}$) were detected at $491_{nm}$ and $595_{nm}$, respectively. Absorbance at $\lambda_{Max}$ was used to plot reference curve.

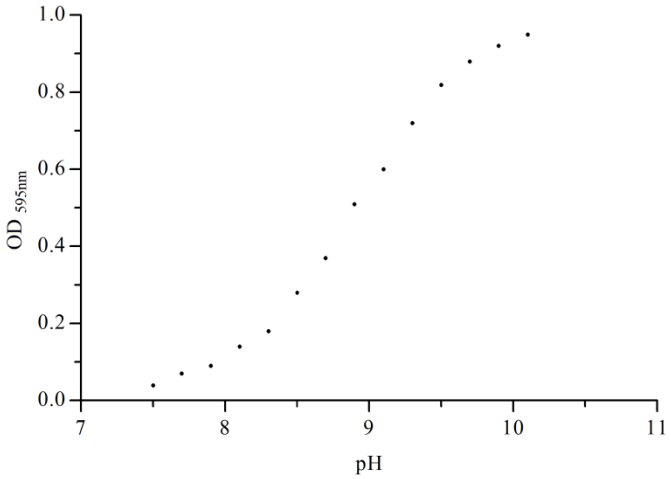


**Figure 4.29** Shows plotted reference curve which used to determine pH shift upon addition of various concentrations of salts and organic solvents.

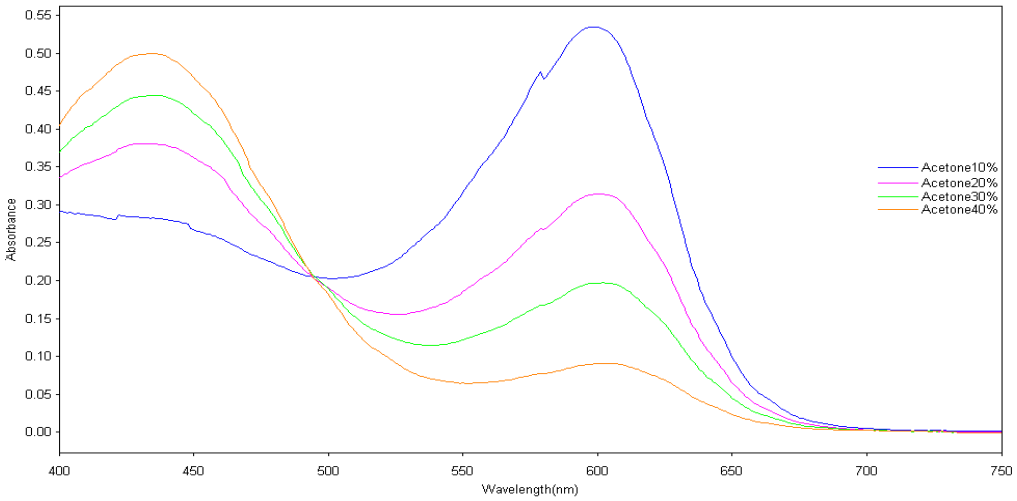


**Figure 4.30** Shows spectrogram of different concentrations of acetone in 50 mM CAPSO buffer pH 9.5 at $595_{nm}$. Change in absorbance at this wave length is due to change of pH as a function of change of acetone concentration.

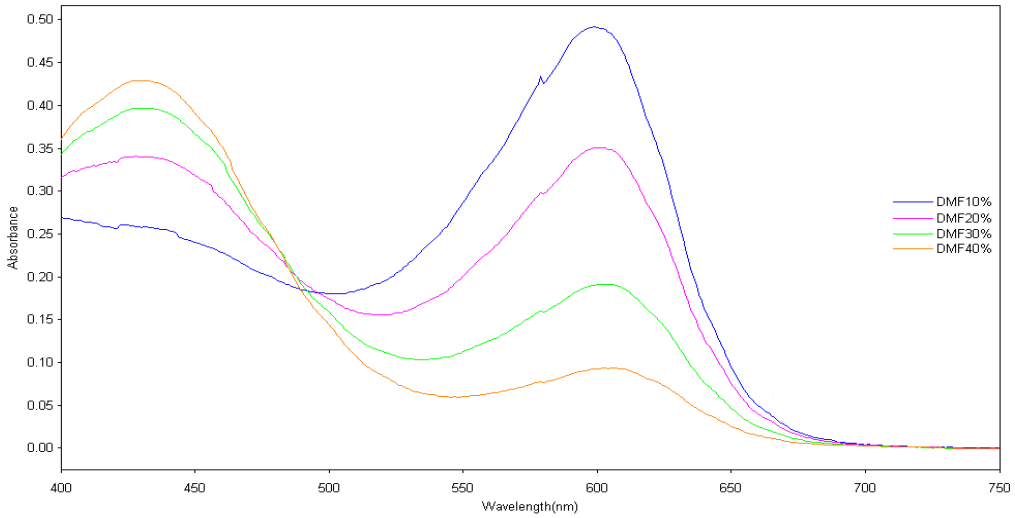


**Figure 4.31** Shows spectrogram of different concentrations of DMF in 50 mM CAPSO buffer pH 9.5 at $595_{nm}$. Change in absorbance at this wave length is due to change of pH as a function of change of DMF concentration.

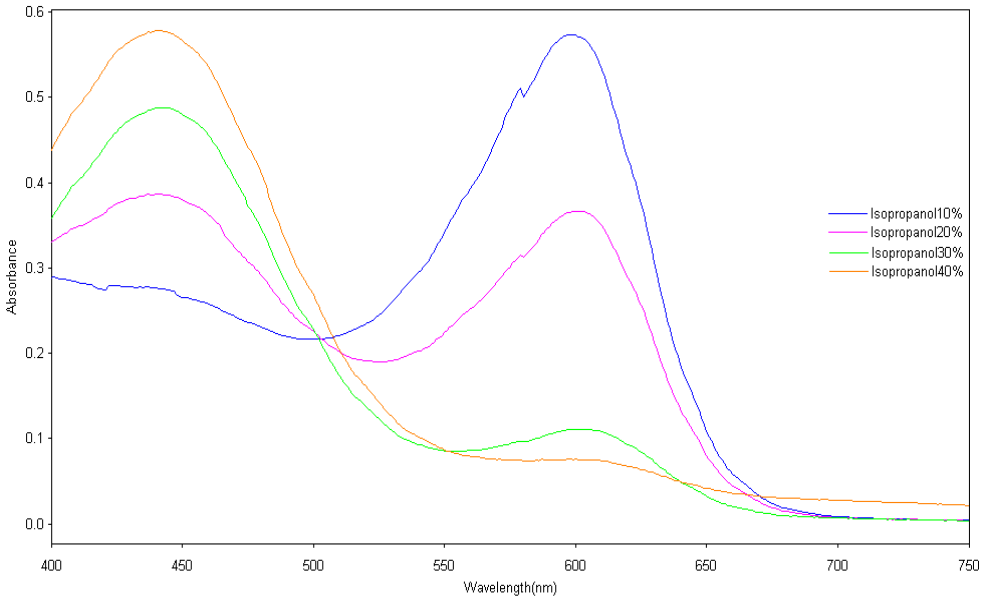


**Figure 4.32** Shows spectrogram of different concentrations of isopropanol in 50 mM CAPSO buffer pH 9.5 at $595_{nm}$. Change in absorbance at this wave length is due to change of pH as a function of change of isopropanol concentration.

**Table 4.4** Shows skewed final pH after addition of different concentrations of miscible organic solvents, change of pH and needed pH of CAPSO buffer to keep the reaction pH at 9.5.

| Organic solvent (%) | Organic solvent | Final pH | Δ pH | pH of needed CAPSO buffer |
|---|---|---|---|---|
| 10 | Acetone | 8.9 | - 0.6 | 10.1 |
| | DMF | 8.8 | - 0.7 | 10.2 |
| | Isopropanol | 9.0 | - 0.5 | 10.0 |
| 20 | Acetone | 8.6 | - 0.9 | 10.4 |
| | DMF | 8.6 | - 0.9 | 10.4 |
| | Isopropanol | 8.7 | - 0.8 | 10.3 |
| 30 | Acetone | 8.4 | - 1.1 | 10.6 |
| | DMF | 8.0 | - 1.5 | 11.0 |
| | Isopropanol | 8.0 | - 1.5 | 11.0 |
| 40 | Acetone | 7.9 | - 1.6 | 11.1 |
| | DMF | 7.8 | - 1.7 | 11.2 |
| | Isopropanol | 7.7 | - 1.8 | 11.3 |

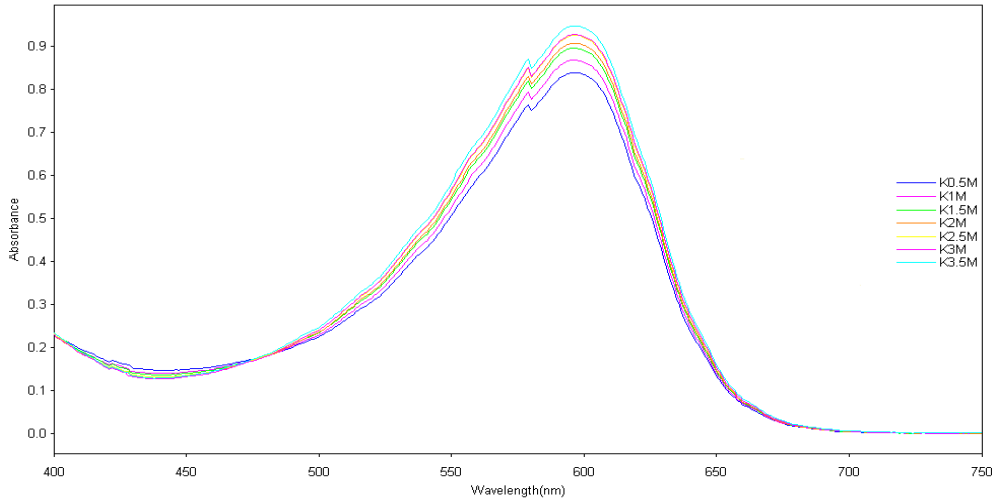


**Figure 4.33** Shows spectrogram of different concentrations of KCl in 50 mM CAPSO buffer pH 9.5 at $595_{nm}$. Change in absorbance at this wave length is due to change of pH as a function of change of KCl concentration.

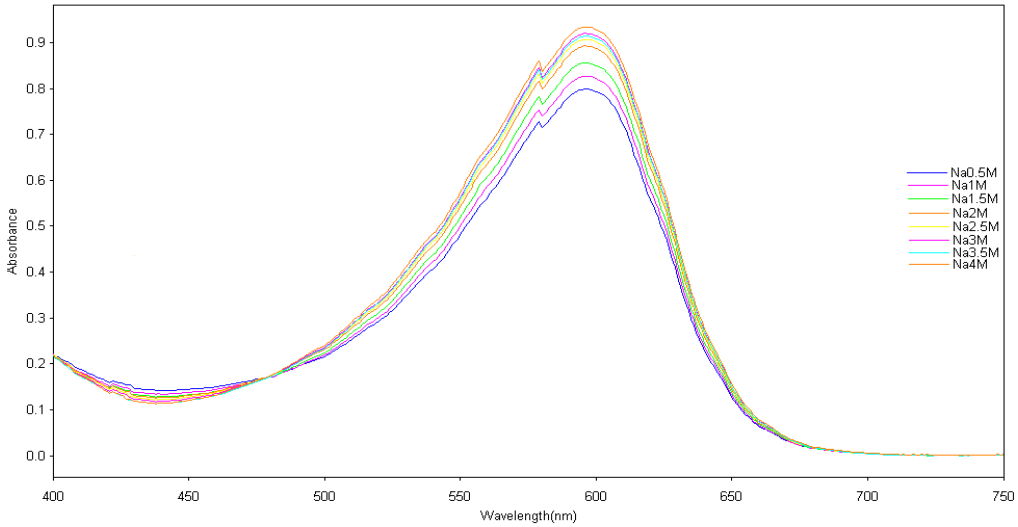


**Figure 4.34** Shows spectrogram of different concentrations of NaCl in 50 mM CAPSO buffer pH 9.5 at $595_{nm}$. Change in absorbance at this wave length is due to change of pH as a function of change of NaCl concentration.

**Table 4.5** Shows skewed final pH after addition of different concentrations of inorganic salts, change of pH and needed pH of CAPSO buffer to keep the reaction pH at 9.5.

| Inorganic salts (M) | Inorganic salts | Final pH | Δ pH | pH of needed CAPSO buffer |
|---|---|---|---|---|
| 0.5 | KCl | 9.58 | 0.08 | 9.42 |
| | NaCl | 9.50 | 0.00 | 9.50 |
| 1.0 | KCl | 9.64 | 0.14 | 9.36 |
| | NaCl | 9.50 | 0.00 | 9.50 |
| 1.5 | KCl | 9.70 | 0.20 | 9.30 |
| | NaCl | 9.51 | 0.01 | 9.49 |
| 2.0 | KCl | 9.75 | 0.25 | 9.25 |
| | NaCl | 9.53 | 0.03 | 9.47 |
| 2.5 | KCl | 9.80 | 0.30 | 9.20 |
| | NaCl | 9.57 | 0.07 | 9.43 |
| 3.0 | KCl | 9.85 | 0.35 | 9.15 |
| | NaCl | 9.59 | 0.09 | 9.41 |
| 3.5 | KCl | 9.89 | 0.39 | 9.11 |
| | NaCl | 9.63 | 0.13 | 9.37 |

## 4.12 Effects of various concentrations of different inorganic salts and miscible organic solvents on different variants of D-PhgAT

The effect of various proportions of different inorganic salts (NaCl and KCl) and miscible organic solvents are shown in figures 4.35 and 4.36. Table 4.6 shows the miscible organic solvents and inorganic slat concentrations where 50% of enzyme activity ($C_{50}$) was remained.

### 4.12.1 Effects of various concentrations of different inorganic salts on different variants of D-PhgAT

The transamination activity of all D-PhgAT variants showed slightly decrease when salt concentration (both NaCl and KCl) increased up to 1.5 M and the dropped largely in higher concentrations. However, all variants were still active at 3.5 M salts. Study of $C_{50}$ values (Table 4.6) revealed that all variants have higher tolerance for KCl and are more active in the presence of this salt compared to NaCl. Moreover variants with halophilic peptide fusions are more active and show higher tolerance at higher salts concentrations.

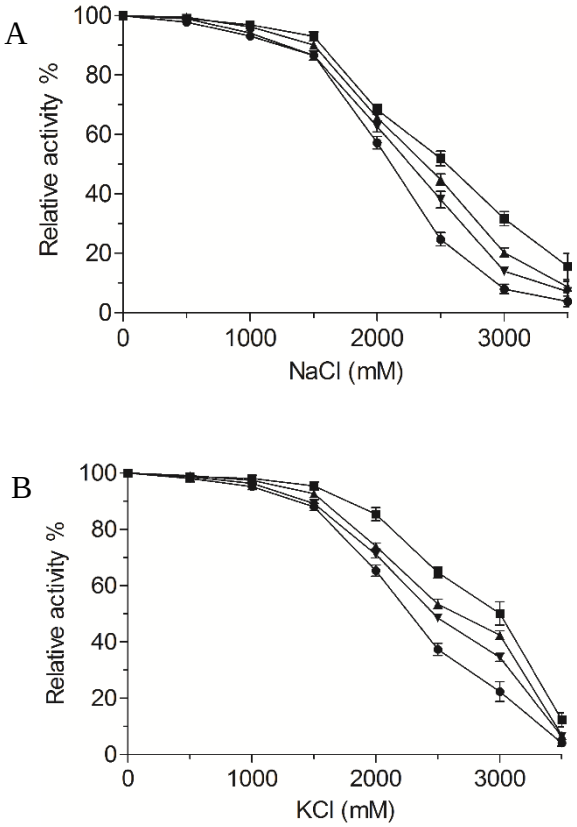


**Figure 4.35** Shows effects of various concentrations of A) NaCl and B) KCl inorganic salts on different variants of D-PhgAT. WT-D-PhgAT (●), $A_1$-D-PhgAT (▲), $A_2$-D-PhgAT (▼) and ALAL-D-PhgAT (■). Bars represent the standard deviation (n = 3).

### 4.12.2 Effects of various concentrations of different miscible organic solvents on different variants of D-PhgAT

Transamination activity of D-PhgAT was determined in reaction mixtures contained up to 40% of selected miscible organic solvents. The transamination activities of all D-PhgAT variants decreased as concentration of organic solvents increased, especially in presence of DMF and acetone where showed lower $C_{50}$ compared to that of isopropanol (Table 4.6). In all cases, halophilic fused variants have been shown to manifest higher $C_{50}$ value compared to wild type, where ALAL-D-PhgAT variant showed the highest $C_{50}$ value at presence of isopropanol.

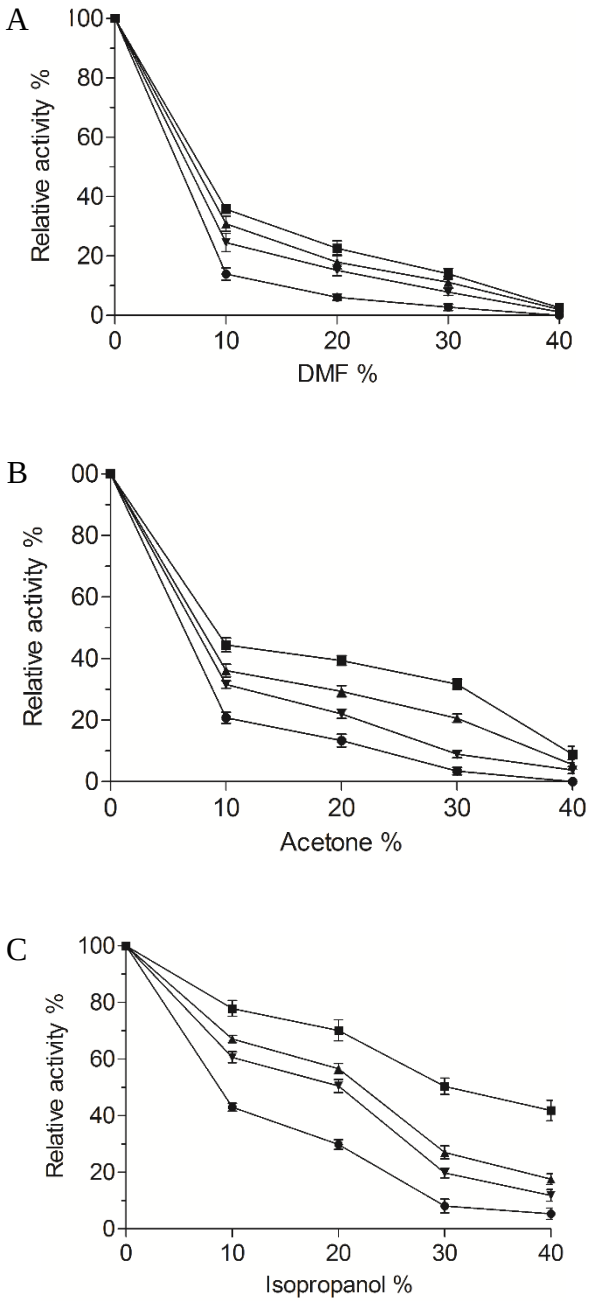


**Figure 4.36** Shows effects of various proportions of A) DMF and B) Acetone C) Isopropanol miscible organic solvents on different variants of D-PhgAT. WT-D-PhgAT (●), $A_1$-D-PhgAT (▲), $A_2$-D-PhgAT (▼) and ALAL-D-PhgAT (■). Bars represent the standard deviation (n = 3).

**Table 4.6** $C_{50}$ values of different variants of D-PhgAT in different organic solvents and salts.

| Protein variants | $C_{50}$ (% V/V) | | | $C_{50}$ (M) | |
|---|---|---|---|---|---|
| | DMF | Acetone | Isopropanol | NaCl | KCl |
| **WT-D-PhgAT** | 5.82 ± 0.86 | 6.27 ± 0.72 | 8.70 ± 0.47 | 2.10 ± 0.03 | 2.28 ± 0.05 |
| **$A_1$-D-PhgAT** | 7.22 ± 0.35 | 7.80 ± 0.49 | 22.30 ± 1.52 | 2.38 ± 0.04 | 2.65 ± 0.03 |
| **$A_2$-D-PhgAT** | 6.60 ± 0. 48 | 7.20 ± 0.53 | 20.10 ± 2.30 | 2.26 ± 0.02 | 2.46 ± 0.02 |
| **ALAL-D-PhgAT** | 7.80 ± 0.62 | 9.00 ± 0.97 | 30.20 ± 2.84 | 2.56 ± 0.03 | 3.00 ± 0.02 |

## 4.13 Thermal stability of D-PhgAT variants in absolute organic solvents

In the current study, thermal stability of different variants of D-PhgAT was determined at the presence of absolute miscible organic solvents: DMF, acetone and isopropanol at 25, 40 and 60 °C. As it is shown in figure 4.37; significant thermal stability of halophilic peptide fused variants was achieved either at the presence of miscible organic solvents or aqueous buffer which was substantially higher for ALAL-D-PhgAT variant. Amongst examined solvents, DMF (log *p*: -1.04) was shown to have highest adverse effect while comparatively isopropanol (log *p*: 0.074) has impressive thermal protective effect. The results showed that thermal stability of D-PhgAT variants were increased as the hydrophobicity of the organic solvents increased.

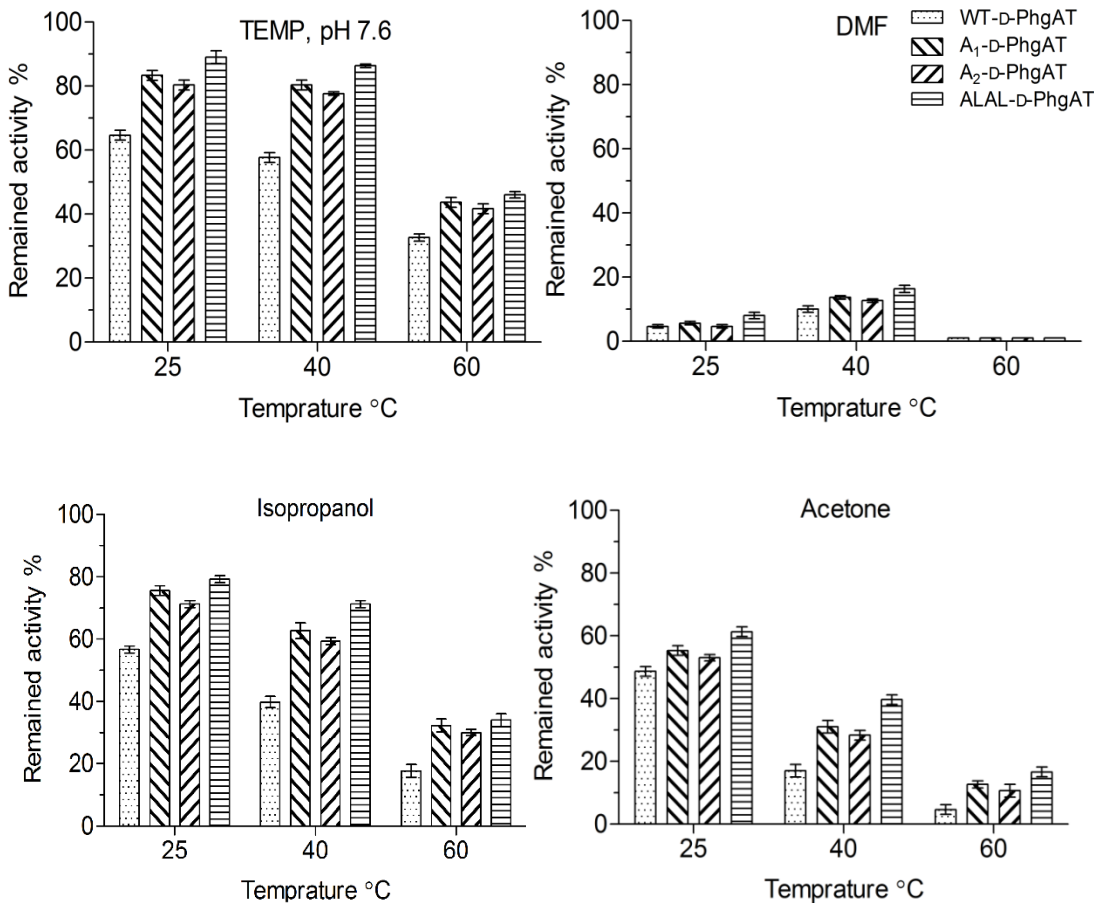


**Figure 4.37** Thermostability of different variants of D-PhgAT at TEMP buffer pH 7.6 as control and different organic solvents (DMF, acetone and isopropanol) in 1 h incubation at different temperatures (25, 40 and 60 °C). Bars represent the standard deviation (n = 3).

# CHAPTER V
# DISCUSSION

## 5.1 Construction of plasmids and expression of different variants of D-PhgAT

In order to increase solubility and stability of D-PhgAT, two optimized oligonucleotides of two α-helixes ($A_1$ and $A_2$) and a hybrid of them with the middle loop (ALAL) from *Hs* Fdx were fused at N-terminus domain of *dpgA* gene in pET-17b plasmid vector carrying the ampicillin resistance gene under T7 lac promoter. The expression happened in *E. coli* tuner (DE3) pLysS which contains a second low-level expression plasmid (pLysS) that codes for the T7 lysozyme at petty levels. This plasmid also caries chloramphenicol resistance gene. A negligible disadvantage of T7 lysozyme is the reduced expression of *dpgA* gene upon binding to T7 promoter. Addition of IPTG to 0.4 mM final concentration can increase D-PhgAT yield significantly [4].

Expression conditions of D-PhgAT were set at 20 °C, 100 rpm for 16 h. These conditions were previously reported to seek satisfactory D-PhgAT protein production up to 30% of total cell proteins [3]. All variants of D-PhgAT were expressed successfully under this system.

## 5.2 Purification of different variants of D-PhgAT and activity assay

Purification of D-PhgAT variants were successfully carried on by combination of three steps. First step was ammonium sulfate fractional precipitation. Ammonium Sulfate Precipitation as a simple and effective method of fractionating proteins is based on a simple fact that at specific salt concentration (varies for different proteins) the natural tendency of a given protein to overcome aggregation will be nullified. Since at high concentration of ammonium sulfate the surficial charges are neutralized and due to the lack of or weakened repulsive force, protein particles tend to

bind together, aggregate and form large complexes which are easy to precipitate and remove from protein suspension by centrifugation. Since aggregation of each given protein initiates at a specific salt concentration, this method provides a simple and easy way for enrichment and purification of specific proteins in a solution. In case of D-PhgAT, 25 – 45% ammonium sulfate saturation was executed with approximately 60 – 70% protein yield and 1.8 – 1.9 fold purification.

In the second step of purification, the protein pellets from ammonium sulfate fractional precipitation were dissolved in TEMP buffer pH 7.6 containing 1 M ammonium sulfate. Then this protein solution was applied on the Phenyl Sepharose 6 FF hydrophobic interaction chromatography (HIC) column which was pre-equilibrated with the same buffer. Pre-equilibration with buffers that contain high salt concentrations will eliminate free water molecules from microenvironments around highly hydrophobic ligands on the column beads (in this case phenyl residues). This step is critical for binding of hydrophobic protein particles, e.g., D-PhgAT, via their surficial hydrophobic patches and can be baffled by exceed free water molecules. Unbound proteins were washed out by two beds volume of the same buffer and subsequently bound proteins containing D-PhgAT were eluted by four beds volume of linear descending gradient of ammonium sulfate 1 – 0 M in TEMP buffer pH 7.6. In this step, 39 – 44 % yield and 6 – 7 fold of purification was achieved.

For the next step of purification, active fractions from the previous step were pooled, concentrated and desalted by using a 50 kDa cut off centrifugal device and TEMP buffer pH 7.6. Since this cut off centrifugal device has 50 kDa membrane, proteins lower than that will wash out from solution. In contrast, proteins with higher molecular weight (including D-PhgAT homodimer, 47.5 kDa each) will stay in mixture. This pooled, concentrated and desalted protein mixture was used as material for the next step of purification with DEAE Sepharose FF ion exchange chromatography (IEX) column which was pre-equilibrated by TEMP buffer pH 7.6. In contrast with HIC which separate proteins based on their differences in hydrophobicity, IEX separates them based on their differences in charge. For this approach, proteins were bound to oppositely charged chromatographic medium upon loading onto IEX column. Then unbound proteins were washed out by 2 beds volume of the same buffer. Subsequently conditions altered so bound substances, including

D-PhgAT, were eluted differentially. For elution eight beds volume of a gradually ascending gradient of sodium chloride 0 –1 M in TEMP buffer pH 7.6 was used, in which eluted proteins were substituted with $Cl^-$ ions. Then active fractions were pooled, concentrated and desalted by using a 50 kDa cut off centrifugal device and TEMP buffer pH 7.6 as mentioned above. This buffer was served as storage enzyme buffer until enzyme was used in the next experiments. In this step, 28 – 30% yield and 16 – 17 fold of purification was achieved. In each step purity and activity of D-PhgAT was monitored by SDS-PAGE and NanoDrop, respectively. This level of purification is suitable to fulfill purity requirements for the next steps of this study.

## 5.3 Determination of optimal pH activity, p*I* value and solubility of different variants of D-PhgAT

The effect of pH on activity of D-PhgAT variants was determined by spectrophotometric method. All variants of D-PhgAT displayed relatively low transamination activity at the acidic and neutral pH while the activity of all variants gradually enhanced as the pH progressively shifted toward the alkaline condition until reaching maximum at pH 9.5 (in CAPSO buffer) (Figure 4.24). Further increase in pH from 9.5 resulted in decreasing of D-PhgAT activity and no significant activity was observed at pH 11.0 and above. All D-PhgAT variants including the wild-type displayed similar pH-activity profile indicating that there was no significant structural change of the catalytic site and probably of the overall enzyme molecule upon fusion with the halophilic peptides. Our results are in alignment with the previous results and attest no remarkable change in optimal pH-activity of D-PhgAT upon halophilic peptide fusion, compared with WT-D-PhgAT.

In the current study, isoelectric pH (p*I*) values of D-PhgAT variants were determined by using the Immobiline$^{TM}$ DryStrips. Fusion of $A_1$, $A_2$ and ALAL peptides which contain 3, 2 and 13 negatively charged residues, respectively; form *H. salinarum* at the N-terminus domain of D-PhgAT significantly reduced its p*I* value compared with that of WT-D-PhgAT. As shown in Figure 4.25, p*I* values of $A_1$-D-PhgAT, $A_2$-D-PhgAT and ALAL-D-PhgAT are 5.53, 5.76 and 5.28 respectively (Table 4.2); while p*I* value of the WT-D-PhgAT was previously reported to be 6.2 [8].

This is as expected because the p*I* value of a given protein is actually related to its net charge, and the net charge of a given protein is factually related to its unique amino acid signature and p*K* of their ionizable groups at specific pH, where increasing and decreasing in number of net negatively and net positively charged residues, respectively, would result in the decrease of the protein p*I* value [73].

The in-vitro solubility of D-PhgAT variants were determined at 25 °C in TEMP pH 7.6 and CAPSO pH 9.5 buffers by concentration method. As expected and shown in Table 4.3, fusion of highly negative charged halophilic peptides at N-terminus domain of D-PhgAT increased the solubility of $A_1$-D-PhgAT, $A_2$-D-PhgAT and ALAL-D-PhgAT 6.1-, 5.3-, and 8.1-fold, respectively, in TEMP pH 7.6 storage buffer and 5-, 4.5-, and 5.9-fold in CAPSO pH 9.5 reaction buffers, compared to that of the WT-D-PhgAT. Chemically speaking, the protein solubility is the function of its total net charge and the buffer pH [74], where at pH higher than p*I*, deprotonation of residues occurred leading to stronger repulsive force between the protein molecules which consequently prevent aggregation and lead to higher solubility. The other factor that can largely affect protein solubility is the number of hydrophobic residues on the surface of a hydrophobic protein e.g., D-PhgAT. Predominantly, the hydrophobic force pushes these residues into the protein core; whoever, formation of hydrophobic patches on the surface of hydrophobic proteins is usually found. This phenomenon leads to higher tendency of proteins to aggregate, precipitate and manifests low solubility. Our results attest previous study [51] that negatively charged peptide fusion can be used to develop more soluble protein variants when highly concentrated protein is crucial. These peptide fusions with high content of polar residues interact with water molecules resulting in lowering protein-protein interaction and thereby favoring protein solubility.

## 5.4 Effects of substrate concentration on catalytic performance of D-PhgAT

Effects of various concentrations of MSG salt as a substrate on the reverse activity of D-PhgAT to produce D-Phg was determined by the HPLC method. Increasing concentrations of MSG salt in the reaction mixture resulted in proportional

increase in activity of D-PhgAT and its halophilic variants up to a certain value for each but beyond that the activity start to drop (Figure 4.27). The highest reaction rate for WT-D-PhgAT was 12.56 ± 1.16 mM $h^{-1}$ with 1250 mM of MSG and those for $A_1$-D-PhgAT, $A_2$-D-PhgAT and ALAL-D-PhgAT were 17.81 ± 0.67, 20.17 ± 1.1 and 23.82 ± 1.47 mM $h^{-1}$, respectively, with 1500 mM of MSG. At higher concentrations than 1250 mM for WT-D-PhgAT and 1500 mM for the halophilic fused variants the reaction rates diminished gradually. Surprisingly, the activity of $A_2$-D-PhgAT was higher than that of the $A_1$-D-PhgAT at all MSG concentrations which has higher solubility compared with $A_2$-D-PhgAT. The reason for this incoherence is not clear and yet to be investigated. The decrease in activity with the high concentrations of the substrate might be due to the effects of substrate inhibition or the lower substrate diffusion to the active site of the enzyme as previously suggested [68]. At 2000 mM MSG, visible precipitation of WT-D-PhgAT was observed while no precipitation was detected with those halophilic fused variants (data not shown). In addition to this after the reaction mixture was diluted till the final concentration of MSG reached 1500 mM, activity of the halophilic fused variants was partially retrieved suggesting that the decrease in activity was due to substrate inhibition rather than denaturation. Of these, ALAL-D-PhgAT displayed the highest reaction rate and the fusion with halophilic peptide improved solubility in high concentration of MSG.

## 5.5 The effects of different concentrations of salts and organic solvents on D-PhgAT activity

The effects of different proportions of miscible organic solvents or salts are show in Figures 4.34 and 4.35. Table 4.6 shows the organic solvents and salts concentrations where 50% of enzyme activity ($C_{50}$) was remained. D-PhgAT transamination activity was determined in reaction mixtures contained 10, 20, 30 and 40% of selected miscible organic solvents. The transamination activities of all D-PhgAT variants decreased as concentration of organic solvents increased, especially in presence of DMF and acetone. This phenomenon could be, at least partly, due to denaturation capacity of these solvents [72 and 75]. Since DMF and acetone have low hydrophobicity (log *p*: -1.04 and -0.20, respectively), they are potent to strip water

molecules from the hydration shell region at the expense of protein flexibility and promote denaturation and inactivation of enzyme. In the case of $A_1$-D-PhgAT, $A_2$-D-PhgAT and ALAL-D-PhgAT the fusion of halophilic peptides that contain high amounts of polar negatively charged residues serve as extra sites for binding of water molecules and maintaining the hydration shell region of protein and lead to partially preserving activity. In spite of large decrease in D-PhgAT activity in presence of DMF and acetone, this enzyme showed higher relative activity in presence of isopropanol (log *p*: 0.074) which indicate it's relatively higher hydrophobicity compared with that of the MDF and acetone. This property of isopropanol results in stripping of less water molecules from the hydration shell region of protein and thereby less denaturation and consequent inactivation of D-PhgAT variants. The highest observed activity has been seen in ALAL-D-PhgAT ($C_{50}$: 30.20 ± 2.84).

In next experiment we examined the effect of salts on D-PhgAT activity by including different proportions of NaCl and KCl in reaction mixture. All D-PhgAT variants showed slightly decrease in activity where salts concentrations (both NaCl and KCl) increased up to 1.5 M and dropped largely in higher concentrations, however all variants were still active at 3.5 M salts. The study of $C_{50}$ values revealed that all variants have higher tolerance for KCl and are more active in the presence of this salt compared with NaCl. Moreover, variants with halophilic peptide fusions are more active and show higher tolerance at higher salts proportions. Based on Hofmeister series NaCl is slightly kosmotropic and KCl is slightly chaotropic salt, therefore they manifest different enzyme inactivation mechanisms which can possibly be explained by affecting physical states of water around the enzyme molecules [54]. Kosmotropic salts which are known as water maker will interact with bulk water molecules in the solvent more than the hydrophobic surficial residues of the enzyme. This phenomenon is referred as preferential exclusion and will force to bury these non-polar residues into the core of the enzyme at the expense of protein flexibility and thereby inactivation of the enzyme. In contrast, chaotropic salts which are referred as water structure breakers are pushed away from bulk water and will interact with aqueous shell region of the enzyme or even bind to it. This phenomenon is known as preferential binding and will lead to weaken hydrophobic interactions, increased the enzyme-solvent accessible area and subsequently denaturation of the enzyme. The negatively charged residues on $A_1$,

$A_2$ and ALAL α-helixes bind to notable amounts of hydrated ions thus decrease surficial hydrophobicity, thus, lower tendency to aggregate unless at higher salt concentrations.

## 5.6 Thermal stability of D-PhgAT variants in absolute organic solvents

In this experiment, thermal stability of different variants of D-PhgAT was determined in the presence of absolute DMF, acetone and isopropanol at 25, 40 and 60 °C. As it is shown in Figure 4.37; significant thermal stability of halophilic peptide fused variants was achieved either in the presence of miscible organic solvents or aqueous buffer which was substantially higher for ALAL-D-PhgAT variant. Amongst examined solvents, DMF (log *p*: -1.04) was shown to have highest adverse effect while comparatively isopropanol (log *p*: 0.074) has impressive thermal protective effect. The results showed that thermal stability of D-PhgAT variants were increased as the hydrophobicity of the organic solvents increased. This phenomenon can be due to conformational rigidity and subsequently raised the resistance against the thermal inactivation in the presence of absolute organic solvents. In this condition and dehydrated state, a great propensity for denaturation is available but due to lack of water as molecular lubricant, the required flexibility for denaturation is absent leading to rigidity of protein [58]. This rigidity and eliminated water participation in hydrogen bonds, reduced dielectric constant and increased strong intra protein interactions cause lower activity in non-aqueous media compared to aqueous buffer. It has been reported that some other organic solvents e.g., glycerol and ethylenglycerol due to formation of multiple hydrogen bond and therefore mimic the water effect [59] and crown ether and cyclodextrins due to formation of stable supra molecular complexes and including residues amine groups in their cavities and consequently reduced inter- and intra-molecular salt bridges will enable the enzyme to adopt a catalytically more active and soluble conformation in organic solvents [50]. Our results, hereby, showed that the practiced halophilic peptide fusion at N-terminus domain of D-PhgAT in this study, can increase thermal stability of a mesophilic protein, both in aqueous and non-aqueous media.

# CHAPTER VI
# CONCLUSION

D-Phenylglycine aminotransferase from *Pseudomonas stutzeri* ST-201 is useful for enzymatic synthesis of enantiomerically pure D-phenylglycine, with invaluable biotechnological and pharmaceutical potentials. However, D-PhgAT low solubility prevents its application at high substrate concentration. To the best of our knowledge, this is the first study which successfully applies the use of the halophilic peptide fusion to increase solubility and stability of such kind of hydrophobic enzyme. With an aim to increase protein solubility, N-terminus of D-PhgAT was genetically fused with short peptides ($A_1$ α-helix, $A_2$ α-helix, and ALAL which is a hybrid of $A_1$ and $A_2$) from a ferredoxin enzyme of a halophilic archaeon, *Halobacterium salinarum*. The fused enzymes $A_1$-D-PhgAT, $A_2$-D-PhgAT and ALAL-D-PhgAT displayed reduced p*I* and increased in solubility by 6.1-, 5.3-, and 8.1-fold in TEMP pH 7.6 storage, respectively, and 5-, 4.5-, and 5.9-fold in CAPSO pH 9.5 reaction buffers, respectively, compared with WT-D-PhgAT. In addition, all the fused D-PhgAT displayed higher enzymatic reaction rate than the WT-D-PhgAT at all concentrations of L-glutamate monosodium salt used. The highest one, 23.82 ± 1.47 mM $h^{-1}$, was that obtained from having ALAL-D-PhgAT reacted with 1500 mM of the substrate. Moreover, the halophilic fusion significantly increased tolerance of D-PhgAT in the presence of NaCl and KCl with slightly in favor of KCl, where under the same condition at 3.5 M NaCl or KCl all halophilic fused variants showed higher activity than WT-D-PhgAT. Overall results of our in-vitro study clearly indicates that this method not only can increase solubility of D-PhgAT but also can interestingly increase its tolerance to high concentration of MSG as the substrate for the reverse reaction of D-PhgAT. Upon fusion of D-PhgAT with halophilic peptides, transamination activity was decreased as concentration of miscible organic solvent increased from 0 to 40%. The reduction in activity is seen to be higher in presence of less hydrophobic organic solvents. In this case the highest $C_{50}$ (30.20 ± 2.84) was seen

in presence of isopropanol and for ALAL-D-PhgAT variant. In the next study, thermal stability of different variants of D-PhgAT was determined in presence of absolute miscible organic solvents at different temperatures. The results showed that the halophilic fused variants has higher thermal stability compared with wild type in log *p* related wise that is belong to ALAL-D-PhgAT with highest remained activity (79.33 ± 1.15) at 25 °C. This discovery indicates the high potential of employing this new knowledge for production of D-phenylglycine and D-4-hydroxyphenylglycine, the essential side chain moieties for manufacturing of the highly demanded semisynthetic antibiotics e.g., penicillins and cephalosporins.

# REFERENCES


1 Wiyakrutta S and Meevootisom V. (1997). A stereo-inverting D-phenylglycine aminotransferase from *Pseudomonas stutzeri* ST-201: purification, characterization and application for D-phenylglycine synthesis. Journal of Biotechnology 55 (3): 193-203.

2 Kongsaeree, P., C. Samanchart. (2003). "Crystallization and preliminary X-ray crystallographic analysis of D-phenylglycine aminotransferase from *Pseudomonas stutzeri* ST201." Acta Crystallographica Section D 59 (5): 953-954.

3 Laowanapiban, P. (2001). D-phenylglycine aminotransferase from *Pseudomonas stutzeri* ST-201: Gene cloning, Sequence analysis, Comprative structural modeling and Over-expression in *Escherchia coli*. Ph.D., Mahidol University.

4 Jearakulprasert, M. (2008). Optimization of His-tagged D-phenylglycine animotransferase gene expresion, enzyme purification and immobilization. M.Sc, Mahidol University.

5 Leuchtenberger, W., K. Huthmacher. (2005). "Biotechnological production of amino acids and derivatives: current status and prospects." Applied Microbiology and Biotechnology 69 (1): 1-8.

6 Jariyachawalid, K., P. Laowanapiban. (2012). "Effective enhancement of *Pseudomonas stutzeri* D-phenylglycine aminotransferase functional expression in *Pichia pastoris* by co-expressing *Escherichia coli* GroEL-GroES." Microbial Cell Factories 11 (1): 47.

7 Iyer, P. V. and L. Ananthanarayan (2008). "Enzyme stability and stabilization Aqueous and non-aqueous environment." Process Biochemistry 43 (10): 1019-1032.

8 Chantarasiri, A., V. Meevootisom. (2012). "Effective Improvement of D-Phenylglycine Aminotransferase Solubility by Protein Crystal Contact

Engineering." Journal of Molecular Microbiology and Biotechnology 22 (3): 147-155.

9 Adamczak, M. (2004). "Strategies for Improving Enzymes for Efficient Biocatalysis." Food Technol. Biotechnol 42 (4): 251–264.

10 Eijsink, V. G. H., S. Gåseidnes. (2005). "Directed evolution of enzyme stability." Biomolecular Engineering 22 (1–3): 21-30.

11 Bornscheuer, U. T., G. W. Huisman. (2012). "Engineering the third wave of biocatalysis." Nature 485 (7397): 185-194.

12 Karan, R., M. Capes. (2012). "Function and biotechnology of extremophilic enzymes in low water activity." Aquatic Biosystems 8 (1): 4.

13 Marg Bl Fau - Schweimer, K., H. Schweimer K Fau - Sticht. (2005). "A two-alpha-helix extra domain mediates the halophilic character of a plant-type ferredoxin from halophilic archaea." Biochemistry 44: 29-29.

14 Copeland, R. A. (2000). Enzymes. United States of America, Wiley-VCH, Inc.

15 PrWeb (2011). "Global Industrial Enzymes Market to Reach US$3.74 Billion by 2015, According to a New Report by Global Industry Analysts, Inc." http://www.prweb.com/releases/industrial_enzymes/proteases_carbohydrases/prweb8121185.htm.

16 Xiao, J., A. Burn. (2008). Increasing Solubility of Proteins and Peptides by Site-Specific Modification with Betaine. Bioconjugate Chemistry 19 (6): 1113-1118.

17 Ciarán Ó, F. (1995). "Understanding and increasing protein stability." Biochimica et Biophysica Acta (BBA) - Protein Structure and Molecular Enzymology 1252 (1): 1-14.

18 Schmid, R. (1979). Stabilized soluble enzymes Advances in Biomedical Engineering. Springer Berlin / Heidelberg 12: 41-118.

19 Misset, O. and A. V. Dijk (1998). Diagnosing the inactivating process of enzymes. Progress in Biotechnology. F. J. P. J. L. I. A. Ballesteros and P. J. Halling, Elsevier. 15: 3-18.

20 Weingartner, H., C. Cabrele. (2012). How ionic liquids can help to stabilize native proteins. Physical Chemistry Chemical Physics 14 (2): 415-426.

21 Roberto, F. (2009). Stabilization of multimeric enzymes: Strategies to prevent subunit dissociation. Enzyme and Microbial Technology 45 (6–7): 405-418.

22 T. Satyanarayana, C. R. a. S. S. (2005). Extremophilic microbes: Diversity and perspectives. Current science 89: 78-90.

23 Deguchi, S., H. Shimoshige. (2011). "Microbial growth at hyperaccelerations up to 403,627 × *g*." Proceedings of the National Academy of Sciences.

24 Moniruzzaman, M., N. Kamiya. (2010). "Activation and stabilization of enzymes in ionic liquids." Organic & Biomolecular Chemistry 8 (13): 2887-2899.

25 Steiner, J. G. a. W. (2004). The Biocatalytic Potential of Extremophiles Extremozymes. Food Technol. Biotechnol. 42 (4): 223-235.

26 Mevarech, M., F. Frolow. (2000). "Halophilic enzymes: proteins with a grain of salt." Biophysical Chemistry 86 (2–3): 155-164.

27 Ando, N., B. Barstow. (2008). "Structural and Thermodynamic Characterization of T4 Lysozyme Mutants and the Contribution of Internal Cavities to Pressure Denaturation†." Biochemistry 47 (42): 11097-11109.

28 Pedersen, J. S., D. E. Otzen. (2002). Directed Evolution of Barnase Stability Using Proteolytic Selection. Journal of Molecular Biology 323 (1): 115-123.

29 Eijsink, V. G. H., A. Bjørk. (2004). "Rational engineering of enzyme stability." Journal of Biotechnology 113 (1–3): 105-120.

30 Ogino H Fau - Miyamoto, K., H. Miyamoto K Fau - Ishikawa. (1995). "Organic-solvent-tolerant bacterium which secretes organic-solvent-stable lipolytic enzyme." Appl Environ Microbiol. 61 (12): 4258–4262.

31 Plou, F. J., M. V. Calvo. (1998). Stabilization of hydrolases by chemical modification with fatty acids or polyethylene glycol. Progress in Biotechnology. F. J. P. J. L. I. A. Ballesteros and P. J. Halling, Elsevier. 15: 115-120.

32 Inada, Y., M. Furukawa. (1995). "Biomedical and biotechnological applications of PEG- and PM-modified proteins." Trends in Biotechnology 13 (3): 86-91.

33 López-Gallego, F., T. Montes. (2005). "Improved stabilization of chemically aminated enzymes via multipoint covalent attachment on glyoxyl supports." Journal of Biotechnology 116 (1): 1-10.

34 Fernández, M., A. Fragoso. (2005). "Stabilization of α-chymotrypsin by chemical modification with monoamine cyclodextrin." Process Biochemistry 40 (6): 2091-2094.

35 Mateo, C., J. M. Palomo. (2007). "Improvement of enzyme activity, stability and selectivity via immobilization techniques." Enzyme and Microbial Technology 40 (6): 1451-1463.

36 Fernandez–Lafuente, R., J. M. Guisan. (2000). "Immobilization of functionally unstable catechol-2,3-dioxygenase greatly improves operational stability." Enzyme and Microbial Technology 26 (8): 568-573.

37 Fukuchi, Satoshi, Yoshimune, Kazuaki, Wakayama, Mamoru, Moriguchi, Mitsuaki, Nishikawa, Ken. (2003). Unique Amino Acid Composition of Proteins in Halophilic Bacteria. Journal of Molecular Biology. 327 (2): 347-357.

38 Mozhaev, V. V., Y. L. Khmelnitsky. (1989). "Catalytic activity and denaturation of enzymes in water/organic cosolvent mixtures." European Journal of Biochemistry 184 (3): 597-602.

39 Silva, C., C. J. Silva. (2007). Laccase immobilization on enzymatically functionalized polyamide 6,6 fibres. Enzyme and Microbial Technology 41 (6–7): 867-875.

40 Nita, M., A. Raducan. (2007). "Stabilization of catalase in the presence of additives." Analele Universitatii Bucuresti Chimie 16 (9): 1-5.

41 Haard, N. F. (1998). "Specialty enzymes from marine organisms." Food Technology 52 (7): 64–67.

42 Karaseva Ei Fau - Metelitsa, D. I. and D. I. Metelitsa. (2006). "Stabilization of glucoso-6-phosphate dehydrogenase by its substrate and cofactor in an ultrasonic field." Russ J Bioorg Chem 32 (5):485-93.

43 Khajeh, K., M. M. Shokri. (2006). "Acidic and proteolytic digestion of α-amylases from Bacillus licheniformis and Bacillus amyloliquefaciens:

Stability and flexibility analysis." Enzyme and Microbial Technology 38 (3–4): 422-428.

44 Yanli Mi, G. W., Laura Thoma (2004). Cryoprotection Mechanisms of Polyethylene Glycols on Lactate Dehydrogenase During Freeze-thawing. The aaps journal 6 (3): 45–54.

45 Bhatnagar, B. S., M. J. Pikal. (2008). "Study of the individual contributions of ice formation and freeze-concentration on isothermal stability of lactate dehydrogenase during freezing." Journal of Pharmaceutical Sciences 97 (2): 798-814.

46 Yoon, S.-H. and J. F. Robyt (2005). Activation and stabilization of 10 starch-degrading enzymes by Triton X-100, polyethylene glycols, and polyvinyl alcohols. Enzyme and Microbial Technology 37 (5): 556-562.

47 Smialowski, P., A. J. Martin-Galiano. (2007). Protein solubility: sequence based prediction and experimental verification. Bioinformatics 23 (19): 2536-2542.

48 Trevino, S. R., J. M. Scholtz. (2007). Amino Acid Contribution to Protein Solubility: Asp, Glu, and Ser Contribute more Favorably than the other Hydrophilic Amino Acids in RNase Sa. Journal of Molecular Biology 366 (2): 449-460.

49 Golovanov, A. P., G. M. Hautbergue. (2004). "A Simple Method for Improving Protein Solubility and Long-Term Stability." Journal of the American Chemical Society 126 (29): 8933-8939.

50 Mine, Y., K. Fukunaga. (2003). "Enhanced enzyme activity and enantioselectivity of lipases in organic solvents by crown ethers and cyclodextrins." Journal of Bioscience and Bioengineering 95 (5): 441-447.

51 Lee, E., Y. Kim. (2005). "Stabilizing Peptide Fusion for Solving the Stability and Solubility Problems of Therapeutic Proteins." Pharmaceutical Research 22 (10): 1735-1746.

52 Islam, M. M., M. A. Khan. (2012). "Analysis of amino acid contributions to protein solubility using short peptide tags fused to a simplified BPTI variant." Biochimica et Biophysica Acta (BBA) - Proteins and Proteomics 1824 (10): 1144-1150.

53 Seishi Shimizu, W. M. M. a. N. M. (2006). The Hofmeister series and protein-salt interactions. Journal of Chemical Physics 124 (23): 234905-234909.

54 Moelbert, S., B. Normand. (2004). "Kosmotropes and chaotropes: modelling preferential exclusion, binding and aggregate stability." Biophysical Chemistry 112 (1): 45-57.

55 Vreeland, R. H., W. D. Rosenzweig. (2000). Isolation of a 250 million-year-old halotolerant bacterium from a primary salt crystal. Nature 407 (6806): 897-900.

56 Tehei, M., B. Franzetti. (2002). The search for traces of life: the protective effect of salt on biological macromolecules. Extremophiles 6 (5): 427-430.

57 Grant, W. D. (2004). "Life at low water activity." Philosophical Transactions of the Royal Society of London. Series B: Biological Sciences 359 (1448): 1249-1267.

58 Hartsough, D. S. and K. M. Merz (1992). "Protein flexibility in aqueous and nonaqueous solutions." Journal of the American Chemical Society 114 (26): 10113-10116.

59 Torres, S. and G. R. Castro (2004). Non-Aqueous Biocatalysis in Homogeneous Solvent Systems. Enzyme 42 (4): 271-277.

60 Rubin-Pitel, S. B. and H. Zhao (2006). Recent Advances in Biocatalysis by Directed Enzyme Evolution. Comb Chem High Throughput Screen 9 (4): 247-257.

61 Klibanov, A. M. (2001). "Improving enzymes by using them in organic solvents." Nature 409 (6817): 241-246.

62 Tebbe, A., C. Klein. (2005). Analysis of the cytosolic proteome of Halobacterium salinarum and its implication for genome annotation. Proteomics 5 (1): 168-179.

63 Fukuchi, S., K. Yoshimune. (2003). "Unique Amino Acid Composition of Proteins in Halophilic Bacteria." Journal of Molecular Biology 327 (2): 347-357.

63 Tadeo, X., B. López-Méndez. (2009). Structural Basis for the Aminoacid Composition of Proteins from Halophilic Archea. PLoS Biol 7 (12): 1000257.

64 Paul S Fau - Bag, S. K., S. Bag Sk Fau - Das. (2008). Molecular signature of hypersaline adaptation: insights from genome and proteome composition of halophilic prokaryotes. Genome Biology 9 (4): article R 70.

65 Bandyopadhyay Ak Fau - Krishnamoorthy, G., H. M. Krishnamoorthy G Fau - Sonawat. (2001). "Structural stabilization of [2Fe-2S] ferredoxin from *Halobacterium salinarum*." Biochemistry 40 (5): 1284-1292.

66 Puigbò, Pere, Guzmán, Eduard, Romeu, Antoni, Garcia-Vallvé, Santiago. (2007). OPTIMIZER: a web server for optimizing the codon usage of DNA sequences. Nucleic Acids Research. 35 (2): 126-131.

67 Zhiming Tu, G. H. a. K. X. L. (2005). An improved system for competent cell preparation and high efficiency plasmid transformation using different Escherichia coli strains. Electronic Journal of Biotechnology 8 (1): 114-120.

68 Rojanarata, T., D. Isarangkul. (2004). Controlled-release biocatalysis for the synthesis of D-phenylglycine. Biocatalysis and Biotransformation 22 (3): 195-201.

69 Vignesh D Fau - Parameswari, Paul, Parameswari P Fau - Jin, Kim Hae, Jin Kh Fau - Pyo, Lim Yong. (2010). SeqCalc: A portable bioinformatics software for sequence analysis. Bioinformation 5 (3): 85-88.

70 Evans, P., Wyatt, K., Wistow, G. J., Bateman, O. A., Wallace, B. A., Slingsby, C. (2004). The P23T Cataract Mutation Causes Loss of Solubility of Folded γD-Crystallin. Journal of Molecular Biology. 343 (2): 435-444.

71 Mozhaev, V. V., M. V. Sergeeva. (1990). "Multipoint attachment to a support protects enzyme from inactivation by organic solvents: α-Chymotrypsin in aqueous solutions of alcohols and diols." Biotechnology and Bioengineering 35 (7): 653-659.

72 Miroliaei, M. and M. Nemat-Gorgani (2002). "Effect of organic solvents on stability and activity of two related alcohol dehydrogenases: a comparative study." The International Journal of Biochemistry & Cell Biology 34 (2): 169-175.

73 Shaw, K. L., G. R. Grimsley. (2001). The effect of net charge on the solubility, activity, and stability of ribonuclease Sa. Protein Science 10 (6): 1206-1215.

74 Nick Pace, C., S. Treviño. (2004). "Protein structure, stability and solubility in water and other solvents." Philosophical Transactions of the Royal Society of London. Series B: Biological Sciences 359 (1448): 1225-1235.

75 Khmelnitsky, Y. L., V. V. Mozhaev. (1991). "Denaturation capacity: a new quantitative criterion for selection of organic solvents as reaction media in biocatalysis." European Journal of Biochemistry 198 (1): 31-41.

# APPENDIX

# CULTURE MEDIA, REAGENTS, BUFFERS AND CHEMICAL SOLUTIONS USED IN CURRENT STUDY

## 1. Culture media

### 1.1 Luria Bertani (LB) broth and agar, 1 Lit

| | |
|---|---|
| Tryptone | 10 g |
| Yeast extract | 5.0 g |
| NaCl | 10 g |

Adjust to pH 7.0 if necessary and sterilize by autoclaving at 121 °C for 15 min. For L.B. agar medium, 1.5% agar was added prior to autoclaving and approximately 20 mL of medium was poured into 100 mm plates.

### 1.2 Luria Bertani (LB) agar, low salt, 1 Lit

| | |
|---|---|
| Tryptone | 10 g |
| Yeast extract | 5.0 g |
| NaCl | 5.0 g |
| Agar | 15 g |

Adjust to pH 7.0 if necessary and sterilize by autoclaving at 121 °C for 15 min. Approximately 20 mL of medium was poured into 100 mm plates.

### 1.3 Super Optimal broth with Catabolite repression (SOC broth), 1 Lit

| | |
|---|---|
| Tryptone | 20 g |
| Yeast extract | 5 g |
| NaCl | 584.4 mg |
| $MgCl_2.6H_2O$ | 508.2 mg |
| $MgSO_4.H_2O$ | 1.348 g |

Adjust to pH 7.0 if necessary and sterilize by autoclaving at 121 °C for 15 min. For S.O.C agar medium, 1.5% agar was added prior to autoclaving. Medium was allowed to cool down to 50 °C and then glucose from a 1 M filter sterilized (0.45 µm MILLEX®HA Filter Unit) stock solution was added to a final concentration of 20 mM. Approximately 20 mL of the medium was poured into 100 mm plates.

## 2. Reagents and buffers used for agarose gel electrophoresis

### 2.1 Loading Dye

Commercially available 6X DNA loading dye, Fermentas #R0611 was used.

### 2.2 TBE buffer (10X stock), 1 Lit

| | |
|---|---|
| Tris-base | 108 g |
| Boric acid | 55 g |
| EDTA (0.5 M pH 8.0) | 40 ml |

TBE buffer was sterilized by autoclaving and kept at 4 °C. 10X TBE buffer was diluted to appropriate concentration just prior to use.

## 3. Preparation and transformation of competent *E. coli* cells

### 3.1 TB ($CaCl_2$) solution, 1 Lit

| | |
|---|---|
| PIPES | 3.021 g |
| $CaCl_2.2H_2O$ | 2.205 g |
| KCl | 18.637 g |

Adjust to pH 6.7 with 1 M KOH and then 10.88 g of $MnCl_2.4H_2O$ was added. Then the solution was filter sterilized by using 0.45 µm MILLEX®HA Filter Unit and kept at 4 °C until used. TB ($CaCl_2$) solution was used ice chilled.

### 3.2 Dimethyl sulfoxide (DMSO) 40%

Forty µL of DMSO was mixed with 60 µL of sterilized deionized water in 1.5 mL Eppendorf tube and kept at -20 °C until use. One µL of 40% DMSO was used in transformation protocol.

## 4. Antibiotics

### 4.1 Ampicillin stock solution (100 mg/mL)

For preparation of ampicillin stock solution, 1 g of ampicillin as sodium salt was dissolved in sterilized deionized water to final volume of 10 mL. Solution was filter sterilized by using 0.45 µm MILLEX®HA Filter Unit and 1 mL aliquots was kept at -20 °C until use.

### 4.2 chloramphenicol stock solution (34 mg/mL)

For preparation of chloramphenicol stock solution, 340 mg of chloramphenicol was dissolved in 10 mL absolute ethanol and stored at -20 °C until used.

## 5. Purification of protein

### 5.1 Lysis buffer pH 7.6

| | |
|---|---|
| Tris | 20 mM |
| EDTA pH 8.0 | 1 mM |
| β-mercaptoethanol | 0.01% |
| Pyrodoxal-5′-phosphate (PLP) | 100 µM |

The pH of solution was adjusted to 7.6 by 1 M HCl solution and then was filtered through 0.45 µm cellulose acetate membrane just prior to use by vacuum filtration.

**5.2 TEMP buffer pH 7.6**

| | |
|---|---|
| Tris | 20 mM |
| EDTA pH 8.0 | 1 mM |
| β-mercaptoethanol | 0.01% |
| Pyrodoxal-5′-phosphate (PLP) | 2.5 µM |

The pH of solution was adjusted to 7.6 by 1 M HCl solution and then to eliminate air bubbles and any solid particle, buffer was filtered through 0.45 µm cellulose acetate membrane by vacuum filtration just prior to use.

**5.3 TEMP buffer pH 7.6 containing 1 M ammonium sulfate**

One liter of TEMP buffer pH 7.6 prepared with the same receipt in appendix 5.2 containing 1 M ammonium sulfate (132.14 g) and was filtered through 0.45 µm cellulose acetate membrane by vacuum filtration to eliminate air bubbles and any solid particle just prior to use.

**5.4 TEMP buffer pH 7.6 containing 1 M sodium chloride**

One liter of TEMP buffer pH 7.6 prepared with the same receipt in appendix 5.2 containing 1 M sodium chloride (58.44 g) and was filtered through 0.45 µm cellulose acetate membrane by vacuum filtration to eliminate air bubbles and any solid particle just prior to use.

## 6. D-PhgAT kinetic assay

Reaction mixture with 1000 µL final volume contains:

| | |
|---|---|
| D-4-hydroxyphenylglycine | 10 mM |
| α-ketoglutarate | 10 mM |
| CAPSO buffer pH 9.5 | 50 mM |
| Pyrodoxal-5′-phosphate (PLP) | 5 µM |
| EDTA | 5 µM |
| Sterilized deionized water* | *** |

| | |
|---|---|
| protein sample | 20 µL |

*Sterilized deionized water was added to final volume of 980 µL. Reaction was monitored at $340_{nm}$ for 180 sec upon addition of 20 µL protein sample.

## 7. SDS-PAGE gel electrophoresis

### 7.1 Separating 12% polyacrylamide gel (one gel with 1 mm spacer)

| | |
|---|---|
| Sterilized deionized water | 1.675 mL |
| Tris-HCl pH 8.8 1.5 M | 1.25 mL |
| SDS 10% solution | 50 µL |
| Polyacrylamide 30% solution | 2 mL |
| Ammonium persulfate 10% solution | 25 µL |
| TEMED | 2.5 µL |

### 7.2 Stacking 4% polyacrylamide gel (one gel with 1mm spacer)

| | |
|---|---|
| Sterilized deionized water | 1.5 mL |
| Tris-HCl pH 8.8 1.5 M | 0.625 mL |
| SDS 10% solution | 25 µL |
| Polyacrylamide 30% solution | 0.325 mL |
| Ammonium persulfate 10% solution | 12.5 µL |
| TEMED | 2.5 µL |

### 7.3 5X SDS-PAGE sample loading buffer (5 mL stock solution)

| | |
|---|---|
| Tris-HCl pH 6.8 0.5 M | 0.625 mL |
| SDS 10% solution | 1 mL |
| Glycerol | 0.5 mL |
| β-mercaptoethanol | 0.25 mL |
| Bromophenol blue 0.05% solution | 0.125 mL |
| Sterilized deionized water | 2.5 mL |

**7.4 10X SDS-PAGE running buffer (1 liter stock solution)**

| | |
|---|---|
| Tris base | 30g |
| Glycine | 144g |
| SDS 10% solution | 100 mL |

SDS-PAGE running buffer is not autoclavable. In case of long term storage, only Tris base and glycine solution was autoclaved and SDS was added just prior to use. 10X buffer was diluted with sterilized deionized water to 1X working buffer prior to use.

## 8. Coomassie blue staining and destaining

**8.1 Coomassie blue staining solution (500 mL)**

| | |
|---|---|
| Coomassie Blue R-250 | 0.5g |
| Methanol | 200 mL |
| Glacial acetic acid | 50 mL |
| Sterilized deionized water | 250 mL |

**8.2 Destaining solution I (1 liter)**

| | |
|---|---|
| Methanol | 400 mL |
| Glacial acetic acid | 70 mL |
| Sterilized deionized water | 530 mL |

**8.3 Destaining solution II (1 liter)**

| | |
|---|---|
| Methanol | 50 mL |
| Glacial acetic acid | 70 mL |
| Sterilized deionized water | 880 mL |

## 9. Isoelectric focusing (IEF) reagents

### 9.1 Rehydration buffer (5 mL stock solution)

| | |
|---|---|
| Urea | 2.4 g |
| CHAPS | 0.1 g |
| IPG buffer | 25 µL |
| Bromophenol blue | trace grains |

Volume was adjusted to 5 mL with sterilized deionized water. Rehydration buffer was kept as -20 °C in 200 µL aliquots until use. Dithiothreitol (DTT) was added freshly to rehydration buffer to final concentration of 100 mM just prior to use.

### 9.2 SDS equilibration solution (10 mL)

| | |
|---|---|
| Tris-HCl pH 8.8 1.5 M | 0.335 mL |
| Urea | 3.6 g |
| Glycerol | 3 mL |
| SDS | 0.2 g |
| Bromophenol blue | trace grains |

SDS equilibration solution was kept at -20 °C until use. 100 mg dithiothreitol was added freshly to 10 mL of SDS equilibration solution just prior to use.

## 10. Reagents and buffers for plasmid extraction (Alkaline lysis)

### 10.1 Buffer P1, 100 mL

| | |
|---|---|
| Glucose | 50 mM |
| Tris-HCl pH 8.0 | 25 mM |
| EDTA pH 8.0 | 10 mM |

This buffer is commercially available and supplied with QIAprep® Spin Miniprep Kit (QIAGEN). In case of preparation in lab, this buffer was sterilized by using 0.45 µm

MILLEX®HA Filter Unit and kept at 4 °C until used. Just prior to use, 10 mg Ribonuclease A (RNase A) was added.

**10.2 Buffer P2**

| | |
|---|---|
| NaOH | 0.2 N |
| SDS | 1% (w/v) |

This buffer is commercially available and supplied with QIAprep® Spin Miniprep Kit (QIAGEN). In case of preparation in lab, 0.4 N NaOH and 2% (w/v) SDS should be prepared separately and mix at a ratio of 1:1 just prior to use and store at room temperature.

**10.3 Buffer N3, 100 mL**

| | |
|---|---|
| Potassium acetate (5 M stock solution) | 60 mL |
| Glacial acetic acid | 11.5 mL |
| Distilled water | 28.5 mL |

This prepared N3 buffer is 3 M and 5 M for potassium and acetate respectively. This buffer could be autoclaved at 121 °C for 15 min and then stored at room temperature.

**10.4 TE buffer (10X stock solution)**

| | |
|---|---|
| Tris-HCl pH 8.0 | 100 mM |
| EDTA pH 8.0 | 10 mM |

This buffer could be autoclaved at 121 °C for 15 min and then stored at room temperature.

## 11. Chemical solutions

**11.1 α-ketoglutarate (100 mM)**

Fresh 0.1 M solution of α-ketoglutarate was prepared just prior to use by dissolving 0.191 g of α-ketoglutarate disodium salt in 9 mL distilled water. After dissolving, solution final volume was adjusted to 10 mL. Solution was sterilized by using 0.45 µm MILLEX®HA Filter and kept on ice until use for no longer than 48 h.

### 11.2 Acrylamide solution (30%)

High purity 30% acrylamide/bis-acrylamide solution with total monomer to cross-linker ration of 37.5:1 (2.6% C) was obtained from Bio-Rad® (China) as a safer alternative to handling acrylamide powder. In case of preparing this solution in laboratory under safety control, 141.1 g of acrylamide and 3.9 g of *N*′,*N*′-bis-methylene-acrylamide were heated at 37 °C in 800 mL distilled water. Final volume was adjusted to 1000 mL by distilled water. Solution, then, was filtered by using 0.45 µm MILLEX®HA Filter and stored in dark bottle at 4 °C until use.

### 11.3 Ammonium persulfate solution (10%)

Fresh 10% solution of ammonium persulfate was prepared just prior to use. For preparation of this solution, 10 mg of highly pure ammonium sulfate (Bio-Rad, USA) was dissolved in 100 µL distilled water by vigorous mixing in a micro centrifuge tube. This solution stored at 4 °C and is best to be used in 2 weeks.

### 11.4 CAPS buffer (250 mM)

For preparation of 250 mM stock of CAPS ((3-[Cyclohexylamino]-1-propane-sulfonic acid)) buffer, 5.532 g of powder was dissolved in 90 mL distilled water and pH was adjusted to 10-11. Distilled water was added to adjust to final volume of 100 mL. This solution was autoclave sterilized for 15 min at 121 °C and stored at 4 °C until use.

### 11.5 CAPSO buffer (500 mM, 10X)

For preparation of 500 mM stock of CAPSO **(**3-(Cyclohexylamino)-2-hydroxy-1-propanesulfonic acid) buffer, 11.86 g of CAPSO powder (anhydrous) was dissolved in 90 mL of distilled water and pH was adjusted to 9.5. Distilled water was added to adjust to final volume of 100 mL. This solution was autoclave sterilized for 15 min at 121 °C and stored at 4 °C until use.

### 11.6 Citrate buffer (250 mM)

For preparation of 250 mM stock of citrate buffer, 5.25 g of citric acid monohydrate powder was dissolved in 90 mL of distilled water and pH was adjusted

to desire working value. Distilled water was added to adjust to final volume of 100 mL. This solution was autoclave sterilized for 15 min at 121 °C and stored at 4 °C until use.

**11.7 D-4-hydroxyphenylglycine (100 mM)**

Fresh 100 mM solution of D-4-hydroxyphenylglycine was prepared just prior to use. For preparation of this solution, 0.167 g of D-4-hydroxyphenylglycine was dissolved in 10 mL distilled water and stored at 4 °C until use for no longer than 24 h.

**11.8 KCl solution (4 M)**

For preparation of 4 M stock of KCl solution, 7.45 g of KCl powder was dissolved in distilled water to final volume of 100 mL. This solution was autoclave sterilized for 15 min at 121 °C and stored at room temperature until use.

**11.9 NaCl solution (5 M)**

For preparation of 5 M stock of NaCl solution, 29.22 g of NaCl powder was dissolved in distilled water to final volume of 100 mL. This solution was autoclave sterilized for 15 min at 121 °C and stored at room temperature until use.

**11.10 PIPES buffer (250 mM)**

For preparation of 250 mM stock of PIPES sodium salt (Piperazine-N,N′-bis-(Ethanesulfonic acid)) buffer, 8.38 g of powder was dissolved in 90 mL distilled water and pH was adjusted to desired working value. Distilled water was added to adjust to final volume of 100 mL. This solution was autoclave sterilized for 15 min at 121 °C and stored at 4 °C until use.

**11.11 PLP (25 mM)**

For preparation of 250 mM stock of PLP (Pyrodoxal-5′-Phosphate) solution, 0.061 g of powder was dissolved in 10 mL distilled. Solution, then, was filtered by using 0.45 µm MILLEX®HA Filter and 1 mL aliquots were stored in 1.5 mL micro-centrifuge tubes at -20 °C until use.

### 11.12 SDS solution (10%)

For preparation of 10% SDS (Sodium *n*-dodecyl sulfate) solution, 10 g of highly pure electrophoresis grade SDS powder was totally dissolved in 90 mL 65 °C pre-heated distilled water and stirred, then volume was adjusted to 100 mL and kept at room temperature.

### 11.13 Tris-HCl (0.5 M, pH 6.8)

For preparation of 0.5 M Tris (2-amino-2-hydroxymethyl-propane-1,3-diol) HCl buffer, 6.057 g of Tris base powder was dissolved in 90 mL of distilled water. Hydrochloric acid (6 N) was used to adjust pH to 6.8, and then final volume was adjusted to 100 mL. This solution can be autoclave sterilized for 15 min at 121 °C and store and at 4 °C.

### 11.14 Tris-HCl (1 M, pH 8.8)

For preparation of 1 M Tris (2-amino-2-hydroxymethyl-propane-1,3-diol) HCl buffer, 12.114 g of Tris base powder was dissolved in 90 mL of distilled water. Concentrated hydrochloric acid (11.65 N) was used to adjust pH to 8.8, and then final volume was adjusted to 100 mL. This solution can be autoclave sterilized for 15 min at 121 °C and store and at 4 °C.

# BIOGRAPHY

| | |
|---|---|
| **NAME** | Mr. Hossein Javid |
| **DATE OF BIRTH** | September 22 1980 |
| **PLACE OF BIRTH** | Shiraz, Iran |
| **INSTITUTION ATTENDED** | **1998 - 2002:** B.Sc. of Biology (Microbial Sciences), Faculty of Science, Islamic Azad University (IAU), Iran.<br>**2002 - 2005:** M.Sc. of Biology-Microbiology, Faculty of Science, Islamic Azad University (IAU), Iran.<br>**2009 - 2014:** Ph.D. of Microbiology, Faculty of Science, Mahidol University, Bangkok, Thailand |
| **RESEARCH GRANTS** | Partial scholarship from the Doctor of philosophy program in Microbiology, faculty of science, Mahidol University, Bangkok, Thailand.<br>Research Assistantship scholarship, Faculty of Graduate Studies, Mahidol University, Bangkok, Thailand. |
| **PRESENTATION** | Isolation of Polycyclic Aromatic Hydrocarbons (PAHs) degrading bacteria from Tashk lake and study of the effect of salt in Bioremediation. 2006. The 8$^{th}$ National congress of Microbiology. |

**Publications**

**1.** Effects of halophilic peptide fusion on solubility, stability and catalytic performance of D-phenylglycine aminotransferase. 2014. Journal of Microbiology and Biotechnology. (Accepted)

**2.** Isolation of halophilic and halotolerant microorganisms from Bakhtegan Lake and the effect of Physico-chemical factors on their frequency. 2007. Scientific and research journal of water and wastewater. **18** (63): 81-87.

**3.** Isolation of Polycyclic Aromatic Hydrocarbons (PAHs) decomposing bacteria from Tashk lake and salt concentrations effects on them. 2007. Iranian Scientific Fisheries Journal. **16** (3): 103-112.

**4.** Gastrointestinal infectious agents in water resources of Jahrom City (senior student project). 2004. Science Bulletin of IAU. **5** (3): 21-22.

**5.** Microbial plastics. 2003. The Journal of Iranian society of Microbiology. **2** (8): 4-9.